Silica Reinforced Tyre Rubbers

Annemieke ten Brinke

2002

Ph.D. thesis
University of Twente

Twente University **Press**

Also available in print:
http://www.tup.utwente.nl/catalogue/book/index.jsp?isbn=9036517583

Silica Reinforced Tyre Rubbers

The research described in this thesis was financially supported by the Dutch Technology Foundation (STW).

Twente University **Press**

Publisher:
Twente University Press,
P.O. Box 217, 7500 AE Enschede, the Netherlands,
www.tup.utwente.nl

Cover design: Jo Molenaar, [deel4 ontwerpers], Enschede
Print: Océ Facility Services, Enschede

ISBN 9036517583

SILICA REINFORCED TYRE RUBBERS

MECHANISTIC ASPECTS OF THE ROLE OF COUPLING AGENTS

PROEFSCHRIFT

ter verkrijging van
de graad van doctor aan de Universiteit Twente,
op gezag van de rector magnificus,
prof.dr. F.A. van Vught,
volgens besluit van het College voor Promoties
in het openbaar te verdedigen
op vrijdag 30 augustus 2002 te 15.00 uur

door

Janna Willemina ten Brinke
geboren op 6 september 1974
te Rijssen

Dit proefschrift is goedgekeurd door de promotor

prof.dr.ir. J.W.M. Noordermeer

"The fear of the Lord is the beginning of knowledge"
(Proverbs 1:7a)

"De vreze des Heeren is het beginsel der wetenschap"
(Spreuken 1:7a)

Aan mijn ouders

Contents

Chapter 1

General Introduction

1.1 Introduction

Vehicle tyres are the most prominent rubber articles regarding volume and importance. They are also the most important design and spring element of the vehicle. More than half of the Natural Rubber and Synthetic Rubbers produced in the world are consumed in the tyre industry.[1]

Early tyre development took place mainly in Great Britain. The Scottish engineer, Robert William Thomson invented the world's first pneumatic tyres in 1845. They consisted of rubber tubes filled with air protected by a canvas cover with leather treads. Although these air-filled tyres offered less resistance to the irregularities of road surfaces than either iron or solid rubber tyres the invention was forgotten, because of the high costs and difficulties to remove these tyres. More then forty years later, in 1888 John Boyd Dunlop revived the pneumatic tyre. The first commercially available pneumatic tyres consisted of an inner-tube surrounded by a "cover" made up of several layers of woven canvas-type fabric, held together by rubber bonding. These "covers" were coated with rubber, which was thickened in the tread area and were locked onto the rim in various ways. This invention and its first applications were for bicycle tyres.[2-5]

The woven canvas proved to be problematic. The fabrics chafed as the tyre flexed and, along with the friction caused by the layers of fabric, excessive heat was generated. The natural rubber compound broke down very quickly with the average life of the tyre being only around three thousand kilometres. To prevent flexing, inflation pressures had to be in the region of around 400 kPa, which made the vehicle extremely uncomfortable, defeating the whole idea of the pneumatic tyre.[2]

The introduction of carbon black as a reinforcing agent in 1904,[4,6] lead to strongly increased tread wear resistance. Commonly carbon black is used for reinforcement and normally provides or enhances good physical properties for the cured rubber compound. Since 1912 in tyre treads the previously used zinc oxide is replaced by a high loading of carbon black to develop adequate physical properties,[4] while a small amount of zinc oxide is still added because it is necessary for the curing reaction. Nowadays pneumatic tyres are conventionally prepared with a rubber tread, which can be a blend of various rubbers, which is typically reinforced with a reinforcing filler: commonly carbon black.

Since the early nineteen forties, carbon blacks have been complemented by the group of highly active silicas. Technological reasons have long prevented silicas from being used in tyre compounds. Conventionally, carbon black is considered to be a more effective reinforcing filler for rubber tyre treads than silica if the silica is

used without a coupling agent. Indeed, at least in comparison with carbon black, there tends to be a lack of, or at least an insufficient degree of, physical and/or chemical bonding between the silica particles and the rubber. This is necessary to enable the silica to become a reinforcing filler for the rubber for most purposes, including tyre treads, if the silica is used without a coupling agent. To overcome such deficiencies, compounds capable of reacting with both the silica surface and the rubber molecule, generally known as coupling agents, are often used.[7]

A tyre is a much more complex object than it looks. Actually a tyre is many things: geometrically, it is a torus; mechanically, a flexible-membrane pressure container; structurally, a high-performance composite; and chemically, a tyre consists of materials made up from long chain macromolecules.[8] The functions of a tyre can be considered in relation to three basic roles: (a) vehicle mobility, (b) performance and integrity, and (c) comfort. Performance, including driving and braking torque and rolling resistance, exerts or transfers forces or moments in forward direction. Vehicle mobility, including cornering, steering response, and abrasion, acts in the lateral direction, and the forces involved in comfort act vertically.[8]

The tyre engineer and of course the customer knows exactly what a good tyre should be like: (a) it should generate the highest possible traction force between tyre and road; (b) the steering characteristics should be exact and predictable under all handling situations; and (c) it should have the lowest possible rolling resistance and (d) give the highest possible mileage. In all these requirements the tyre tread compound plays a major, if not a key role. (a) The tyre traction is determined by the friction properties of the tread compound. Even under wet road conditions – where the drainage of the water from the contact area and the capability of the tread to disrupt the lubrication of the water film are involved in order to establish dry contact to the road – the tread plays a major role, as the friction coefficient of the tread determines the achievable traction level of the tyre. (b) The steering characteristics depend, apart from construction features, on the stiffness of the tread compound, i.e. on its dynamic modulus and again on the friction properties. (c) The rolling resistance of the tyre depends largely on the loss modulus of the tread compound and the resultant heat build-up depends on its thermal conductivity. (d) The mileage obtainable from a tyre depends on a large number of factors. Ultimately, when all other influences are kept constant, the mileage depend on the abrasion resistance of the tread compound, a complex property which itself depends on strength, fatigue and resistance to the effects of aging.[9]

A major problem facing tyre designers has traditionally been to solve the compromise between low rolling resistance, high wet grip and high wear resistance. Rolling resistance is the amount of energy a tyre absorbs as it revolves and deflects. The lower the rolling resistance the less fuel is required to propel the vehicle forward. Lowering the rolling resistance, however, commonly results in a reduction in wet grip performance, which of course is unacceptable.[10,11] A major step in solving this problem can be achieved by the replacement of (part or all) carbon black by silica in the tyre's tread compound. This has enabled

manufacturers to produce tyres which provide improved wet grip properties, better winter performance and lower rolling resistance all at the same time.[10,11]

The reason why this technology can be considered so revolutionary is best described as follows;
Grip is affected by the degree to which a tyre is distorted at high frequencies – in other words the degree to which it complies to small stones and unevenness in the road surface. Grip is best served by rubber compounds, which absorb high levels of energy (high hysteresis compounds).[11]

Rolling resistance, on the other hand, is affected by low frequency distortion – the deflection of the tyre as it revolves. Low rolling resistance requires compounds, which absorb low quantities of energy (low hysteresis compounds). The contrast with grip is why it has been impossible in the past to provide tyres, with both reduced rolling resistance and increased wet grip.[11] With the addition of silica, however, tyre engineers have been able to produce compounds, which provide higher hysteresis at high frequencies but lower hysteresis at low frequencies than achievable with carbon black.[11]

The use of silica can result in a reduction in rolling resistance of 20 % and more relative to carbon black. Assuming correct tyre pressures are maintained and making allowance for varying speeds and different driving characteristics, a 20 % reduction in rolling resistance corresponds to a 5 % fuel saving, which according to Michelin in their promotion of the Michelin “Energy Tyre”, can save the average motorist the amount of money, covering the cost of the tyres.[11]

The use of silica can also improve wet skid performance. By incorporating silica in their winter tyre range, Vredestein claims to have improved wet skid performance by as much as 15 %, substantially improving braking distances at the same time.[11]

Silica also provides substantial benefits in winter tyres and all-season tyres. Compounds using silica are more elastic and flexible at lower temperatures allowing better grip and braking during wintry weather.[11]

Many investigations on carbon blacks, silicas, and organosilane coupling agents[12] not only yielded new insights into the mechanism of reinforcement, but also provided vital new incentives for the development of tyre compounds and tyres with much better performance.[6] Due to the increased use of silica for reinforcement in tyre technology and its potential in other rubber applications, it is generally felt that a further study of the mechanism of silica adhesion, or compatibilisation with the rubber matrix by coupling agents, is justified.

1.2 Aim of the project

The aim of the investigations described in this thesis is to obtain a better understanding of the reaction between silica, coupling agent and rubber. A better understanding of this reaction might help the understanding of the reinforcement mechanism for silica filled rubbers,[13,14] which in turn may help developing tyres

with an even better balance of properties. Further, it may potentially lead to a broader application base for silica reinforcement also in other (dynamic) rubber applications.

The reaction of the coupling agent to the silica surface was intensively studied by different authors.[13,15-24] Therefore, we have chosen to study the reaction between coupling agent and rubber in more detail. This is the part of the reaction mechanism, which is still not completely understood. The work described in this thesis is therefore directed to the effect of various silane coupling agents on processing as well as on dynamic mechanical properties. The work is primarily focussed on tyre applications, based on the “green tyre” silica tread compound.

1.3 Structure of this thesis

The background of the use of silica in rubber especially for tyre applications, the influence on tyre rolling resistance, Payne effect and the use of coupling agents and their effect is briefly described in Chapter 2 of this thesis. Chapter 3 deals with the synthesis and characterisation of alternative coupling agents.

The study in Chapter 4 deals with investigations of the influence of the rubber-reactive part of the coupling agent on processing, curing and dynamic mechanical properties of the rubber compound. The coupling agents studied are equivalents of the industrially most commonly used bis(triethoxysilylpropyl) tetrasulphide, (TESPT) and vary in sulphur rank and carbon rank when compared to TESPT.

Chapters 5 and 6 deal with new coupling agents and their effect on processing and dynamic mechanical properties of the “green tyre” tread compound.

Chapter 7 describes the results of ^{1}H NMR relaxation measurements, performed as an alternative method to sense interactions, either physical or chemical of nature, between silica and rubber by means of coupling agents.

References

1. W. Hofmann, "Rubber Technology Handbook", Hanser/Gardner, Munich, 1996.
2. Internet page, *www.firestone.co.za/passenger/tips/consumer_history.htm.*
3. Internet page, *vintagecars.about.com/library/weekly/aa082298.htm?once= true&.*
4. C. M. Blow and C. Hepburn, "Rubber Technology and Manufacture", Plastics and Rubber Institute, London, 1982.
5. J. L. White, "Rubber Processing: technology, materials, and principles", Hanser, Munich, 1995.
6. S. Wolff, Rubber Chem. Technol., 69, 325 (1996).
7. D. J. Zanzig, P. H. Sandstrom, M. J. Crawford, J. J. A. Verthe and C. A. Losey (to The Goodyear Tire & Rubber Company), EP 0 638 610 A1 (27-07-1994).
8. J. E. Mark, "Science and Technology of Rubber", Academic Press, San Diego, 1994.
9. K. A. Grosch, Rubber Chem. Technol., 69, 495 (1996).

10. B. Freund, F. Forster and R. Lotz, Paper No. 77 presented at a meeting of ACS, Rubber Division, Cleveland, Ohio, 17-20 October,1995.
11. Internet Page, *www.tyres-online.co.uk/technology/silica.asp.*
12. E. P. Plueddemann, "Silane coupling agents", Plenum Press, New york, 1991.
13. M. J. Wang, S. Wolff and J. B. Donnet, Rubber Chem. Technol., 64, 559 (1991).
14. S. Wolff, Tire Sci. Technol., 15, 276 (1987).
15. M.-J. Wang and S. Wolff, Rubber Chem. Technol., 65, 715 (1992).
16. M.-J. Wang, S. Wolff and J.-B. Donnet, Kautsch. Gummi Kunstst., 45, 11 (1992).
17. S. Wolff and M. J. Wang, Rubber Chem. Technol., 65, 329 (1992).
18. A. Hunsche, U. Görl, A. Müller, M. Knaack and T. Göbel, Kautsch. Gummi Kunstst., 50, 881 (1997).
19. A. Hunsche, U. Görl, A. Müller, M. Knaack and T. Göbel, Kautsch. Gummi Kunstst., 50, 881 (1997).
20. A. Hunsche, U. Görl, H. G. Koban and T. Lehmann, Kautsch. Gummi Kunstst., 51, 525 (1998).
21. U. Görl and A. Parkhouse, Kautsch. Gummi Kunstst., 52, 493 (1999).
22. U. Görl, A. Hunsche, A. Müller and H. G. Koban, Rubber Chem. Technol., 70, 608 (1997).
23. U. Görl and J. Muenzenberg, Paper No. 38 presented at a meeting of ACS, Rubber Division, Anaheim, California, May 6-9, 1997.
24. A. Blume, Paper No. 73 presented at a meeting of ACS, Rubber Division, Chicago, Illinois, April 13-16, 1999.

Chapter 2

Advantages of silica over carbon black as reinforcing filler and the effect of coupling agents in tyre applications

2.1 Introduction

Natural and synthetic rubbers, also called elastomers are rarely applied in their pure form. They are “too weak” to ful-fil practical requirements because of lack of hardness, strength properties and wear resistance. Fillers are used in order to improve the properties of rubber compounds. Fig 2.1 shows the effect of reinforcing fillers on different compound properties. Rubber articles derive many of their mechanical properties from the admixture of these reinforcing (active) fillers at quantities of 30% up to as much as 300% relative to the rubber part.

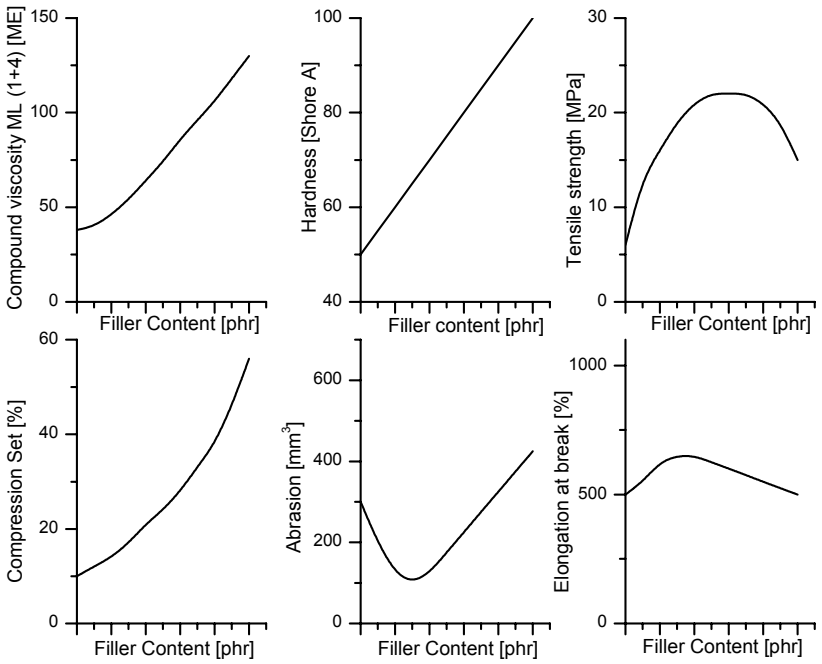

Fig 2.1: The influence of the amount of reinforcing fillers on compound properties.

Carbon black is in use as the most versatile reinforcing filler for rubber, complemented by silicas in the early nineteen fourties. In tyre manufacturing silicas

are more and more used nowadays, mainly to decrease the rolling resistance.[1] The increased attitude of protecting the environment gives rise to a demand for tyres combining a long service life with driving safety and low fuel consumption, achieved by this lower rolling resistance. However, the change from carbon black to silica is not at all obvious because of technical problems involved. In particular, the mixing of rubber with pure silicas is difficult, because of the polarity-difference between silica and rubber. Therefore, coupling agents are applied in order to bridge this polarity difference. The elucidation of the action in the reinforcement process, and the development and production of bifunctional organosilanes as coupling agents, finally paved the way for silicas to enter this area of application.[2]

2.2 Tyre performance

A tyre has to ful-fil many qualifications. Out of all these qualifications, three main performance criteria stand out: traction, wear resistance and rolling resistance.

A tyre must deliver high traction and cornering forces on wet and dry roads, also called wet and dry grip. The steering characteristics under all handling situations should be predictable. This high traction force between tread and road is necessary to create a good grip on the road surface, thereby avoiding slippage. Traction depends on three main tyre features: the tyre construction; the tyre tread compound and tread profile design; the road conditions.

A tyre must also show low wear and good durability and give a satisfactory driving comfort: the resistance to abrasion should be as high as possible to create a high mileage.[3,4]. With regard to environment and driving costs, the rolling resistance should be as low as possible, leading to low fuel consumption. Rolling resistance, being one of the main performance criteria covered in this thesis, will be dealt with in more detail in paragraph 2.2.1.

These three most important properties: rolling resistance, treadwear and wet grip form the so called: “magic triangle” of tyre properties, which means that a balance must be found between these properties. These requirements are conflicting, as it is impossible to improve all three characteristics at the same time. A compromise between these characteristics should always be achieved.[5]

2.2.1 Rolling resistance

The last three decades, tyre producers have put much emphasis on reduction of the tyre rolling resistance, while simultaneously improving other aspects of tyre performance.[6] A tyre consumes energy as it is constantly changing its shape as the sidewalls deflect and the tread flattens into the contact patch. This consumes a small but definite amount of energy by virtue of hysteresis and consequently fuel.[4]

A tread with high hysteresis losses will have a higher rolling resistance and greater road-holding than a tread made out of resilient rubber. By use of proper tread compounds, the hysteresis characteristics can be controlled, thereby providing lower rolling resistance without affecting wet grip and wear resistance.[4] Rolling resistance plays a surprisingly large role in fuel consumption: for passenger cars and light trucks, a decrease in rolling resistance with minimum 10 % can yield fuel

consumption improvements ranging from 0.5 to 1.5 %, and for heavy trucks, an improvement of 10 % can yield fuel savings of 1.5 to 3.0 %.[3] That is to say, that for passenger cars and light trucks 5 to 15 % of the fuel energy is consumed by rolling resistance and 15 to 30 % for heavy trucks.

Tyre rolling resistance is defined as the energy consumed per unit distance of travel as a tyre rolls under load. The energy consumed by the tyre is converted into heat. The proper unit of rolling resistance is [J/m], which equals [N], the unit of force. It should be kept in mind though, that there is a distinct qualitative difference between the two units. Rolling resistance is a energy per unit length and, hence, a scalar – not a vector as the unit [N] would imply. Thus, the rolling resistance, F_R is given by the equation:

$$F_R = \frac{dH}{dl} \tag{2.1}$$

where dH denotes the energy converted by the tyre into heat over the distance dl travelled. Or, since dl = vdt, where v is the road speed of the tyre, and dt is the time taken for a distance dl,

$$F_R = \frac{\dot{H}}{v} \tag{2.2}$$

Where the rate of heat development $\dot{H}$ (≡ dH/dt) is often termed power loss, P_R:

$$\dot{H} \equiv P_R \tag{2.3}$$

Then,

$$F_R = \frac{P_R}{v} \tag{2.4}$$

Holt and Wormeley[7] considered the energy balance of the tyre-roadwheel system. They argued that part of the input power delivered by the motor is converted into heat by the tyre, and the rest, the output power, is used to drive the car. Thus,

$$P_R = P_{in} - P_{out} \tag{2.5}$$

where P_{in} is the tyre input power provided by the motor, and P_{out} is the tyre output power supplied to traction of the car. The rest, P_R, is expended as heat by the tyre through deformation and friction. Therefore,

$$F_R = \frac{P_{in} - P_{out}}{v} \tag{2.6}$$

This is the general definition of rolling resistance. It includes all losses within the tyre structure, between tyre and roadway, and within the roadway. Bearing losses are excluded however.[3]

2.2.2 Relation between rolling resistance and dynamic mechanical properties

Rubber is a viscoelastic material: as it deforms, a fraction of the energy is stored elastically, and the remainder is dissipated as heat in a hysteretic manner. These hysteretic losses within a tyre, as well as aerodynamic drag and friction in the contact patch and with the rim, are irrecoverable losses and contribute to the total drag force on a moving vehicle.[6]

Viscoelastic behaviour is most commonly characterised in a so-called oscillatory dynamic mechanical test. The application of an oscillatory shear strain γ of angular frequency ω,

$$\gamma(t) = \gamma_0 \sin \omega t \tag{2.7}$$

results for a linear viscoelastic material in a sinusoidal stress σ, out of phase with the strain:

$$\sigma(t) = \sigma_0 \sin(\omega t + \delta) \tag{2.8}$$

The strain lags behind the stress by a phase angle δ.

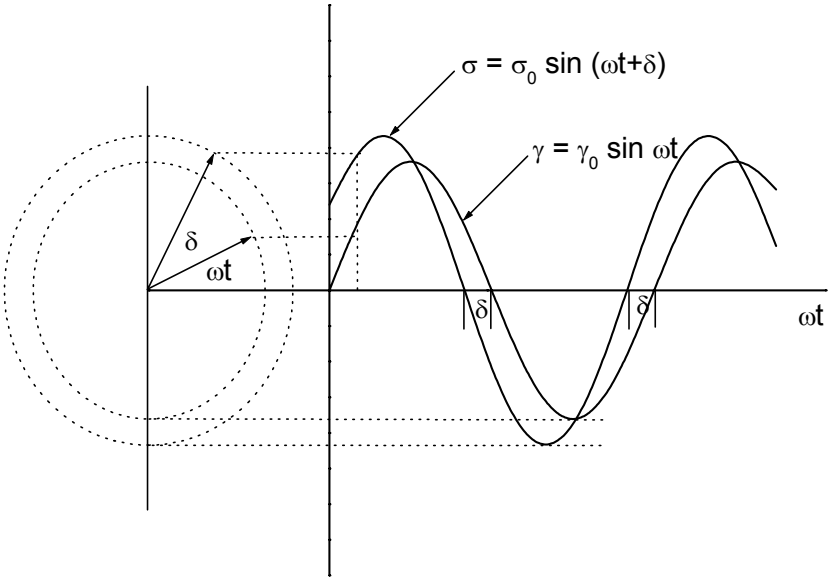

Fig. 2.2: Vector representation of an oscillating stress leading an alternating strain by a phase angle δ.

A vector representation of the dependence of γ and σ on ωt is shown in Fig. 2.2. Equation (2.8) can be rewritten as follows:

$$\sigma(t) = (\sigma_0 \cos\delta)\sin\omega t + (\sigma_0 \sin\delta)\cos\omega t \tag{2.9}$$

This equation shows that the stress consists of two components: one in phase with the strain (σ_0 cos δ); the other 90° out of phase (σ_0 sin δ). Therefore, the relationship between stress and strain in this dynamic experiment can be redefined by writing:

$$\sigma(t) = \gamma_0 \left[G' \sin \omega t + G'' \cos \omega t \right] \tag{2.10}$$

in which:

$$G' = \frac{\sigma_0}{\gamma_0} \cos \delta \tag{2.11}$$

and

$$G'' = \frac{\sigma_0}{\gamma_0} \sin \delta \tag{2.12}$$

Thus the component of stress $G'\gamma_0$ is in phase with the oscillatory strain; the component $G''\ \gamma_0$, is 90° out of phase. G' is termed storage modulus, and G" the loss modulus. The tangent of the phase angle, also called loss tangent is:

$$\tan \delta = \frac{G''}{G'} \tag{2.13}$$

The effects of rubber materials on rolling loss are profound and complex. Rolling loss depends not only on the basic polymers, their blending ratios, the other compounding ingredients and the state of cure, but also on the stresses, strains, temperatures and frequencies these materials experience at different locations in the tyre structure. Schuring[3] assumed that nearly all energy losses in a tyre must be generated in the rubber. The general dissipative mechanism of viscoelastic materials such as rubber is reasonably well understood; but its mathematical formulation is rather complex, except in simple models. The model preferred for tyres is the one-dimensional, sinusoidal deformation of linear viscoelastic materials in a geometrically simple specimen, as exemplified above. In reality, rubber deformations in a tyre are neither one-dimensional nor sinusoidal. Each volume element of a tyre, as it goes through one tyre revolution, is subjected to a three-dimensional, non-sinusoidal strain cycle, which hampers a mathematical analysis. The analysis is complicated further by non-linearities of the material response, and by temperature and frequency effects. These are complexities, which forced tyre researchers to resort to the much simpler linear, sinusoidal model: Fig. 2.2. The model is only a rough guide but, if handled judiciously, it is quite useful.

As cited by Medalia,[8] the deformation of a tyre tread can be resolved approximately into a constant strain (bending) and a constant stress (compression) condition. Since the geometric mean of the hysteresis under these two conditions is approximately proportional to tan δ, tyre tread hysteresis is as a first approximation, proportional to tan δ.

2.2.3 Rubber polymer influences on tyre performance

The tan δ level has a highly predictive value for the most important properties of a tyre tread. The significance of the tan δ curve for a number of important functions of a tread rubber is shown in Fig. 2.3.

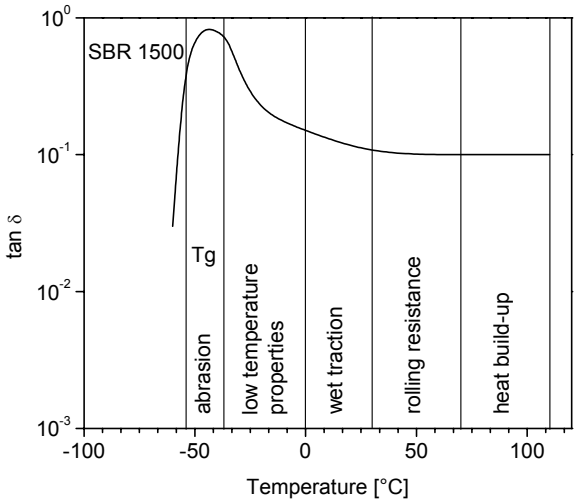

Fig. 2.3: Tread rubber evaluation, tan δ as a function of temperature.[9]

A prediction of the suitability of the tyre tread for winter use can be made with the help of the behaviour in the low temperature range, where the beginning of the glass state indicated by a strong upturn of the loss tangent marks the limit of elastic behaviour. As an indication of skidding behaviour (grip, traction) on wet, icy or dry roads, the level of the loss tangent around 0°C till approximately +30°C can be taken. The range between +30°C and approximately +70°C comprises the running temperatures of a tyre. Under these temperature conditions the loss factor essentially determines the degree of rolling resistance. At temperatures exceeding this limit the tyre enters into a region of maximum stress and reaches the limit of safe operation with the risk of destruction. The tan δ-values in this range indicate the heat build-up behaviour and allow an estimate of incipient thermal decomposition and the limit of good tyre performance.[9]

Since the peak in tan δ correlates with the glass transition temperature T_g of the polymer, this value became a tool for the selection of a suitable tyre rubber. The dependence of tan δ on temperature was studied for several rubber polymers by Nordsiek. The summary of the experimental results supports the concept of the relation between rubber molecular mobility and viscoelastic behaviour. The choice of the rubber polymer with the optimum glass transition temperature T_g therefore plays a key role in achieving a compromise between many tyre requirements.[9,10] The influence of different rubber polymers is not further investigated in this thesis. In all cases the same combinations of Solution-SBR and BR are employed.

2.3 Filler reinforcement

2.3.1 Carbon black vs. silica

Carbon black is most commonly used as reinforcing filler. Application of carbon black results in an increase in strength properties, wear resistance and fatigue resistance. In addition, due to its colour it is an excellent absorber of light. It therefore absorbs most of the ultraviolet components of sunlight, which can otherwise initiate oxidative degradation of the rubber.

The effects of the presence of carbon black on the dynamic mechanical properties of various types of filled rubber has been studied by many authors, e.g.[11-14] and was reviewed by Medalia[15]. The general conclusion from this early work was that the incorporation of carbon black in different types of rubber gives in most of the cases an increases in the storage and loss moduli, G' and G", and an increase in hysteresis, tan δ. Increases in strain amplitude give decreases in storage modulus G': the so-called Payne effect, see later.

Particularly since the introduction of the Energy® tyre by Michelin, silica has become more important as reinforcing filler for the rubber industry. The main reason is the greater reinforcing power of silica when compared to carbon black. The additional effect of temperature dependence of tan δ for reinforced rubber compounds is the result of the characteristics of reinforcing fillers to form a filler network. Comparing the tan δ values at different temperatures for silica and carbon black, a considerably lower tan δ value is found for silica at lower temperatures. In the rubbery state at temperatures beyond 20 °C the tan δ and hysteresis is still higher for carbon black: Fig 2.4.

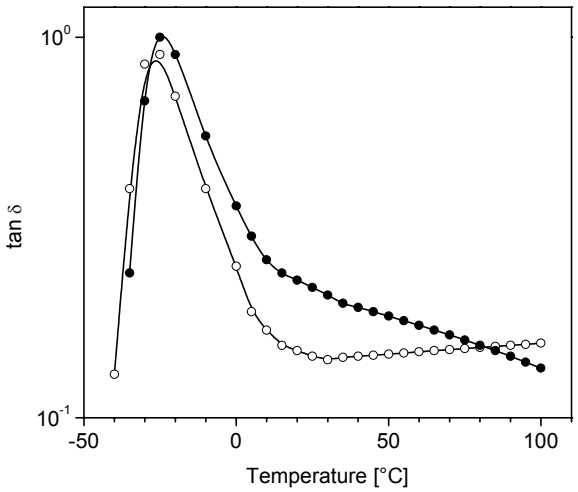

Fig 2.4: Theoretical graph of the temperature dependence of tan δ for a silica (○) and a carbon black (●) reinforced compound.

Replacement of carbon black by silica therefore results in a decrease of tan δ at higher temperatures, and thereby in a reduction in the rolling resistance. The use of silica in addition leads to a comparable tan δ at lower temperatures, providing a comparable ice- and wet grip of a tyre.[1]

The higher hysteresis of carbon black at higher temperatures is mainly due to the energy dissipation during repeated destruction and reconstruction of the filler network, which leads to a rapid decrease of tan δ with increasing temperature primarily due to a reduction of filler-filler interaction as well as filler-polymer interaction. Conversely the hysteresis of the silica-filled rubber increases with increasing temperature, finally showing a crossover point with carbon black at about 90 °C. Again, this may be anticipated from strongly and highly constructed filler clusters. As the temperature increases, weakening of the filler-filler interaction would result in an increase in the portion of filler network, which can be broken down and reformed during cyclic deformation at low strain amplitudes.[16] In Table 2.1 the influence of silica and carbon black on different tyre properties is given in a qualitative manner.

Table 2.1: The effect of silica and carbon black on different tyre properties. (+ = better; – = worse; ~ = same/comparable)

Property	Carbon Black	Silica
Rolling resistance	-	+
Ice- or wet grip	~	~ or +
Wear resistance	+	-

Compounding with silica enables tyre technicians to reduce the filler content, because of the greater reinforcing power of silica. A decrease in filler content corresponds to a higher amount of elastic rubber in proportion to the damping filler phase in the compound and is an effective way to reduce rolling resistance. The curve of tan δ is shifted downwards in temperature towards the unfilled rubber.[17]

The dependence of the G'-modulus on strain for a reinforced rubber vulcanisate is shown in Fig. 2.5. The G'-modulus of a filled rubber vulcanisate is built-up of: (a) a strain-independent contribution of the rubber network, which is the result of the proportionality of the G'-modulus to νRT, where ν is the number of moles of elastically effective network chains per unit volume, as a result of vulcanisation; (b) a strain-independent hydrodynamic effect of the filler, which was first derived by A. Einstein[18,19], and later exemplified for rubber in the Guth, Gold and Smallwood equation[20,21]:

$$G = G_0\left(1 + 2.5\phi + 14.1\phi^2\right) \tag{2.14}$$

where G and G_0 are the moduli of the filled and unfilled system respectively and ϕ is the volume fraction of the filler; (c) a strain-independent effect due to chemical/physical rubber to filler interactions; and (d) a strain-dependent contribution of the filler, which is also known as the Payne effect.[22]

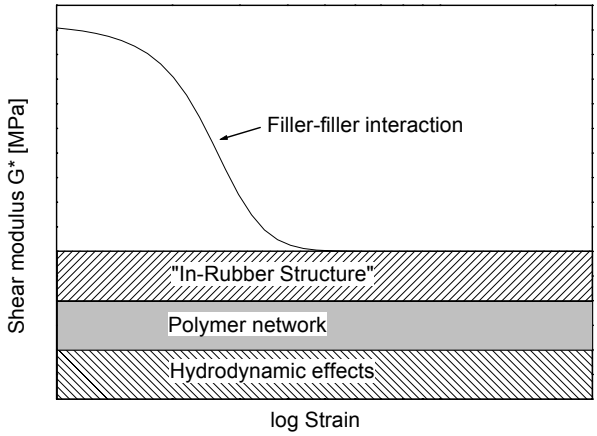

Fig. 2.5: The G-modulus as a function of strain for a reinforced rubber vulcanisate.*

It has been proposed that the reinforcement mechanism of carbon black is essentially due to the formation of a co-continuous network. Upon straining the sample, the polymer network stores energy and the carbon black network is disrupted, which releases energy in the form of heat. Upon removal of the strain, the stored energy present in the polymeric matrix reforms the filler network. These exchanges of energy are possible because the filler network is mechanically "trapped" in the net of the polymeric network, which is the deformation carrier. This mechanism has been proposed by several authors[22-24] and is supported by the experiments of Gerspacher et al.[25,26] The disruption of the silica network generally takes place at a higher strain compared to carbon black. The energy loss for a rolling tyre is therefore less for a silica reinforced compound when compared to a carbon black compound, resulting in a lower tan δ and consequently a lower rolling resistance of the tyre.[27]

At low temperature or high frequency deformations, the polymer plays the main role. The effect of the polymer, which is still part of the filler polymer network, is complemented by the influences of filler subnetworks or clusters.[28] At moderate-high temperature / high frequency or at low temperature / low frequency deformations, the filler-filler interactions are mostly responsible for the reinforcement and hysteretic effects.[29] The filler particles are, considering their volume concentration, in the "percolation" state i.e., the carbon black particles touch each other in a "filler-network".[22,30,31]

In order to explain the Payne effect in another way, Göritz supposed a Langmuir type polymer chain adsorption to the carbon black. The network density in the neighbourhood of a filler particle increases due to adsorption of network chains to the filler particle. A distribution of differently strong links between filler particles and segments of elastomer chains exists. During mixing, the first macromolecules which come in contact with the filler see the whole free surface. When a first link is

formed, neighbouring segments have a high probability to attach to the next interaction position and so on. This process comes to an end when all neighbouring sites on the filler surface are occupied. Chains, which arrive at the surface at a later moment, find the area widely covered and their possibilities of stabilisation are reduced. The last chains attached to the sites have very weak links to the particle. The storage modulus of a filled rubber sample, caused by entropy elasticity is directly proportional to the network density, the Boltzmann constant and the temperature. In the adsorption mechanism the network density is composed of three different parts: (a) the chemical network density; (b) the density of network chains attached by stable bonds to the filler surface; and (c) the density of unstable bonds between chains and filler. An increasing desorption of chains with increasing amplitude leads to a reduced network density. With increasing dynamic deformation these weakly bonded chains are torn off the filler surface and the density of unstable bonds between chains and filler decreases. By means of the theory of entropy elasticity it is then possible to describe the strain dependent modulus using a derivation similar to the theory of Langmuir concerning adsorption of gases to planar metal surfaces.[32]

The applicability of both theories, filler networking and polymer adsorption was studied by Freund and Niedermeier.[33] Carbon black, graphitised carbon black, silica and hydrophobated silica were used to vary filler agglomeration and polymer adsorption strength both in non-polar NR and polar NBR. Payne-type testing of all compounds including a relaxation study led to the conclusion that filler networking is the dominant Payne mechanism in the case of silicas, whereas polymer adsorption dominates in the case of carbon blacks.

2.3.2 Influences of the type of silica

The reinforcing effect of silica is related to its morphology. The morphology of silica can be divided into three characteristic structures, namely primary particles, aggregates and agglomerates. A primary particle has cross-sectional dimensions of 5 – 100 nm. Aggregates of multiple primary particles are formed by chemical and physical-chemical interactions: dimensions: about 100 – 500 nm. The aggregate can be quantified by the size of the primary particles as expressed in their specific surface area, the number of primary particles and their geometrical arrangement in the aggregate. The term “structure” encompasses all these three parameters to give a general measure of the aggregate. The aggregates are then condensed into agglomerates by Van der Waals forces. Typical dimensions of agglomerates are in the order of magnitude of 1 – 40 μm.[34] Silica agglomerates are disintegrated during rubber mixing, more or less to the size of aggregates or even primary particles. Silica aggregates are comparable to those of carbon blacks, but have a higher structure. This structure accounts for the greater reinforcing power relative to carbon black. Because of its high specific component of surface energy, silica has a strong tendency to agglomerate, and is difficult to disperse in rubber and rapidly re-agglomerates after mixing.

The dispersion of high-surface area silica in a silica-filled tread compound was measured using an optical microscope. Results showed that approximately 1% of the field of view of the micrograph still had agglomerates greater than 1 μm. A

compound containing a common commercial silica had approximately 6% area in the field of view larger than 1 μm. Therefore this first silica was characterised as being "highly or easy-dispersible" in rubber. Further, for this easy-dispersible silica the use of a silane coupling agent did not further increase its dispersion in rubber to a significant extent. A higher tan δ at 0° C along with a lower tan δ at 60° C was found with this high dispersion silica. Consequently, a high dispersion precipitated silica makes it possible to obtain low tread wear and high wet traction together with low rolling resistance. Moreover, a lower viscosity is obtained with the high dispersion precipitated silica, which enhances mixing and extrusion processability. A good dispersion allows a greater silica/filler contact area and a better homogeneity of the filler distribution within the compound.

Hi-Sil EZ is an easy dispersible precipitated silica that has been commercialised for use as a reinforcing filler of general purpose elastomers. Use of this silica affords excellent processability into rubber while maintaining important durability properties such as tear strength and cut-growth resistance.[35,36]

Novel precipitated silica particles presenting an improved capacity for dispersion and deagglomeration in reinforcing elastomer matrices were invented by Rhone Poulenc. When used as a reinforcing filler for elastomers, the final compounds had markedly improved mechanical properties relative to such elastomers reinforced with commercial silicas, like Ultrasil VN3 (DEGUSSA) and KS 404 (AKZO). The lowest Mooney viscosity was found for a compound with this novel silica and a higher reinforcing capability.[37-39] This Rhone Poulenc high dispersible silica was used as a reinforcing filler in the experiments described in this thesis.

Table 2.2: Surface properties of different commercial silicas.

Silica	BET [m^2/g]	CTAB [m^2/g]
HiSil® EZ[35]	167	153
Zeosil® 1165 MP[38]	170	155
Ultrasil® VN 3[38]	180	162
KS® 404[38]	170	151

Silica-treated carbon black was studied as a novel reinforcing filler for rubber compounds, as a partial defence against the silica-replacement of carbon black. Rubber compounds containing the silica-treated carbon black have similar performance to silica, which is suitable for application in tyre tread compounds with respect to hysteresis and electric conductivity. A compound that included silica-coated carbon black had lower tan δ in the higher temperature region and higher tan δ in the lower temperature region similar to a silica compound.[40,41]

2.4 Silane coupling agents

2.4.1. Basic mechanisms

Apart from the difficulty involved with mixing, see paragraph 2.1, silica being an acidic substance by virtue of acidic surface silanol groups, de-activates sulphur curing of rubber which usually requires alkaline conditions. This cure retarding effect and the difficult mixing and dispersion behaviour of hydrophilic silica are often corrected with a silane coupling agent. Due to a better dispersion and

polymer bonding, the formation of secondary filler structures (reagglomeration) is then reduced.[42]

A bifunctional organosilane coupling agent is generally characterised by two functions: one for the adhesion to the hydrophilic silica surface, the silane moiety, the other for adhesion to or enhancement of the compatibility with the hydrophobic polymer matrix: Fig 2.6.[1] The formation of filler-rubber linkages via organosilanes has a major influence on the properties of rubber compounds.[43] By lowering the specific component of surface energy of silica the level of adsorption of hydrocarbon rubber on the filler surface can be enhanced and subsequently filler-filler interactions are reduced. Coupling agents are used as a surface modification, either applied on the silica particle itself before the mixing, or by admixing to the rubber compound.[1]

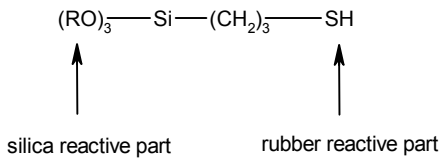

Fig. 2.6: Example of a bifunctional organosilane: 3-mercaptopropyltrialkoxy silane.

The addition during mixing in situ has been reported to be only 70 percent as efficient as pre-treatment. In situ modification of silica with silane coupling agents requires a number of precautions regarding the mixing sequence and mixing temperature, as well as careful adjustment of mixing conditions for every silane-containing compound. In silanised silicas, the silane already has undergone a chemical reaction with the silica, which renders the above precautions superfluous.[42] In addition, the already reacted coupling agents improve the ease with which the silica may be mixed with the rubber matrix.

Wolff assumed the following mechanism for the reaction between silica and the silane coupling agent on the one hand and the rubber matrix and the silane coupling agent on the other hand: Fig. 2.7.

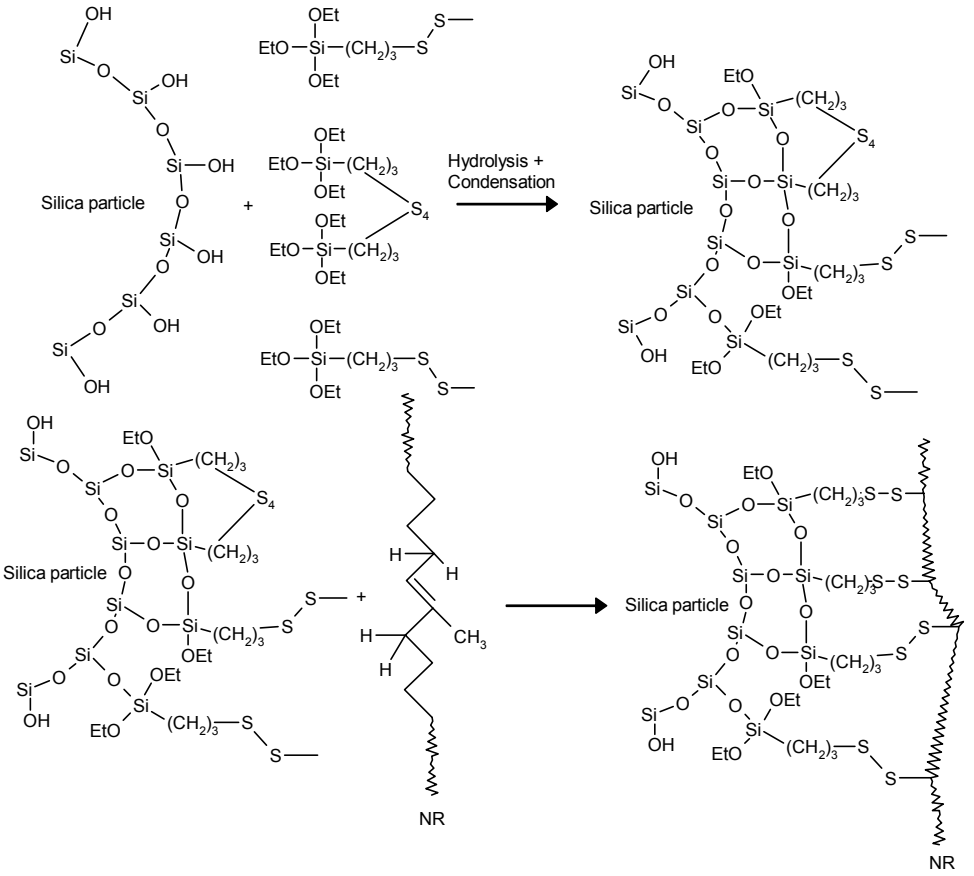

Fig. 2.7: Modification reaction of silicas with TESPT and formation of rubber-to-filler bonds.[44]

Kilian[45] questioned the validity of the assumption that a chemical reaction between the silane coupling agent and the rubber matrix takes place. The coupling agents do react covalently with the silica surface, but upon deformation pronounced evidence of slippage of "anchored" rubber molecules along the silica surface was found. In effect, using coupling agents only seems to enhance the hydrophobicity of the silica surface. This raised questions, whether there are chemical substances which effectively interact with the silica surface and the sulphur cure (and may further enhance the reinforcing power of silica).[1]

The reaction of the silane coupling agent with silica has been studied extensively by several authors. According to Hunsche et al., first a single bond with the silica surface is formed. This primary reaction is followed by a hydrolysis reaction, prior to condensation reactions between pairs of neighbouring silane molecules already bound to the silica surface: the secondary reaction.[46-50]

Görl et al.[51-55] studied the reaction of the coupling agent with the rubber matrix. From the results of a model compound study, the reaction was proposed to take place via an intermediate asymmetric polysulphide, a reaction product of a rubber

accelerator and the coupling agent. This intermediate product is formed by the reaction of the coupling agent, already linked to the silica surface and a disulphide accelerator. In the subsequent reaction the polysulphide is substituted into the allyl position of the rubber with release of the accelerator part. A covalent bond between the rubber and the filler was assumed to be formed by this reaction, resulting in a chemical bridge between rubber and filler.

2.4.2 Silane coupling agents for silicas

3-Mercaptopropyltrimethoxy silane was proposed and propagated as one of the first coupling agents for rubber applications.[56] Addition of 3-mercaptopropyltrimethoxy silane increased tensile strength, tear strength and modulus, improved hysteresis and lowered permanent set of a silica-filled natural rubber compound.[42] However, two properties of this coupling agent turned out to be disadvantageous. As a mercaptan, this mercapto silane emanated a disagreeable odour during mixing, especially at elevated temperatures. It also caused scorch problems and therefore its use remained limited.

Using trichlorosilane as a starting point, more than one hundred different organosilanes were synthesised by Wolff and co-workers.[57,58] These compounds were then tested for their utility in silica-filled rubber compounds. Only two silanes were found to be suitable as coupling agent, namely:

$(C_2H_5O)_3 – Si – (CH_2)_3 – S_4 – (CH_2)_3 – Si – (OC_2H_5)_3$
Bis(triethoxysilylpropyl)tetrasulphide (TESPT),

$(C_2H_5O)_3 – Si – (CH_2)_3 – SCN$
3-Thiocyanatopropyltriethoxy silane (TCPTS).

All other silanes had drawbacks regarding handling, odour, ease of transport, storage stability, kinetics of the modification and/or curing reactions, toxicological safety of the substances and their reaction products. The bis(triethoxysilylpropyl) tetrasulphide (TESPT) is applied in the Michelin “Green Tyre”.[59]

As mentioned above the silanisation reaction takes place in two steps. In the first step, the first ethoxy group reacts very quickly with the isolated and/or geminal silanol groups on the silica, either directly or after hydrolysis: Fig 2.8. One or two ethoxy groups per triethoxysilyl group remain after the TESPT has reacted with the silica. In a second, slower reaction step, these ethoxy groups are hydrolysed, thus crosslinking neighbouring TESPT molecules by means of siloxane bonds.[46-49] In the case of silanisation with TESPT, it must be borne in mind that the TESPT bound to the silica contains the highly reactive tetrasulphide group, which is able to undergo a thermal reaction with the polymer (see Chapter 4). This thermal reaction takes place when the mixing temperature becomes too high, leading to a rise in viscosity due to thermal crosslinking of the compound. This danger does not exist if TCPTS is used for the silanisation. Silica modified with TCPTS forms only monosulphidic rubber-to-filler bonds in accelerator/sulphur cure systems, and is therefore mainly restricted to the use in mechanical goods and the preparation of modified silica. With TESPT, on the other hand, the reaction time increases if the

optimum temperature is not attained. The modification of silica with either TESPT or TCPTS leads to a marked reduction in compound viscosity.[2]

Fig. 2.8: Reaction mechanism of the silanisation reaction.[46-49]

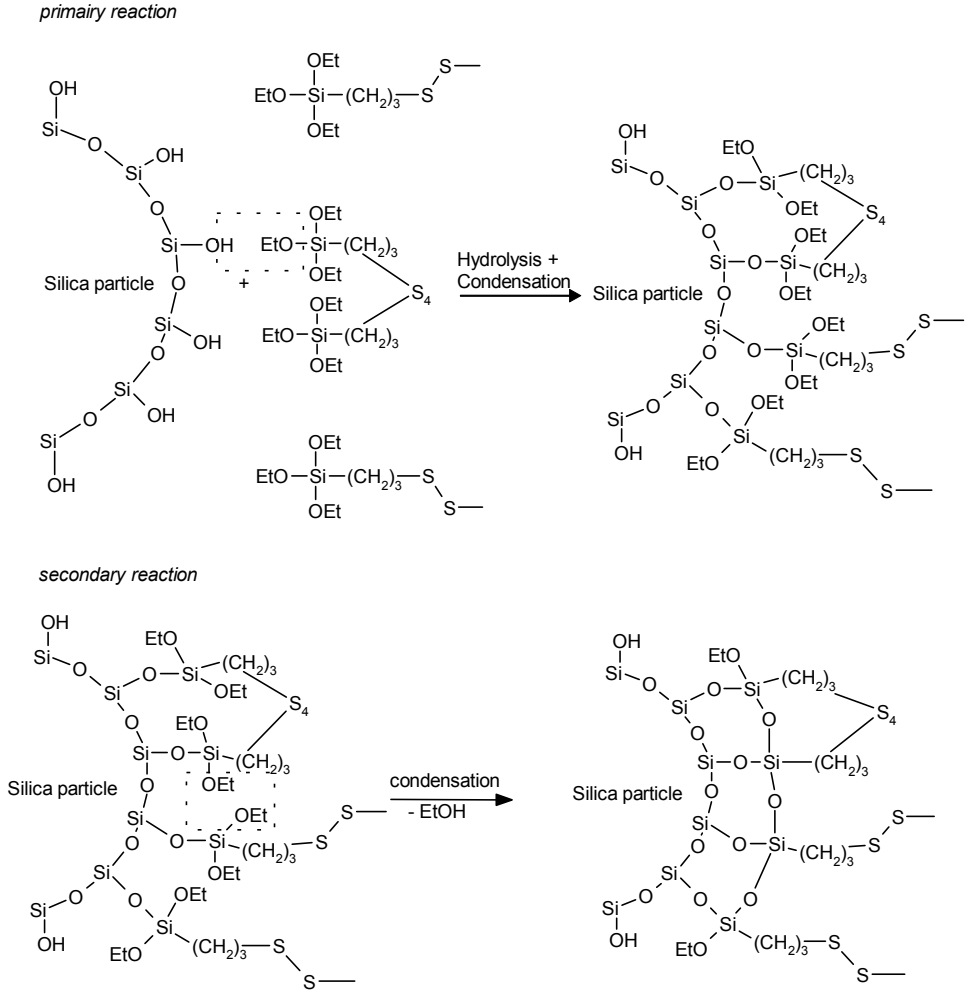

Various other sulphur-containing silanes have been prepared and used to study the effect of structural features on their reinforcing action in silica-filled styrene-butadiene rubber (SBR). A general structure of these silanes is given in Fig. 2.9.

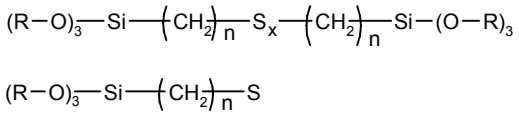

where R=methyl, ethyl of propyl, n=1 or 3 and x=1,2,3 or 4

Fig 2.9: General structure of studied silane coupling agents.[60]

The influence of the hydrolysable group on the silane coupling activity was determined by the comparison of methoxy, ethoxy and propoxy derivatives. The rate of the silanisation reaction turns out to depend on the alkoxy-group of the silane. It decreases in the following order:

CH_3O- > C_2H_5O- > C_3H_7O- > C_4H_9O- etc.

With the propoxy group, the reaction rate is generally too slow. Although the methoxy group reacts very rapidly, for toxicological reasons it is not used as a silanising agent – at least for the in situ process – because it evolves methanol. This leaves the ethoxy group, which reacts quickly enough and which is toxicologically sufficiently harmless if necessary precautions are taken.

Mercapto-substituted alkylsilanes affect the cure kinetics more than the other alkylsilanes, with a considerably more pronounced scorch shortening. Silanes with their sulphur-containing groups in α-position were found to be more effective in increasing the vulcanisation rate then silanes with their sulphur-containing groups in γ-position. On the other hand, the presence of γ-derivatives resulted in a higher reinforcement than in the case of coupling agents with the rubber-reactive group in the α-position. γ-Derivatives resulted in considerably higher modulus improvement. The coupling effect, which was measured by tensile moduli, increased with the length of the sulphur chain. However, the mercaptosilanes were found to be the most effective in coupling. A linear relationship between modulus and scorch time shortening and between bound rubber content and the tensile modulus (=coupling effect) was found.[60]

The effects of silane coupling agents with structures similar to TESPT but with various sulphur ranks, on the viscosity, curing characteristics and mechanical and dynamic mechanical properties of low rolling resistance silica filled SBR/polybutadiene tyre tread compounds were investigated.[61,62] The effect of holding constant the total sulphur level of the formulation by the addition of elemental sulphur to silanes with a lower average sulphur rank was also determined. The processing and property changes depended on whether the sulphur was added in the mixer or in the curing package.

Coupling agents (Fig. 2.10) with the following formulas were tested and compared with TESPT: [63,64]

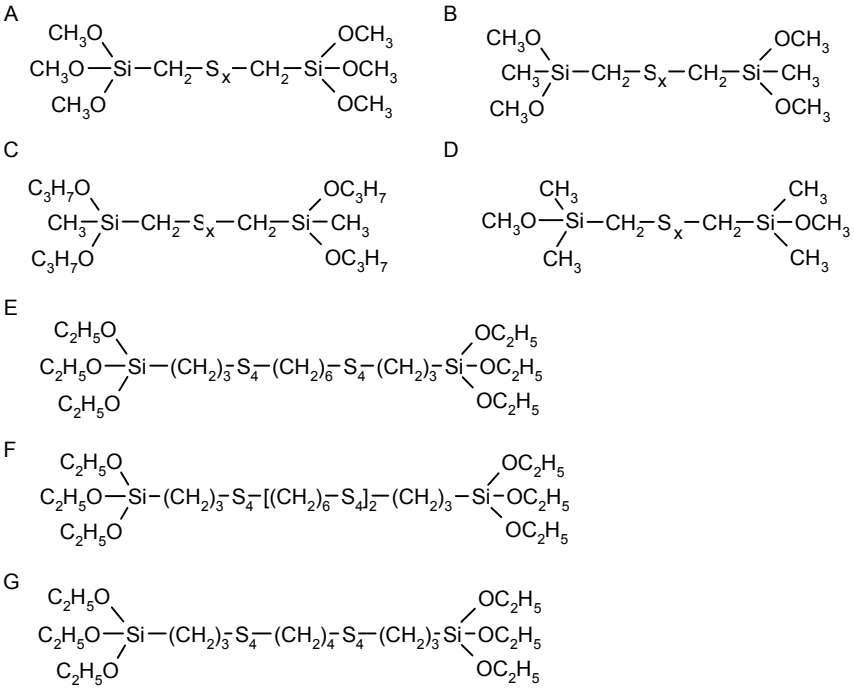

Fig. 2.10: Structures of various studied silane coupling agents.

Increased moduli, hardness and elasticity were found and a much lower tan δ at 60 °C, predictive of the rolling resistance of a tyre, was found. Surprisingly, also a higher tan δ at 0 °C was observed for the coupling agents A, B, C and D, which can be compared with a better wet grip of a tyre.[63] (Fig. 2.10) For coupling agents E, F and G (Fig. 2.10) no tan δ at 0 °C was measured.[64]

2.5 Other coupling agents

The mostly used coupling agents are silane coupling agents. Also some other, non-silane compounds have been tested. In this paragraph some of these non-silane coupling agents will be discussed. It should be noted however, that the reaction mechanism of these coupling agents with silica has not been reported.

2.5.1 Thiophosphoryl compounds as coupling agents for silica

The interaction of bis(diisopropyl)thiophosphoryl disulphide (DIPDIS) (Fig. 2.11) with silica and hydrocarbon rubber was studied by Mandal et al. [65]

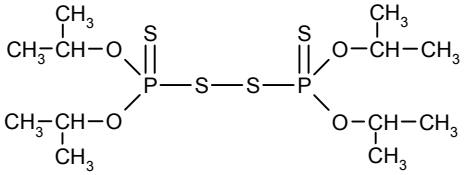

Fig. 2.11: Structure of DIPDIS.

Using gas liquid chromatography it was found that at 140 °C the concentration of free DIPDIS diminished, which indicated a coupling reaction. Isopropyl alcohol was found to be eliminated. From Infrared-spectra it was also evident that DIPDIS reacts with silica. The following reaction scheme was presented:

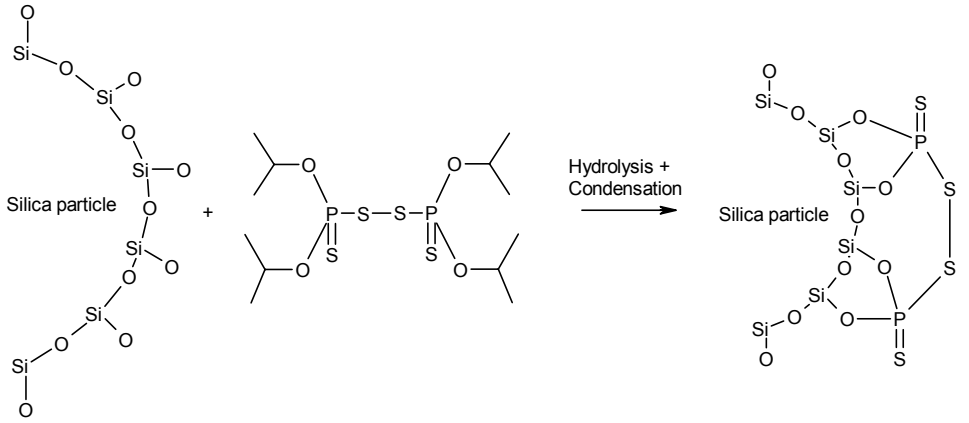

Fig. 2.12: Reaction of silica with DIPDIS.[65]

The reaction of DIPDIS with a hydrocarbon rubber was also studied using gas liquid chromatography. The labile disulphide linkage present in DIPDIS may undergo cleavage and the fragments thus obtained may become chemically linked with a hydrocarbon rubber. From the chromatograms it was evident that DIPDIS reacts with natural rubber during mill mixing and that at 170 °C the reaction was complete. The reaction between DIPDIS and natural rubber was presented as follows[65]:

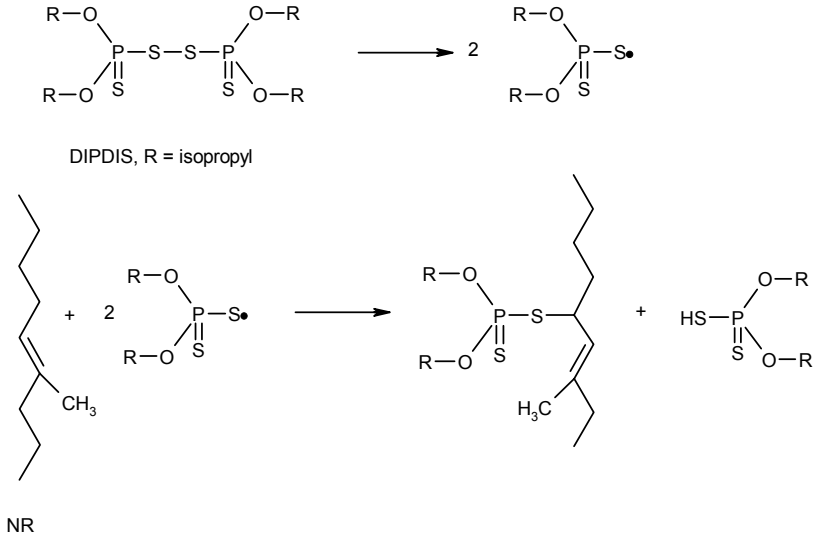

Fig 2.13: Reaction of natural rubber with DIPDIS.[65]

From the results it was apparent that DIPDIS can simultaneously combine with natural rubber and silica during cure and thus is likely to influence the physical

properties of the vulcanisates in a similar way as silane coupling agents e.g. TESPT.[65]

2.5.2 Other non-silane coupling agents for silica

Organo sulphonamides (Fig. 2.14) have been used as a silica coupler.[66] The properties (modulus, tan δ, hardness and abrasion) of a natural rubber compound, containing a benzene sulphonamide as a coupling agent were compared with a compound containing the conventional silane coupling agent, TESPT.[66]

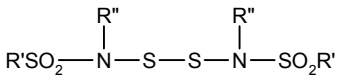

Fig. 2.14: General structure of organo sulphonamides.

From the results it was concluded that the properties of these compounds were comparable.

The zinc-, ammonium- and sodium salts of salicylic acid (Fig. 2.15) were tested as silica coupling agents in silica-reinforced rubber compounds.[67]

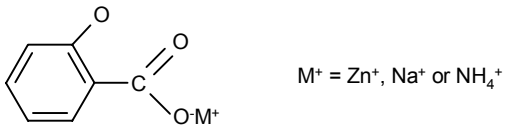

Fig. 2.15: General structure of salts of salicylic acid.

The properties of a silica-reinforced natural rubber compound containing sodium salicylate as a silica coupler were compared with a compound containing the conventional TESPT.

The sodium salicylate was observed to provide substantial equivalence in these properties to the conventional TESPT. This was considered to be an advantage because it was calculated, that rubber properties equivalent to the silane coupler might be achieved with a potentially lower cost.[67]

Zinc-, sodium- and ammonium phenoxyacetate (Fig. 2.16) were evaluated as an alternative for the commonly used silane coupling agent TESPT. Silica-reinforced natural rubber compounds containing one of these coupling agents were prepared.

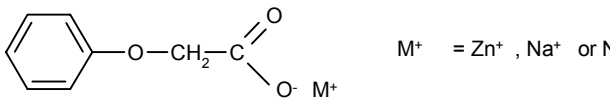

Fig. 2.16: General structure of phenoxyacetate salts.

The zinc phenoxyacetate and the sodium phenoyxacetate were observed to provide substantial equivalence in properties to a conventional silica coupling

agent, TESPT. The same advantage was found as for sodium salicylate, namely the same rubber properties achieved with a potentially lower cost.[68]

Because of the disadvantages of the silane coupling agents aromatic bismaleimides of the following formula (Fig. 2.17) were tested as silica couplers. A silica-reinforced natural rubber compound containing an aromatic bismaleimide as silica coupler was tested and compared with a compound containing TESPT.[69]

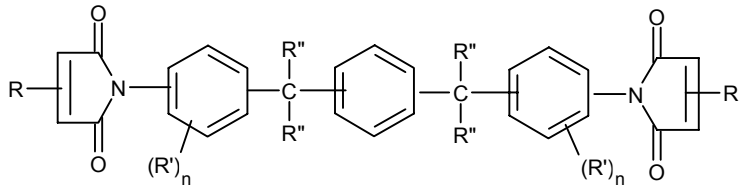

Fig. 2.17: General structure of aromatic bismaleimides.

No conclusions were made by the authors, but from the results it can be concluded that the properties of both compounds were comparable. So, possibly the aromatic bismaleimide is a good alternative, because it does not have the scorch problems and it does not have the problem of hydrolysis upon storage, which a silane coupling agent has and finally leads to a less reactive compound.

Nicotinamide (Fig. 2.18) was tested as a silica coupler in a silica-reinforced natural rubber compound. The properties of this compound were compared with a compound containing TESPT.[70]

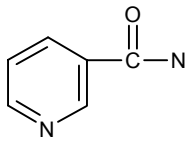

Fig. 2.18: Structure of nicotinamide.

From the results it was concluded that nicotinamide used as a coupling agent in silica reinforced compounds gave approximately the same properties as TESPT.

Dialkyleneamide polysulphides (Fig. 2.19) were claimed as silica coupling agents, and compared with TESPT. The properties of a silica-reinforced polyisoprene rubber containing a dialkyleneamide polysulphide were determined and compared with a TESPT containing compound.

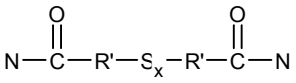

Fig. 2.19: General structure of dialkylenamide polysulphides (x = 2 to 7).

From the results it was concluded that the use of dialkylenamide polysulphides resulted in higher modulus, hardness properties (at room temperature) and rebound values than the control (TESPT).[71]

The addition of mercaptopyridines (Fig. 2.20) to rubber-silica compositions resulted in higher modulus, lower elongation, higher hardness and higher network density. The results indicated more extensive rubber-rubber crosslinking and/or rubber-filler coupling. However, the SBR compositions containing these mercaptopyridines were more scorch sensitive than a TESPT containing SBR compound.[72]

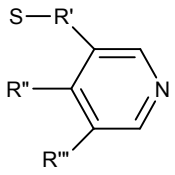

Fig. 2.20: General structure of mercaptopyridines.

Finally, since the introduction of silane coupling agents for silica filled rubber compounds a lot of research has been done in order to search for other, cheaper and/or better coupling agents for silica. Phosphonates[73], borate compounds[74], polysulphidic polyethersilanes[75], asymmetric siloxy compounds[76-79] and sodium-, potassium- or lithium salts thereof[80], unsaturated siloxy compounds[81], ether containing siloxy compounds[82], nitrogen containing siloxy compounds[83], blocked mercaptosilanes[84], sulphanylsilanes[85], sulphur functionalised polyorganosiloxanes [86] and all kinds of variations on TESPT[87-89] have been and still are being claimed as coupling agents for silica filled compounds, resulting in better or at least comparable compound properties compared to a TESPT-containing compound.

2.6 Summary and considerations for our research plan

Silica reinforcement of rubber is a very complicated technology, which is still very much in development. Literature and patent evidence are growing with a steady pace. As to the silica: the state of the art is, that with the exception of the availability of the easily dispersible silicas – like Hi-Sil® EZ and Zeosil® 1165 MP – there has not been much further development lately. With respect to carbon black technology: the main activity seems to concentrate on the development of silica-coated carbon blacks, which perform like intermediates between carbon black and silica.

A coupling agent is an absolute prerequisite for a proper performance of a silica-reinforced rubber compound, for reasons of:

- ease of dispersion;
- shielding of acidic groups to prevent cure retardation;
- obtaining the right balance between tan δ 0 °C for optimal wet grip and tan δ 60 °C for rolling resistance.

Although silicas pre-treated with coupling agents are in principle available, it is standard technology in the rubber industry to add the coupling agent in situ during the mixing operation. A great variety of coupling agents has been and is being explored up till today with varying effectiveness:
- silanes in great variety, mainly variations on TESPT (§ 2.4.2);
- thiophosphoryl compounds (§ 2.5.1);
- many others, like organo sulphonamides, salts of salicylic acid, phenoxy acetate salts, etc., for which it is impossible to derive a common denominator for reason of their functionality, based on the available information (§ 2.5.2).

The most commonly used coupling agent is TESPT, with which all other coupling agents are compared on functionality. Literature and patent data suggest indeed that improvements over TESPT in balance of properties are possible.

Based on these conclusions, the research described in this thesis focuses on optimisation of the coupling agent with emphasis on:
- optimisation of TESPT and variations on its structure;
- variations on the thiophosphoryl compounds;
- combined silane-accelerator and thiophosphoryl-accelerator systems along the lines of Mandal and Basu.[90]

References

1. P. Cochet, L. Barriquand, Y. Bomal and S. Touzet, Paper No. 74 presented at a meeting of ACS, Rubber Division, Cleveland, Ohio, Oct. 17-20, 1995.
2. S. Wolff, Rubber Chem. Technol., 69, 325 (1996).
3. D. J. Schuring, Rubber Chem. Technol., 53, 600 (1980).
4. I. Indian Rubber Institute, "Rubber Engineering", McGraw-Hill, New York, 0-07-135875-7, 2000.
5. R. Engehausen, A. Rawlinson and J. Trimbach, Tire Technol. Int. Ann. Review, 2001, 36 (2001).
6. D. E. Hall and J. C. Moreland, Paper No. 29 presented at a meeting of ACS, Rubber Division, Dallas, Texas, April 4-6.
7. W. L. Holt and P. L. Wormeley, Technol. Papers of Bur. Stand., 19, 213 (1925).
8. A. J. Medalia, J. Coll. and Interf. Sci., 32, 115 (1970).
9. K. H. Nordsiek, Kautsch. Gummi Kunstst., 38, 178 (1985).
10. R. Panenka, Tire Technol. Int. Ann. Review, 2001, 86 (2001).
11. H. Roelig, Rubber Chem. Technol., 12, 384 (1939).
12. W. S. J. Naunton and J. R. S. Waring, Trans. Inst. Rubber Ind., 14, 340 (1939).
13. S. D. Gehman, D. E. Woodford and R. B. Stambaugh, Ind Eng. Chem., 33, 1032 (1941).
14. R. B. Stambaugh, Ind. Eng. Chem., 34, 1358 (1942).
15. A. I. Medalia, Rubber Chem. Technol., 51, 437 (1978).
16. M. J. Wang, Rubber Chem. Technol., 71, 520 (1998).
17. L. Gatti, Tire Technol. Int. Ann. Review, 2001, 39 (2001).
18. A. Einstein, Ann. der Physik, 19, 289 (1906).
19. A. Einstein, Ann. der Physik, 34, 591 (1911).
20. E. Guth and O. Gold, Phys. Rev., 53, 322 (1938).
21. H. M. Smallwood, J. Appl. Phys., 15, 758 (1944).

22. A. R. Payne, Rubber Chem. Technol., 39, 365 (1966).
23. E. M. Dannenberg, Rubber Chem. Technol., 48, 410 (1975).
24. G. Kraus, Rubber Chem. Technol., 37, 6 (1964).
25. M. Gerspacher, C. P. O'Farrell and H. H. Yang, Kautsch. Gummi Kunstst., 47, 349 (1994).
26. M. Gerspacher, C. P. O'Farrell, H. H. Yang and W. A. Wampler, Paper No. C presented at a meeting of ACS, Rubber Division, Montreal, Quebec, Canada, May 5-8, 1996.
27. J. B. Donnet, Kautsch. Gummi Kunstst., 47, 628 (1994).
28. M. Gerspacher, O. P. O'Farrell, L. Nikiel and H. H. Yang, Rubber Chem. Technol., 69, 569 (1996).
29. M. Klüppel, R. H. Schuster and G. Heinrich, Rubber Chem. Technol., 70, 243 (1997).
30. M. Gerspacher, Rubber Chem. Technol., 64, 118 (1991).
31. A. Voet, Rubber Chem. Technol., 41, 1208 (1968).
32. P. G. Maier and D. Göritz, Kautsch. Gummi Kunstst., 49, 18 (1996).
33. B. Freund and W. Niedermeier, Kautsch. Gummi Kunstst., 51, 444 (1998).
34. G. Wypych, "Handbook of Fillers", ChemTec Publishing, New York, 2nd, 1-895198-19-4, 1999.
35. L. R. Evans, J. T. Dew, L. T. Hope, T. G. Krivak and W. H. Waddell, Paper No. 51 presented at a meeting of ACS, Rubber Division, Philadelphia, Pennsylvania, May 2-5, 1995.
36. L. R. Evans, J. T. Dew, L. T. Hope, T. G. Krivak and W. H. Waddell, Gummi Fasern Kunstst., 49, 456 (1996).
37. Y. Chevallier and M. Rabeyrin (to Rhone-Poulenc Chimie), US Pat. 5,403,570 (Jun. 26, 1992).
38. Y. Chevallier and M. Rabeyrin (to Rhone-Poulenc Chimie), US Pat. 5,547,502 (Nov. 16, 1994).
39. Y. Chevallier and M. Rabeyrin (to Rhone-Poulenc Chimie), US Pat. 5,587,416 (Jun. 7, 1995).
40. K. Mahmud, M.-J. Wang, J. A. Belmont and S. Reznek (to Cabot Corporation), WO Pat. 98/13428 (02-04-1998).
41. T. Kawazura, F. Yatsuysnagi, M. Kawazoe, K. Ikai and H. Kaidou, Paper No. 72 presented at a meeting of ACS, Rubber Division, Chicago, Illinois, 13-16 April, 1999.
42. E. M. Dannenberg, Elastomerics, 30 (1981).
43. L. R. Evans and W. H. Waddell, Kautsch. Gummi Kunstst., 48, 718 (1995).
44. S. Wolff, Tire Sci. Technol., 15, 276 (1987).
45. H. G. Kilian, M. Strauss and W. Hamm, Rubber Chem. Technol., 67, 1 (1994).
46. A. Hunsche, U. Görl, A. Müller, M. Knaack and T. Göbel, Kautsch. Gummi Kunstst., 50, 881 (1997).
47. A. Hunsche, U. Görl, H. G. Koban and T. Lehmann, Kautsch. Gummi Kunstst., 51, 525 (1998).
48. U. Görl and A. Hunsche, Paper No. 76 presented at a meeting of ACS, Rubber Division, Louisville, Kentucky, Oct. 8-11, 1996.
49. U. Görl, A. Hunsche, A. Müller and H. G. Koban, Rubber Chem. Technol., 70, 608 (1997).

50. U. Görl and J. Muenzenberg, Paper No. 38 presented at a meeting of ACS, Rubber Division, Anaheim, California, May 6-9, 1997.
51. U. Görl and A. Parkhouse, Kautsch. Gummi Kunstst., 52, 493 (1999).
52. A. Hasse and H. D. Luginsland, presented at a meeting of International Rubber Conference, Helsinki, Finland, June 12-15, 2000.
53. H. D. Luginsland, J. Fröhlich and A. Wehmeier, Paper No. 3 presented at a meeting of Deutsche Kautschuk Gesellschaft, Fortbildungsseminar "Soft Matter Nano-Structuring and Reinforcement", Hannover, Germany, May 22, 2001.
54. H. D. Luginsland, J. Fröhlich and A. Wehmeier, Paper No. 59 presented at a meeting of ACS, Rubber Division, Providence, Rhode Island, April 24-27, 2001.
55. U. Görl, J. Münzenberg, D. Luginsland and A. Müller, Kautsch. Gummi Kunstst., 52, 588 (1999).
56. L. P. Ziemansky, Rubber World, 163, 53 (1970).
57. F. Thurn, K. Burmester, J. Pochert and S. Wolff (to Degussa), US Pat. 3,873,489 (25-05-1975).
58. F. Thurn and S. Wolff, Kautsch. Gummi Kunstst., 28, 733 (1975).
59. R. Rauline (to Compagnie Generale des Etablissements Michelin - Michelin & Cie), E. Pat. 0 501 227 A1 (12-02-'92).
60. P. Vondrácek, M. Hradec, V. Chvalovsky and H. D. Khanh, Rubber Chem. Technol., 57, 675 (1984).
61. R. W. Cruse, M. H. Hofstetter, L. M. Panzer and R. J. Pickwell, Paper No. 75 presented at a meeting of ACS, Rubber Division, Louisville, Kentucky, Oct. 8-11, 1996.
62. R. W. Cruse, M. H. Hofstetter, L. M. Panzer and R. J. Pickwell, Rubber & Plastics News, April 21, 14 (1997).
63. T. Scholl and H.-J. Weidenhaupt (to Bayer AG), Eur. Pat. 0 680 997 A1 (April 21, 1995).
64. T. Scholl, H.-J. Weidenhaupt and U. Eisele (to Bayer AG), Eur. Pat. 0 670 347 B1 (20-02-1995).
65. S. K. Mandal, R. N. Datta, P. K. Das and D. K. Basu, J. Appl. Polym. Sci., 35, 987 (1988).
66. P. H. Sandstrom, R. J. Hopper and J. A. Kuczkowski (to The Goodyear Tire & Rubber Company), Eur. Pat. 0 723 991 A1 (July 31, 1996).
67. L. G. Wideman and P. H. Sandstrom (to The Goodyear Tire & Rubber Company), Eur. Pat. 0 700 956 A1 (29-08-1995).
68. L. G. Wideman, P. H. Sandstrom and D. J. Keith (to The Goodyear Tire & Rubber Company), Eur. Pat. 0 682 067 A1 (02-05-1995).
69. J. Muse, P. H. Sandstrom and L. G. Wideman (to The Goodyear Tire & Rubber Company), Eur. Pat. 0 536 701 B1 (06-10-1992).
70. P. H. Sandstrom and L. G. Wideman (to The Goodyear Tire & Rubber Company), US Pat. 5,504,137 (02-04-1996).
71. L. G. Wideman and P. H. Sandstrom (to The Goodyear Tire & Rubber Company), US Pat. 5,641,820 (24-06-1997).
72. G. Kraus (to Philips Petroleum Co.), US Pat. 4,482,663 (13-11-1984).
73. G. D. Macdonnell (to Philips Petroleum Company), US Pat. 4,386,185 (November 5, 1981).
74. F. U. Ernst, F. Visel, R. J. Zimmer and T. F. E. Materne (to Goodyear Tire & Rubber), Eur. Pat. 0 941 995 A2 (15-09-1999).

75. H. Königshofen, H.-J. Weidenhaupt, U. Eisele and T. Scholl (to Bayer AG), Eur. Pat. 0 864 608 A1 (02-11-1999).
76. T. F. E. Materne, U. E. Frank, M. N. Junio, F. Visel and G. Agostini (to Goodyear Tire & Rubber), Eur. Pat. 0 794 187 A1 (10-09-1997).
77. U. E. Frank, F. Visel, G. Agostini, R. J. Zimmer and T. F. E. Materne (to Goodyear Tire & Rubber), Eur. Pat. 0 945 456 A2 (29-09-1999).
78. F. Visel, G. Agostini, M. P. Cohen and T. F. Materne (to Goodyear Tire & Rubber), Eur. Pat. 0 939 081 A1 (01-09-1999).
79. T. F. Materne (to Goodyear Tire & Rubber), Eur. Pat. 0 939 080 A1 (01-09-1999).
80. T. F. E. Materne, U. E. Frank, F. Visel and R. J. Zimmer (to Goodyear Tire & Rubber), Eur. Pat. 0 794 188 A1 (10-09-1997).
81. T. F. E. Materne, F. Kayser and W. Lauer (to Goodyear Tire & Rubber), Eur. Pat. 1 076 060 A1 (14-02-2001).
82. T. F. E. Materne, F. Kayser and W. Lauer (to Goodyear Tire & Rubber), Eur. Pat. 1 076 061 A1 (14-02-2001).
83. T. F. E. Materne, F. Kayser and W. Lauer (to Goodyear Tire & Rubber), Eur. Pat. 1 076 059 A1 (14-02-2001).
84. R. J. Pickwell, E. R. Pohl, R. W. Cruse and K. J. Weller (to OSi Specialties Inc.), WO Pat. 99/09036 (25-02-1999).
85. C. Batz-Sohn and H.-D. Luginsland (to Degussa Huels AG), Ger. Pat. (DE) 198 44 607 A1 (08-05-2001).
86. W. Lortz, H.-D. Luginsland and R. Krafczyk (to Degussa), Eur. Pat. 0 997 489 A2 (03-05-2000).
87. H.-J. Weidenhaupt, U. Eisele and T. Scholl (to Bayer AG), Eur. Pat. 0 670 347 B1 (02-09-1997).
88. T. Scholl and H.-J. Weidenhaupt (to Bayer AG), Eur. Pat. 0 680 997 A1 (08-11-1995).
89. T. F. E. Materne and F. Kayser (to Goodyear Tire & Rubber), Eur. Pat. 1 061 097 A1 (20-12-2000).
90. S. K. Mandal and D. K. Basu, Rubber Chem. Technol., 67, 672 (1994).

Chapter 3

Synthesis and characterisation of the coupling agents investigated

Results of the synthesis of several coupling agents are described in the current chapter. Triethoxysilylpropyl monosulphide, triethoxysilyl hexane and triethoxysilyl decane were synthesised as equivalents of the commercially most used triethoxysilylpropyl tetrasulphide. Triethoxysilylpropylbenzothiazole disulphide was succesfully synthesised as a silane/accelerator combination. A compound consisting of a silane side and a thiophosphoryl side was also prepared, in which the silane part can react with the silica surface, while the thiophosphoryl part is expected to be able to react with both silica as well as with the rubber matrix.

3.1 Introduction

The three main groups of coupling agents, as proposed in Chapter 2 as research topic for this thesis are: variations on bis(triethoxysilypropyl) tetrasulphide (TESPT), combined silane-accelerator systems and variations on thiophosphoryl compounds. Since most of these chemicals are not commercially available, they had to be synthesised. The synthesis and characterisation of these potential coupling agents is described in the current chapter.

3.2 Experimental

3.2.1 Characterisation of the products

^{1}H-NMR spectroscopy

The structure and purity of the coupling agents synthesised were characterised using ^{1}H-NMR spectroscopy. The coupling agents were dissolved in deuterated chloroform (Aldrich, 99.8 atom-% D; CAS nr [865-49-6]). A Bruker 300 MHz NMR spectrometer was used.

Index of refraction

The index of refraction was measured using a Abbe refractometer, equipped with a thermostatic unit. The index of refraction was measured at 25 °C.

3.2.2 Synthesis of variations on bis(triethoxysilylpropyl) tetrasulphide

The synthesis of the following coupling agents was attempted: bis(triethoxysilylpropyl) monosulphide, bis(triethoxysilylpropyl) trisulphide, bis(triethoxysilyl) hexane and bis(triethoxysilyl) decane.

Synthesis of bis(triethoxysilylpropyl) trisulphide from 3-mercaptopropyl triethoxysilane and monosulphur dichloride resulted in a mixture of 80% trisulphide

and 20% of the tetrasulphide. Since pure products were preferred for a systematic study of the silanes with a structure similar to TESPT, the synthesis of pure bis(triethoxysilylpropyl) trisulphide was not further pursued.

Materials

For the syntheses the following chemicals were used: 3-mercaptopropyltriethoxy silane (Gelest Inc. assay 95%; CAS nr [14814-09-6]), 3-chloropropyltriethoxy silane (Gelest Inc.; CAS nr [5089-70-3]), sodium (Merck, assay of Na >99%; CAS nr [7440-23-5]), diisopropylether (Aldrich, assay 99%; CAS nr [108-20-3]), anhydrous magnesium sulphate (Sigma, assay min. 99.5%; CAS nr [7487-88-9]), toluene (Biosolve, assay min. 99.7%; CAS nr [108-83-3]), 1,5-hexadiene (Aldrich, assay 97%, CAS nr [592-42-7]), platinum-cyclovinylmethyl siloxane catalyst (Gelest Inc., 3-3.5% Pt, CAS nr [68585-32-0]), triethoxy silane (Gelest Inc., CAS nr [998-30-1]) and 1,9-decadiene (Aldrich, assay 96%; CAS nr [1647-16-1]).

Synthesis of bis(triethoxysilylpropyl) monosulphide.

Bis(triethoxysilylpropyl) monosulphide[1] (TESPM) was synthesised by the reaction of the sodium salt of 3-mercaptopropyltriethoxy silane and 3-chloropropyltriethoxy silane, according to the reaction scheme (3.1). The sodium salt was formed prior to the reaction by the addition of 5.2 grams of sodium in small pieces to a solution of 51.6 grams 3-mercaptopropyltriethoxy silane in 500 ml diisopropyl ether, under nitrogen flow. During reaction a white suspension was formed. 54.4 grams of 3-chloropropyltriethoxy silane were added drop wise, as soon as all sodium had reacted. The reaction mixture was allowed to react for another 42 hours under reflux conditions, and was extracted several times with water. The organic layer was dried using magnesium sulphate. After filtration the diisopropyl ether was evaporated using a rotavapor.

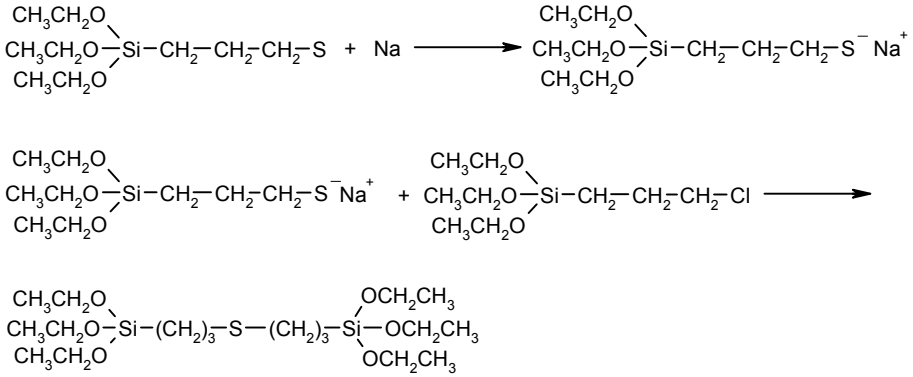

(3.1)

The synthesis of bis(triethoxysilylpropyl) monosulphide as described in the previous paragraph, was also performed by replacement of the solvent diisopropyl ether by toluene. Using toluene a higher reaction temperature was possible, resulting in a faster reaction.

With diisopropyl ether as a solvent the yield of the reaction was 62 wt.%. Using toluene as a solvent a yield of 57 wt.% was achieved. The product was purified by

vacuum distillation in both cases. The product boiling at 158-161 °C and 7 Pa, and with an index of refraction of 1.4392 measured at 25 °C, was characterised using ^{1}H-NMR spectroscopy. In Fig. 3.1 the ^{1}H-NMR spectrum of TESPM is given. The peak assignments are given in Fig. 3.2 and the chemical shifts are given in Table 3.1.

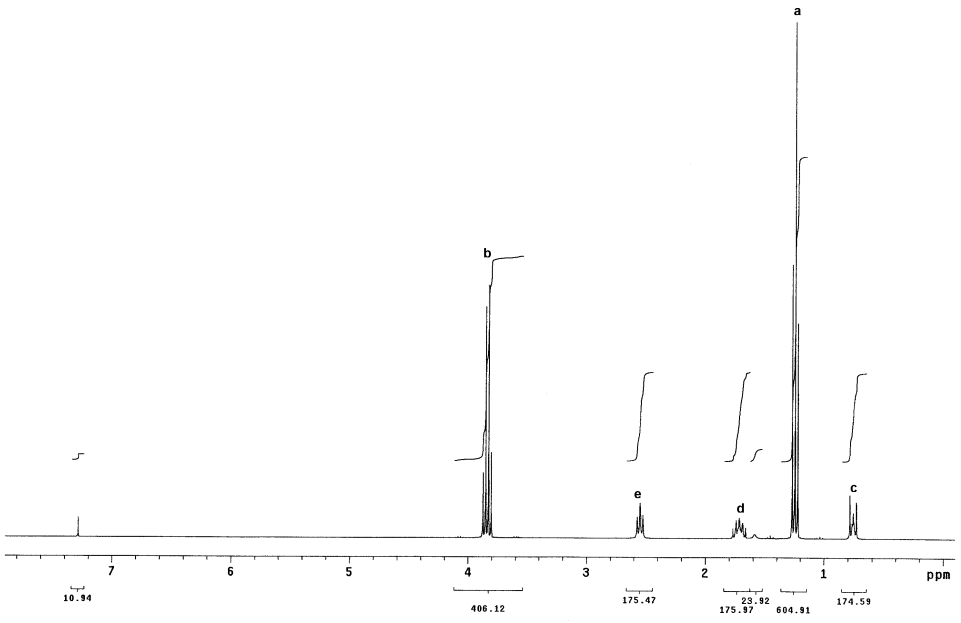

Fig. 3.1: ^{1}H-NMR spectrum of TESPM.

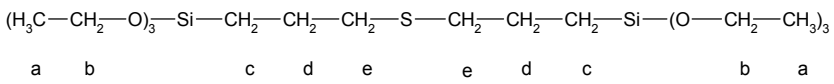

Fig. 3.2: Peak assignments of protons of TESPM.

Table 3.1 Chemical shifts δ of protons of TESPM.

peak	chemical shift δ [ppm]	Type	description
a	1.22	triplet	CH_3
b	3.82	quartet	CH_2, alkoxy side
c	0.72	triplet	CH_2, siloxane side
d	1.70	quintet	CH_2
e	2.54	triplet	CH_2, sulphur side

The ^{1}H-NMR spectrum proves the existence of the peaks, which might be expected for the compound synthesised. No detectable amounts of organic impurities are present in the compound, since only the expected peaks appear in the ^{1}H-NMR spectrum.

Synthesis of bis(triethoxysilyl) hexane

Bis(triethoxysilyl) hexane[2] (HTES) was synthesised by the reaction of triethoxysilane and 1,5-hexadiene, using a platinum-cyclovinylmethylsiloxane catalyst, according to reaction scheme (2). 50.63 grams of triethoxysilane and 12.97 grams of 1,5-hexadiene were dissolved in 65 ml freshly distilled toluene. Under vigorous stirring and nitrogen flow, 2 droplets of the catalyst were added. The reaction mixture was allowed to react for 48 hours at room temperature. Toluene was evaporated using a rotavapor and the product was further purified by vacuum distillation.

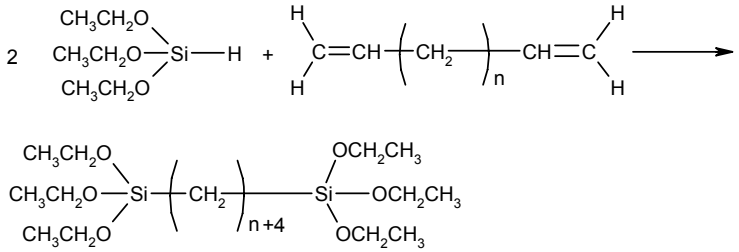

(3.2)

The fraction boiling at 110-117 °C and 8 Pa was collected and characterised with ^{1}H-NMR spectroscopy. The index of refraction of the product at 25 °C was 1.4181. The ^{1}H-NMR spectrum is shown in Fig. 3.3. Peak assignments and chemical shifts are given in Fig. 3.4 and Table 3.2, respectively. The peaks in the ^{1}H-NMR spectrum prove that bis(triethoxysilyl) hexane was formed, without any detectable inorganic impurities.

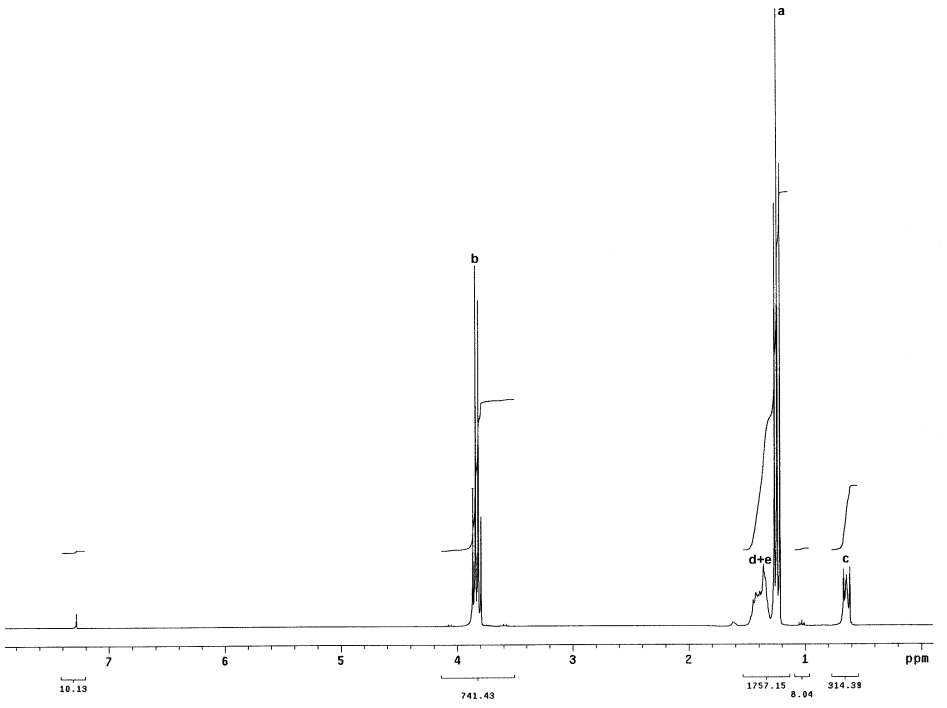

Fig. 3.3: ^{1}H-NMR spectrum of bis(triethoxysilyl) hexane.

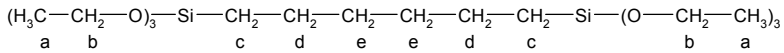

Fig. 3.4: Peak assignments of protons of bis(triethoxysilyl) hexane.

Table 3.2 Chemical shifts δ of protons of bis(triethoxysilyl) hexane.

peak	chemical shift δ [ppm]	type	description
a	1.22	triplet	CH_3
b	3.82	quartet	CH_2, alkoxy side
c	0.62	triplet	CH_2, siloxane side
d	1.38	quintet	CH_2, siloxane side
e	1.44	quintet	CH_2

Synthesis of bis(triethoxysilyl) decane.

Bis(triethoxysilyl) decane[2] (DTES) was synthesised similar to bis(triethoxysilyl) hexane, according to reaction scheme (3.2), from triethoxy silane and 1,9-decadiene using a platinum-cyclovinylmethyl siloxane catalyst. While vigorously stirring, 2 droplets of the catalyst were added to a mixture of 16.34 grams of 1,9-decadiene and 38.77 grams of triethoxysilane in 100 ml freshly distilled toluene. After 48 hours of reaction at room temperature the toluene was evaporated using a rotavapor. Vacuum distillation was used to further purify the product.

A ^{1}H-NMR spectrum was taken from the fraction boiling at 168-174 °C and 7 Pa. Fig. 3.5 shows the ^{1}H-NMR spectrum of DTES. Fig. 3.6 and Table 3.3 give peak assignments and chemical shifts respectively. The ^{1}H-NMR spectrum shows that DTES was formed during reaction. The index of refraction at 25 °C was 1.4253.

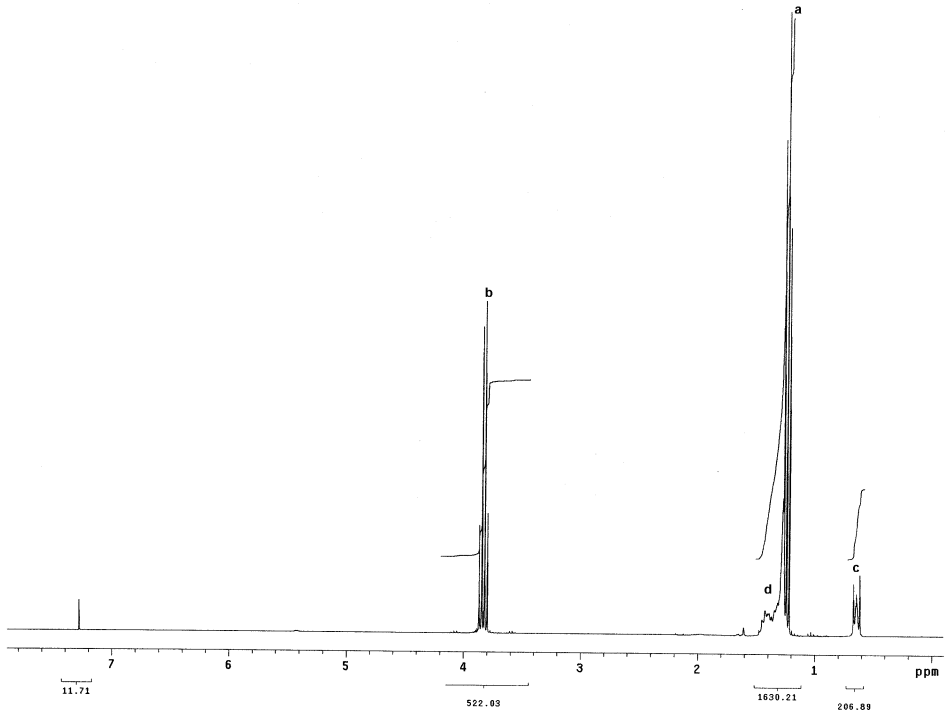

Fig. 3.5: ^{1}H-NMR spectrum of bis(triethoxysilyl) decane.

$(H_3C—CH_2—O)_3—Si—CH_2—(CH_2)_8—CH_2—Si—(O—CH_2—CH_3)_3$
a b c d c b a

Fig. 3.6: Peak assignments of protons of bis(triethoxysilyl) decane .

Table 3.3 Chemical shifts δ of protons of bis(triethoxysilyl) decane.

peak	chemical shift δ [ppm]	type	description
a	1.22	triplet	CH_3
b	3.82	quartet	CH_2, alkoxy side
c	0.62	triplet	CH_2, siloxane side
d	1.40	multiplet	CH_2

3.2.3 Synthesis of silane-accelerator systems

As combinations of a silane and an accelerator, the syntheses of triethoxysilypropyl benzothiazole disulphide and trimethoxysilylpropyl dimethylthiocarbamate were attempted. Trimethoxysilylpropyl dimethylthiocarbamate was prepared from 3-mercaptopropyltriethoxy silane and dimethylthiocarbamoyl chloride. The yield of trimethoxysilypropyl dimethyl thiocarbamate was very low and therefore this combination was not further investigated. The synthesis of triethoxysilylpropyl benzothiazole disulphide will be described in the current paragraph.

Materials

The chemicals used for the synthesis of triethoxysilylpropyl benzothiazole disulphide are: 3-mercaptopropyltriethoxy silane (Gelest Inc., assay 95%; CAS nr [14814-09-6]), 2,2'-dithiobis(benzothiazole) (Aldrich, assay 99%; CAS nr [120-78-

5]), chloroform (Biosolve, assay min. 99.9%; CAS nr [67-66-3]) and toluene (Biosolve, assay min. 99.7%; CAS nr [108-83-3]).

Synthesis of triethoxysilylpropyl benzothiazole disulphide.
Triethoxysilylpropyl benzothiazole disulphide[3-6] can be synthesised by the reaction of 3-mercaptopropyltriethoxy silane and 2,2'-dithiobis(benzothiazole) (MBTS)[4] according to reaction scheme (3.3). 82.5 Grams of MBTS were dissolved in 600 ml chloroform. At room temperature, 59.1 grams of 3-mercaptopropyltriethoxy silane were added drop wise. After 48 hours reaction at room temperature the reaction mixture was cooled with ice and filtered. The chloroform was evaporated using a rotavapor and the reaction product was filtered again. A red viscous filtrate was collected as the desired product.

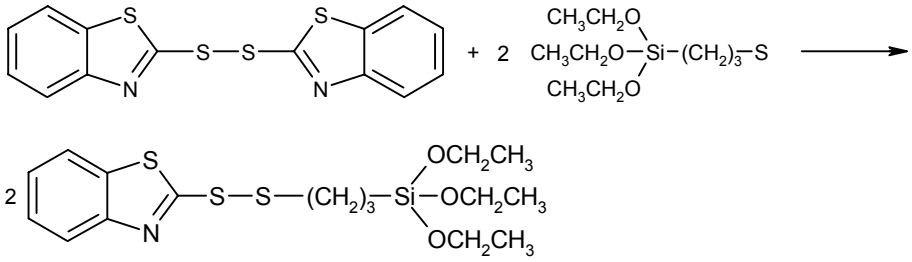

(3.3)

The same reaction was performed with toluene as a solvent, instead of chloroform in order to increase the reaction rate. Therefore 16.6 grams of MBTS were dissolved in 210 ml toluene. The suspension was heated till reflux temperature to dissolve the MBTS. 11.9 Grams of 3-mercaptopropyltriethoxy silane were added drop wise. After 2 hours 90 mole% of the product was formed. The other 10 mole% was bis(triethoxysilylpropyl) disulphide. Toluene was evaporated using the rotavapor. After 23 hours the proportion between product and side product was still 90 mole% to 10 mole%. The product was purified by evaporation of the toluene using the rotavapor. Then diethyl ether was added in order to dissolve organic impurities and the mixture was cooled strongly with liquid nitrogen. The mixture was filtered and the red viscous liquid was collected.

In the first synthesis, using chloroform as a solvent, the composition of the product was, according to the ^{1}H-NMR spectrum, 60 mole % triethoxysilylpropyl benzothiazole disulphide and 40 mole% triethoxysilylpropyl disulphide. When toluene was used as a solvent the reaction temperature could be increased, resulting in a much faster reaction. The product composition was changed to 90 mole% of triethoxysilylpropyl benzothiazole disulphide and 10 mole% of the side product triethoxysilylpropyl disulphide, as can be seen in the ^{1}H-NMR spectrum in Fig. 3.7. The yield was 67 mass%, and the index of refraction at 25 °C was 1.5428. The peak assignments are given in Fig. 3.8 and the chemical shifts are given in Table 3.4. Because of the faster reaction and the higher conversion to triethoxypropyl benzothiazole disulphide the synthesis with toluene as a solvent was used for further research described in this thesis.

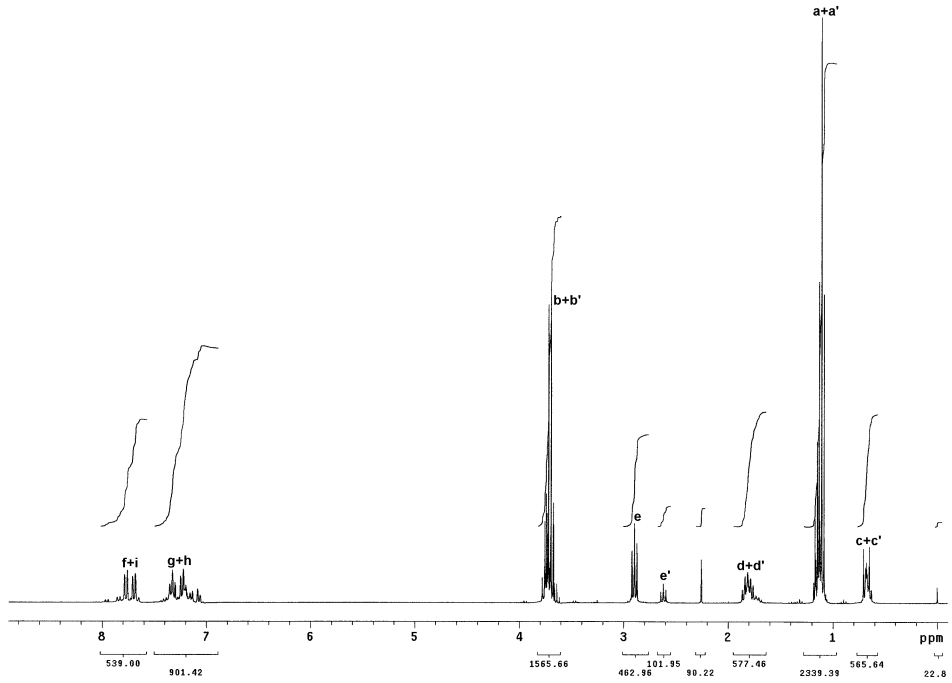

Fig. 3.7: ^{1}H-NMR spectrum of triethoxysilylpropyl benzothiazole disulphide.

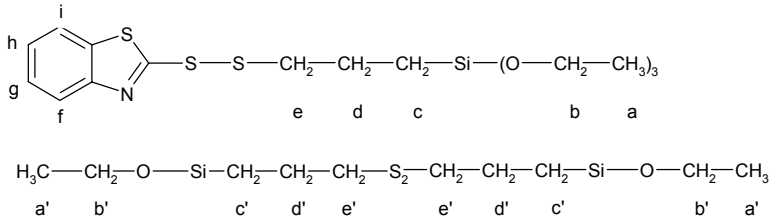

Fig. 3.8: Peak assignments of protons of triethoxysilylpropyl benzothiazole disulphide.

Table 3.4 Chemical shifts δ of protons of triethoxysilylpropyl benzothiazole disulphide.

peak	chemical shift δ [ppm]	type	description
a + a'	1.16	triplet	CH_3
b + b'	3.74	quartet	CH_2, alkoxy side
c + c'	0.70	triplet	CH_2, siloxane side
d + d'	1.82	quintet	CH_2
e	2.92	triplet	CH_2, sulphur side
e'	2.62	triplet	CH_2, sulphur side silane
f + i	7.68-7.84	double doublet	aromatic H, thiazole side
g + h	7.06-7.40	multiplets	aromatic H

3.2.4 Synthesis of variations on thiophosphoryl compounds

In the series of thiophosphoryl compounds as potential coupling agents the following combinations were attempted to be synthesised:

bis(diisopropylthiophosphoryl) disulphide[7] (DIPDIS), bis(diethoxythiophosphoryl) disulphide (DEPDIS), bis(dimethoxythiophosphoryl) disulphide (DMPDIS), diisopropylthiophosphoryl-N-oxydiethylene sulphenamide[8] (DIPTOS), diisopropylthiophosphoryl-2-benzothiazole monosulphide[8] (DIPMBT) and diisopropyl thiophosphoryl triethoxysilylpropyl monosulphide (DIPTESM).

DIPDIS was prepared according to the method described by Pimblott et al.[7] Reaction of diphosphorous pentasulphide and isopropyl alcohol resulted in diisopropoxy dithiophosphate, from which DIPDIS was formed by oxidation. DEPDIS was prepared in a similar way, using ethanol instead of isopropyl alcohol. When DIPDIS or DEPDIS were added as coupling agents to a green tyre tread compound in the first mixing step in the internal mixer, a scorch-like effect occurred, even with low rotor speed. The compounds could not be processed further after the first mixing step. Therefore DIPDIS and DEPDIS were not further investigated.

DMPDIS was prepared by oxidation of dimethoxy dithiophosphate, according to the method described in Methoden der Organischen Chemie Band XII/2, p 811[9,10]. The reaction product of the oxidation was a liquid. From ^{1}H NMR and elemental analysis it was not clear whether the right product was formed. Since the authors of Methoden der Organische Chemie mention a melting point of 51 °C for DMPDIS, the reaction product cannot be sufficiently pure DMPDIS. No other methods for the synthesis of DMPDIS were investigated.

DIPTOS was prepared by the oxidation of diisopropoxy dithiophosphate and N-oxy-diethylene sulphenamide and purified by vacuum distillation. The product boiling at 104 °C and 8 Pa was characterised with ^{1}H NMR spectroscopy. Purification with vacuum distillation however was found to be possible only using small quantities. When larger quantities were used, the product decomposed during vacuum distillation. Therefore DIPTOS could not be further investigated.

DIPMBT was prepared by the reaction of diisopropoxy dithiophosphate and 2,2'-dithiobis(benzothiazole) (MBTS). The ^{1}H-NMR spectrum of the product showed that still a large amount of un-reacted starting material was present. The yield of the reaction was not more then 30 wt.%. The low yield and the occurrence of a large amount of starting material were the reasons why no emphasis was put on the further investigation of DIPMBT.

The synthesis and characterisation of DIPTESM will be described in more detail in the following paragraph.

Materials

For the synthesis of diisopropyl thiophosphoryl triethoxysilylpropyl monosulphide the following chemicals are used: 3-mercaptopropyltriethoxy silane (Gelest Inc., assay 95%; CAS nr [14814-09-6]), diphosphorus pentasulphide (Aldrich, assay 99%; CAS nr [1314-80-3]) isopropyl alcohol (Biosolve, assay 99.8%; CAS nr [67-63-0]), phosphorus pentachloride (Aldrich, assay 95%; CAS nr [10026-13-8]),

diisopropyl ether (Aldrich, assay 99%; CAS nr [108-20-3]), sodium (Merck, assay of Na >99%; CAS nr [7440-23-5].

Synthesis of diisopropylthiophosphoryl triethoxysilylpropyl monosulphide

Diisopropylthiophosphoryl triethoxysilylpropyl monosulphide (DIPTESM) was prepared from diisopropyl chlorothiophosphate and 3-mercaptopropyltriethoxy silane according to reaction scheme (3.4). Since diisopropyl chlorothiophosphate is not commercially available it was prepared by the reaction of diphosphorus pentasulphide with isopropyl alcohol, followed by the substitution of the mercapto-endgroup using phosphorus pentachloride. For the synthesis of DIPTESM then a solution of 5.0 grams of 3-mercaptopropyltriethoxy silane in 25 ml diisopropyl ether was prepared. An amount of 0.5 gram of small pieces of sodium was added. When all sodium had disappeared, 4.5 grams of diisopropyl chlorothiophosphate in 25 ml diisopropyl ether was added dropwise. The mixture was allowed to react for 18 hours under reflux conditions. The reaction mixture was extracted with small amounts of water. The organic layer was dried using a rotavapor. The product was purified by vacuum distillation. (3.4)

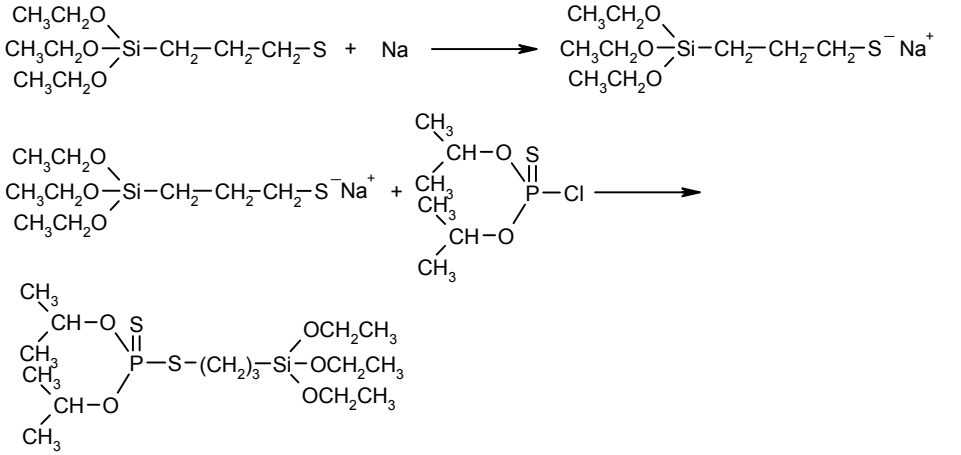

The fraction boiling at 126-138 °C and 7 Pa was characterised by ^{1}H-NMR spectroscopy and elemental analysis. The index of refraction was measured at 25 °C: 1.4641. The ^{1}H-NMR spectrum, Fig 3.10 showed the expected peaks. Peak assignments and chemical shifts are given in Fig 3.11 and Table 3.5, respectively. The results of elemental analysis are given in Table 3.6. Elemental analysis and ^{1}H-NMR spectroscopy proved that diisopropylthiophosphoryl triethoxysilylpropyl monosulphide was formed. The yield of the reaction was 59 mass%.

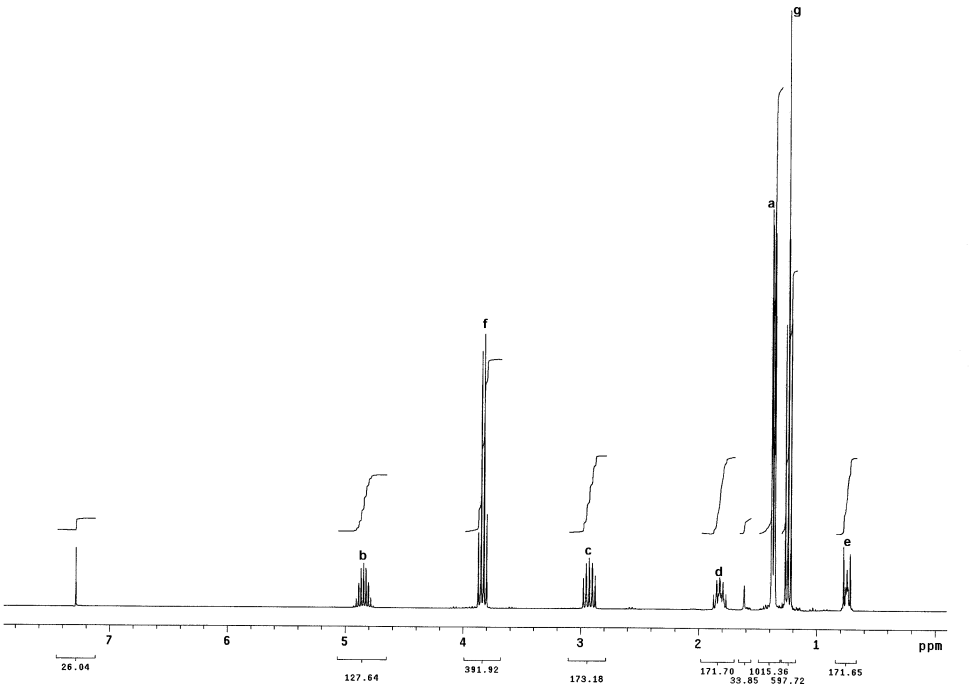

Fig. 3.10: ^{1}H-NMR spectrum of diisopropylthiophosphoryl triethoxysilylpropyl monosulphide.

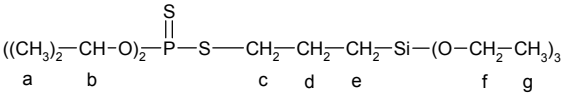

Fig. 3.11: Peak assignments of protons of diisopropylthiophosphoryl triethoxysilylpropyl monosulphide.

Table 3.5 Chemical shifts δ of protons of diisopropylthiophosphoryl triethoxysilylpropyl monosulphide.

peak	chemical shift δ [ppm]	type	description
a	1.36	doublet	CH_3
b	4.82	multiplet	CH, thiophosphoryl side
c	2.90	quintet	CH_2, thiophosphoryl side
d	1.80	quintet	CH_2
e	0.72	triplet	CH_2, siloxane side
f	3.80	quartet	CH_2, alkoxy side
g	1.22	triplet	CH_3, alkoxy side

Table 3.6 Elemental analysis of diisopropylthiophosphoryl triethoxysilylpropyl monosulphide.[a]

Element	mass %	mass % theoretical
C	42.86 ± 0.22	43.0
H	8.73 ± 0.02	8.4
P	7.60 ± 0.02	7.4
S	15.16 ± 0.10	15.4

[a] The error indicates differences in duplicate measurements

3.3 Conclusions

In spite of the difficulties with the syntheses, at least one or more compounds could be prepared for each of the three main groups of potential coupling agents, identified in Chapter 2. Application of these compounds as potential coupling agents will be described in the following chapters of this thesis.

Preparation and purification of the variations on TESPT, was quite easy, except for triethoxysilylpropyl trisulphide. The application of this group of compounds as coupling agents will be described in Chapter 4 of this thesis.

The group of silane-accelerator combinations showed more problems. Synthesis of these type of compounds was less successful, but fortunately one silane-accelerator combination could be synthesised. The effect of this compound, triethoxysilylpropyl benzothiazole disulpide as a potential coupling agent will be described in Chapter 5.

Most difficulties encountered with the synthesis of thiophosphoryl variations. The synthesis and purification of those compounds was the main problem. In some cases however, the synthesis was successful, but those compounds turned out to be so scorch sensitive that they were useless for further investigation as potential coupling agents. Fortunately one combination could be synthesised and could be used as a potential coupling agent without causing insurmountable problems during processing: Chapter 6.

References

1. P. Vondrácek, M. Hradec, V. Chvalovsky and H. D. Khanh, Rubber Chem. Technol., 57, 675 (1984).
2. A. A. Oswald and L. L. Murrell (to Exxon Research and Engineering Co.), US Pat. 4,268,682 (May, 19, 1981).
3. M. P. Cohen and L. G. Wideman (to The Goodyear Tire and Rubber Company), Eur. Pat. 0 785 206 A1 (14-01-1997).
4. M. P. Cohen, D. K. Parker and L. G. Wideman (to The Goodyear Tire and Rubber Company), Eur. Pat. 0 785 207 A1 (14-01-1997).
5. A. L. Ternay Jr., C. Cook and E. Brzezinska, Phosphorus, Sulfur and Silicon, 95-96, 351 (1994).
6. E. Brzezinska and A. L. Ternay Jr., J. Org. Chem., 59, 8239 (1994).
7. J. G. Pimblott, G. Scott and J. E. Stuckey, J. Appl. Polym. Sci., 19, 865 (1975).
8. S. K. Mandal, R. N. Datta and D. K. Basu, Rubber Chem. Technol., 62, 569 (1989).
9. K. Sasse, "Methoden der Organischen Chemie", Georg Thieme Verlag, Stuttgart, 4th, 1964.
10. J. H. Bartlett, H. W. Rudel and E. B. Cyphers (to Esso Research & Engineering Co.), US Pat. 2705694

Chapter 4

The influence of silane sulphur- and carbon rank on processing of a silica reinforced tyre tread compound[#]

The effect of the sulphur rank (4-0) and of the carbon rank (2-10) of equivalents of bis(triethoxysilylpropyl) tetrasulphide TESPT as coupling agents for silica-reinforced tyre tread compounds, is the subject of this study. The coupling agents are added in quantities equimolar to TESPT. Sulphur correction for lower sulphur ranks than TESPT is performed either in the final mixing step or in the first mixing step in an internal mixer.

Without sulphur correction the silanes studied show a marked difference in processing as well as in the final properties of the rubber. When sulphur correction is made in the final mix together with the addition of vulcanisation ingredients, all sulphur-containing silanes behave more like TESPT. The disulphide (TESPD) shows final properties similar to those of TESPT; the mixing behaviour shows improved scorch safety. This is lost when sulphur correction is applied in the first mix.

Sulphur-free silanes do not react on sulphur correction during processing and show only a slight improvement in mechanical properties. A silane without sulphur, having a carbon rank of 10 (DTES) shows the best processing, although final mechanical properties are inferior to TESPT.

4.1 Introduction

It is commonly understood in rubber technology that mechanical properties of rubber compounds, such as tensile strength and tear strength, wear resistance, hysteretic loss and resilience, are greatly improved by the inclusion of reinforcing fillers such as carbon black and silica. These differ from non-reinforcing fillers in their specific primary particle and aggregate sizes, their spatial morphology, or "structure", and their surface characteristics – the occurrence of functional groups and resultant surface free energy.[1] Optimal reinforcing power can be achieved only if the filler is well dispersed in the rubber matrix. The chemical or physical interaction between the filler and the rubber is a further important factor in the reinforcing effect. Traditionally, various carbon blacks have been used as reinforcing fillers.[2] However, the use of silica as a filler in rubber affords a number

[#] Parts of the work described in this Chapter have been published: J.W. ten Brinke, L.A.E.M. Reuvekamp, P.J. van Swaaij, and J.W.M. Noordermeer, Kautsch. Gummi Kunstst. 55, 244 (2002).
The work described in this Chapter has been accepted for publication in Rubber Chem. Technol.

of advantages over carbon black in terms of properties. In tyre treads, silica provides a lower rolling resistance than carbon black at equivalent wear resistance and wet traction.[3,4]

Rubber and carbon black, both being hydrophobic substances, are generally easy to mix. But in the case of silica, hydrogen bond interactions between surface silanol groups in agglomerates are very strong by comparison with the potential interactions between the polar siloxane or silanol groups and the commonly non-polar olefinic hydrocarbon rubbers. These hydrogen bond interactions make it very difficult to mix silica with rubber. Bifunctional organosilane coupling agents are commonly used to chemically modify the surface of the silica in order to enhance interaction with hydrocarbon rubbers. Remarkable improvements in the mechanical properties of the silica-reinforced rubber vulcanisates are obtained, such as improvements in the Young's modulus, tensile strength and elongation at break, lower tan δ at 60 °C and consequently lower heat build-up in the tyre.[5,6]

In normal practice the silica, coupling agent and rubber are introduced simultaneously into the internal mixer. A number of chemical reactions are initiated during mixing:
- bonding of the organosilane to the silica surface;
- reaction between the organosilane and the rubber polymer.

The organosilane coupling agents which are currently most widely used for tyre applications are bis(triethoxysilylpropyl) tetrasulphide (TESPT) (Silquest® A-1289 from OSi Specialties Group/ Crompton Corporation or Si-69® from Degussa AG) and, to a lesser extent, 3-mercaptopropyl triethoxysilane (MPTES).[7,8] Originally TESPT was developed as a curing agent,[9] and in combination with accelerators such as tetramethylthiuram disulphide (TMTD) and N-cyclohexyl-2-benzothiazole sulphenamide (CBS) TESPT crosslinks silica-containing rubbers without further addition of sulphur, at the same time solving mixing problems encountered with silica. Historically, industry has placed greater emphasis on the coupling role of TESPT because of the greater ease of mixing when it is used for such silica-reinforced systems. But with additional experience the realisation came that the cure properties of TESPT must also be considered.[10-22]

The specific reaction of TESPT with silica has been studied by *Görl et al*.[18,23], who concluded that initially a single bond with the silica surface is formed between one ethoxysilyl group of the coupling agent and a silanol group of the silica (primary reaction). This primary reaction is commonly understood to be followed by further condensation reactions between pairs of neighbouring silane molecules which are already bound to the silica surface (secondary reaction). The primary reaction of the coupling agent during mixing is relatively slow at moderate temperatures of, for example, 120 °C, which poses a problem since this temperature is often employed as the dump temperature. In order to achieve shorter reaction times higher batch temperatures are needed. At these elevated temperatures, on the other hand, a third reaction – between the coupling agent and the rubber – is prone to occur, giving rise to scorch problems.[24]

Depending on time and temperature, TESPT can disproportionate into a mixture of polysulphides whose sulphur chain lengths vary from two to eight sulphur atoms. Whether this disproportionation reaction occurs during mixing or later in processing apparently has little effect on the efficiency of TESPT as a coupling agent.[3] It is therefore worth addressing the question whether the tetrasulphide group of TESPT is the optimal sulphur rank, or whether other (lower) sulphur ranks give comparable or even better performance.[25-27] The present paper concentrates on the reaction of the coupling agent with the rubber matrix, and investigates the effect of the sulphur rank of the silane on both processing and dynamic and mechanical properties, using a typical “green tyre” tread compound. Also sulphur-free silanes, varying in carbon chain-length between the silyl-groups are included for further elucidation of the mechanism involved in the function of the coupling agent.

4.2 Experimental

4.2.1 Materials

The compounds for the experiments contained: SBR solution (Buna® VSL 5025 HM, Bayer AG) composed of 75% butadiene with a 50% vinyl content, and 25% styrene, extended with 37.5 phr aromatic oil, with a Mooney viscosity ML (1+4) 100 °C of 65; BR (Kosyn® KBR 01, Korea Kumho Petrochemical Co. Ltd.) with a cis content of >96% and a Mooney viscosity ML (1+4) 100 °C of 44; silica (Zeosil® 1165 MP, Rhodia); aromatic oil (Enerflex® 75, BP Oil Europe); stearic acid (Merck); zinc oxide (Merck); sulphur (J.T. Baker); N-cyclohexylbenzthiazole-2-sulphenamide (CBS) (Santocure® CBS, Flexsys B.V.); diphenyl guanidine (DPG) (Perkacit® DPG, Flexsys B.V.).

The silane coupling agents used were:
Bis(triethoxysilylpropyl) tetrasulphide (TESPT) (Silquest® A-1289, OSi Specialties Group/ Crompton Corporation), Bis(triethoxysilylpropyl) disulphide (TESPD) (Silquest® A-1589, OSi Specialties Group/ Crompton Corporation), Bis(triethoxysilylpropyl) monosulphide (TESPM), 3-Mercaptopropyl triethoxysilane (MPTES) (Silquest® A1891, OSi Specialties Group/ Crompton Corporation), Bis(triethoxysilyl) ethane (ETES) (Gelest Inc., ABCR GmbH & Co), Bis(triethoxysilyl) hexane (HTES), Bis(triethoxysilyl) decane (DTES) . The silanes with their respective chemical structures and sulphur ranks are listed in Table 4.1. TESPM, HTES and DTES were synthesised as described below:

TESPM
3-Mercaptopropyl triethoxysilane (7.69 g) was reacted slowly with sodium (0.74 g) in diisopropyl ether (50 ml). When the sodium reaction was completed 3-chloropropyl triethoxysilane (7.77 g) was added dropwise. The reaction mixture was extracted with water to remove the sodium chloride. After evaporation of the diisopropyl ether, the reaction product was purified by vacuum distillation, giving TESPM (8.9 g, yield 62%) with a boiling point of 160 °C at 0.05 mm Hg. The structure was confirmed by ^{1}H-NMR (300 MHz, $CDCl_3$) δ 3.83 (q, 12H), 2.52 (t, 4H), 1.80 (m, 4H), 1.22 (t, 18H), 0.74 (t, 4H).

Table 4.1 Chemical structures of the silane coupling agents with their corresponding sulphur ranks as determined by elemental analysis.

Component	Sulphur rank
bis(triethoxysilylpropyl) tetrasulphide (TESPT) 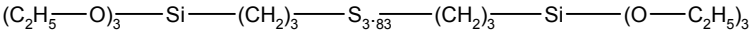	3.8
bis(triethoxysilylpropyl) disulphide (TESPD) 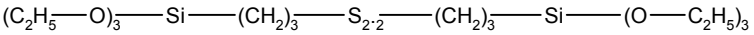	2.2
bis(triethoxysilylpropyl) monosulphide (TESPM) 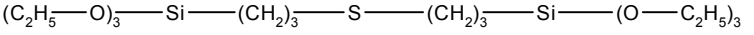	1.0
bis(triethoxysilyl) ethane (ETES) 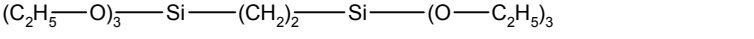	0
bis(triethoxysilyl) hexane (HTES) 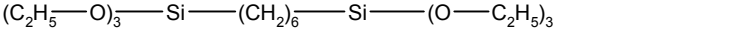	0
bis(triethoxysilyl) decane (DTES) 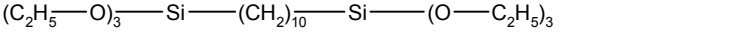	0
3-mercaptopropyl triethoxysilane (MPTES) 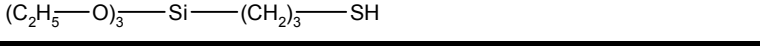	1.0

HTES

HTES was synthesised by hydrosilation of 1,5-hexadiene. A mixture of triethoxysilane (50.63 g), 1,5-hexadiene (12.97 g) and a platinum cyclovinylmethylsiloxane catalyst in 65 ml toluene was stirred under a dry nitrogen flow for 48 hours. Vacuum distillation gave HTES (53.7 g, yield 85%) with a boiling point of 150°C at 0.05 mm Hg. The structure was confirmed by ^{1}H-NMR (300MHz, $CDCl_3$) δ 3.83 (q, 12H), 1.40 (m, 8H), 1.22 (t, 18H), 0.62 (t, 4H).

DTES

DTES was synthesised by hydrosilation of 1,9-decadiene. A mixture of 38.77 g of triethoxysilane, 16.34 g of 1,9-decadiene and a platinum-cyclovinyl-methyl-siloxane catalyst in 100 ml toluene was stirred under a dry N_2 flow for 48 hours. Vacuum distillation gave 36.3 g (yield of 66 %), of DTES with a boiling point of 155-160 °C at 0.05 mm Hg. The structure was confirmed by ^{1}H-NMR (300MHz, $CDCl_3$) δ 3.83 (q, 12H), 1.40-1.22 (m, 16H), 1.22 (t, 18H), 0.62 (t, 4H).

4.2.2 Compound recipes

The experiments were based on a reference tyre tread composition which is shown in Table 4.2 and represents a common “green tyre” recipe in accordance with the Michelin patent.[28] The compound contains 7 phr TESPT and 1.4 phr sulphur. As the molar masses of the various coupling agents used in this study differ from that of TESPT, the quantities of the other coupling agents were adjusted at the outset to represent equimolar quantities. MPTES was added in double molar quantities, because this molecule corresponds to only half a molecule of TESPT. Because the sulphur ranks of these coupling agents also differ from that of TESPT, the sulphur

level in the recipes may also then be adjusted to represent equimolar sulphur levels. Consequently, the two main series were divided in three series of compounds:

- Series I: with equimolar quantities of coupling agents, but without sulphur correction;
- Series II: representing equimolar quantities of coupling agents and equimolar quantities of sulphur in relation to the reference recipe containing TESPT, the extra sulphur added in the last mixing step during the addition of vulcanisation ingredients on the two-roll mill;
- Series III: the same as Series II, but with the extra sulphur already added together with the silane coupling agents during the first mixing step in the internal mixer.

Table 4.2a Tyre tread recipe (phr) with the various coupling agents investigated for Series I.

Component	Reference recipe **I**a	**I**b	**I**c	**I**d	**I**e	**I**f	**I**g
Brabender mixing step 1 + 2							
S-SBR	75.0	75.0	75.0	75.0	75.0	75.0	75.0
BR	25.0	25.0	25.0	25.0	25.0	25.0	25.0
ZnO	2.5	2.5	2.5	2.5	2.5	2.5	2.5
Stearic acid	2.5	2.5	2.5	2.5	2.5	2.5	2.5
Silica	80.0	80.0	80.0	80.0	80.0	80.0	80.0
Aromatic oil	32.5	32.5	32.5	32.5	32.5	32.5	32.5
TESPT	7.0	-	-	-	-	-	-
TESPD	-	6.3	-	-	-	-	-
TESPM	-	-	5.8	-	-	-	-
ETES	-	-	-	4.6	-	-	-
HTES	-	-	-	-	5.4	-	-
DTES	-	-	-	-	-	6.1	-
MPTES	-	-	-	-	-	-	6.2
Sulphur	-	-	-	-	-	-	-
Mill mixing step							
CBS	1.7	1.7	1.7	1.7	1.7	1.7	1.7
DPG	2.0	2.0	2.0	2.0	2.0	2.0	2.0
Sulphur	1.4	1.4	1.4	1.4	1.4	1.4	1.4
Total	229.6	228.9	228.4	227.2	228.0	228.7	228.8

Table 4.2b Tyre tread recipe (phr) with the various coupling agents investigated for Series II and III.

Component	IIb*/ IIIb	IIc*/ IIIc	IId*/ IIId	IIe*/ IIIe	IIf*/ IIIf	IIg*/ IIIg
Brabender mixing step 1 + 2						
S-SBR	75.0	75.0	75.0	75.0	75.0	75.0
BR	25.0	25.0	25.0	25.0	25.0	25.0
ZnO	2.5	2.5	2.5	2.5	2.5	2.5
Stearic acid	2.5	2.5	2.5	2.5	2.5	2.5
Silica	80.0	80.0	80.0	80.0	80.0	80.0
Aromatic oil	32.5	32.5	32.5	32.5	32.5	32.5
TESPT	-	-	-	-	-	-
TESPD	6.3	-	-	-	-	-
TESPM	-	5.8	-	-	-	-
ETES	-	-	4.6	-	-	-
HTES	-	-	-	5.4	-	-
DTES	-	-	-	-	6.1	-
MPTES	-	-	-	-	-	6.2
Sulphur	0.7	1.2	1.6	1.5	1.6	0.7
Mill mixing step						
CBS	1.7	1.7	1.7	1.7	1.7	1.7
DPG	2.0	2.0	2.0	2.0	2.0	2.0
Sulphur	1.4	1.4	1.4	1.4	1.4	1.4
Total	229.6	229.6	228.8	229.5	230.4	229.5

* For Series II the correcting amount of sulphur was added during the mill mixing step.

The recipes corresponding to these three series are all given separately in Table 4.2. The reference recipe containing TESPT, to which the various corrections naturally do not apply, was used as a reference in all three series.

4.2.3 Mixing

The compounds were mixed in three steps. For the first two mixing steps a type-350S Brabender Plasti-corder lab station internal mixer with a mixing chamber volume of 390 ml was used. The mixing procedure for the first two steps is shown in Table 4.3. The starting temperature was 50 °C and the cooling water was kept constant at 50 °C. The rotor speed was set to 100 rpm. The mixer fill factor was 63%. Silica, silane, oil and, for Series III, the sulphur correction were added in two doses, each of half the required quantity.

A problem encountered while adding the second half of the silica, silane and oil during the first mixing step was the tendency of the silica, being fluffy, to escape the downwards movement of the ram, a significant amount then coming to rest on top of the ram. It is time-consuming to sweep the ram while moving it up and down to ensure that all the silica reaches the mixing chamber. On the other hand, the torque of the Brabender Plasti-corder is limited to 400 Nm. If all the silica were to enter the chamber at once, the maximum torque would be exceeded. Experienced manipulation is consequently needed in order to add the silica as quickly as possible, while aiming for a mixer torque peak as close to 400 Nm as possible. In doing so, we tried to minimize the human factor.

Table 4.3 Mixing procedure of the first two steps (Brabender mixer)

Step 1:

Time (min.sec.)	Action
0.00	open ram; load polymers
0.20	close ram
1.20	open ram; add ½ silica, ½ silane, ½ oil, ZnO and stearic acid ½ correction of sulphur (Series III)
1.50	close ram
2.50	open ram; add ½ silica, ½ silane, ½ oil ½ correction of sulphur (Series III)
3.30	close ram
4.30	open ram (sweep)
4.45	close ram
6.45	dump compound

Step 2:

Time (min.sec)	Action
0.00	load compound
5.00	dump compound

The temperature of the compounds was measured online during mixing, using the thermocouple embedded in the discharge door of the mixer. The temperature measured at the end of the mixing step was taken as the dump temperature. It must be borne in mind that this temperature, measured at the interface of the compound and the steel chamber wall, is somewhat (approx. 10 °C) lower than the actual temperature of the compound. Using a pyrometer, attempts were made to measure the dump temperature more accurately by sensing the temperature of the dumped compound, but this did not lead to a more reliable value and was further discarded. The rotor speed and mixing time were selected such as to obtain an average dump temperature of between 140 and 155 °C.

After both mixing steps the compounds were sheeted out on a Schwabenthan 100 ml two-roll mill. Accelerators and sulphur were added in a third mixing step on the same two-roll mill at a temperature setting of about 40 °C.

4.2.4 Compound viscosity and cure properties

The compound Mooney viscosity ML (1+4) at 100 °C was measured by a 2000 E Mooney viscometer from Alpha Technologies. The cure properties of the compounds were determined using an RPA 2000 dynamic mechanical rheological tester from Alpha Technologies at a temperature of 160 °C and a strain of 2.79% during a 30-minute test cycle. The compounds were cured using a WLP 1600/5*4/3 Wickert laboratory press at 160 °C and 100 bar pressure, for a period corresponding to $t_c(90)$ of the specific compound. The dimensions of the cured specimens were 90 x 90 mm x 2 mm thick.

4.2.5 Mechanical characterisation

Dynamic mechanical measurements on the still uncured compounds were taken with the RPA 2000 tester from Alpha Technologies at 100 °C and a frequency of 0.500 Hz. Mechanical characterisation of the cured compounds was performed using a Zwick Z020 tensile tester in accordance with ISO 37.

The loss tangent was measured with the RPA 2000 at 60 °C, 3.49% strain and a frequency of 15 Hz, after first curing the compound in the RPA at 160 °C for $t_c(90)$ and subsequent cooling to 60 °C.

4.3 Results

Series I and II versus Series III in Brabender mixing step 1

The Series I and II recipes employed for the mixing steps in the Brabender mixer are essentially the same, because for Series II the correction for sulphur was made only during the third, mill mixing step. Their mixing behaviours will be discussed together in this first section and compared with Series III.

The seven different silanes studied in these series clearly differ in mixing behaviour, as can be seen in Figure 4.1: mixer torque vs. time for the first mixing step. The thickest line applies to recipe Ia, which represents the reference "green tyre" compound containing TESPT. This line coincides within experimental scatter with the curve for compounds Ie / IIe (HTES). The medium-thick line applies to recipes Ig / IIg which represent the compound containing MPTES and forms a group with the curves for the compounds containing ETES, TESPD and TESPM. These lines differ from the others, especially following dosage of the second half of the silica, silane and oil. The most conspicuous difference, however, is in the mixer torque during the later stages of the mixing step: the compounds containing TESPT and HTES absorb significantly lower torques/energies than the TESPD, TESPM, MPTES and ETES containing compounds. The compounds If / IIf (DTES) shows the lowest energy consumption of all compounds.

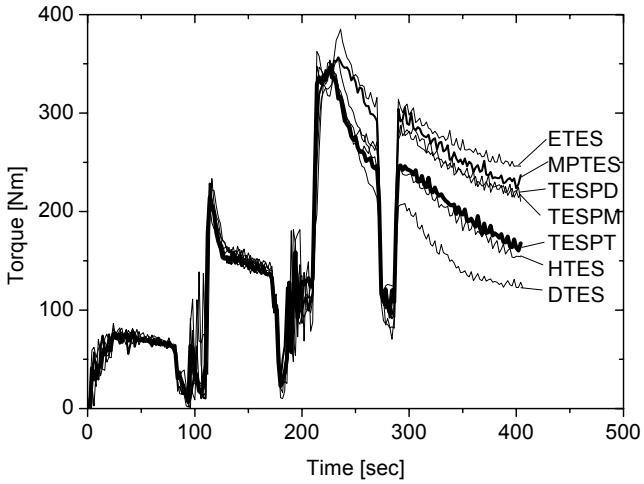

Fig.4.1: Torque vs. mixing time during the first mixing step for Series I and II together: lowest curve: DTES; intermediate two curves: TESPT (= ▬) and HTES; upper four curves: TESPD, TESPM, ETES and MPTES (= ▬).

In Figure 4.2 the mixer torques vs. time are shown for Series III in the first Brabender mixing step. It can be clearly seen that the addition of corrective quantities of sulphur relative to the sulphur contained in TESPT brings the curves for the compounds containing TESPD and TESPM down to the same level as for TESPT. The curve for MPTES (medium-thick line) first drops to approximately the same level as TESPT before starting to climb again after 350 s. Further evidence will show that this is the result of scorch, a familiar occurrence with MPTES under these conditions.[3] The curves for the compounds containing ETES, HTES and DTES are not influenced at all by the addition of corrective amounts of sulphur.

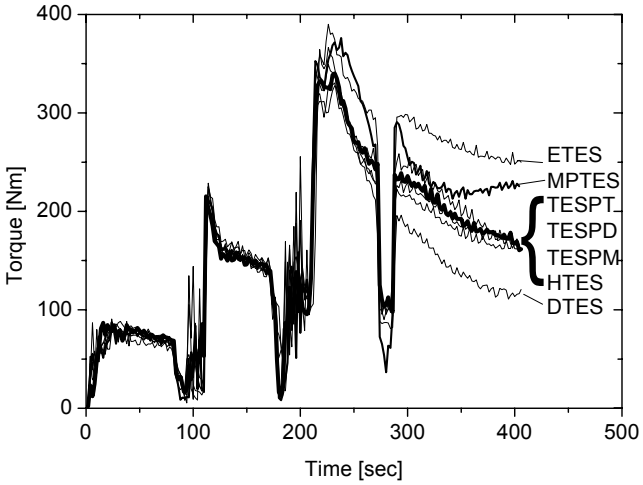

Fig. 4.2: Torque vs. mixing time during the first mixing step for Series III: lowest curve: DTES; intermediate four curves: TESPT (= ▬), TESPD, TESPM and HTES; upper curves: ETES and MPTES (= ▬).

The torque during the final stages of mixing is commonly understood to decrease as a result of reduced batch viscosity, which is in turn due to an increasing batch temperature and improved dispersion of the filler into the rubber matrix. Unfortunately, it is very difficult to separate these two effects in terms of the heat balance of the mixing process. The breakdown of silica agglomerates and the shielding of their hydrophilic surfaces by the reaction with the coupling agents lead to less filler-filler interaction, resulting in a decrease in the compound viscosity and consequently a lower mixer torque. On the other hand, the lower mixer torque also results in less viscous dissipation and consequently less heat generation. This in turn keeps the batch temperature lower, resulting again in a higher viscosity. It is not at all obvious which of the two counteracting effects eventually prevails.

The mixing energies and dump temperatures for these compounds, as listed in Table 4.4, are an aid to understand the results shown in Figures 4.1 and 4.2. The compounds which follow the higher torque vs. time curve consume about 10 – 20% more mixing energy than TESPT. The compound containing DTES, which follows

the lowest torque vs. time curve consumes about 12% less mixing energy than TESPT. A lower mixing energy generally corresponds to a lower dump temperature.

Table 4.4 Characteristics of Brabender mixing.

Compound	First mixing step		Second mixing step	
	Energy [kJ/g]	Dump temp. [°C]	Energy [kJ/g]	Compound Mooney after 2nd step ML (1+4) 100°C
Ref. **I**a	1.91	144	1.39	50.2
Ib / **II**b	2.02	151	1.32	45.6
Ic / **II**c	2.07	155	1.34	46.1
Id / **II**d	2.18	168	2.03	103.9
Ie / **II**e	1.89	147	1.35	47.1
If / **II**f	1.66	130	1.18	39.8
Ig / **II**g	2.13	155	1.38	51.4
IIIb	1.94	141	1.28	45.7
IIIc	1.90	144	1.51	57.0
IIId	2.23	169	2.09	202.4
IIIe	1.92	142	1.52	55.5
IIIf	1.64	130	1.22	42.6
IIIg	2.07	150	1.53	78.2 (scorch)

Strain sweep measurements as an indicator of silica dispersion for Series I and II versus Series III, after Brabender mixing step 1

As a first indicator of the degree of dispersion obtained in this first mixing step, strain sweep measurements were taken on the compounds in the RPA 2000 at 100 °C and 0.500 Hz. Results are given in Figures 4.3a-c and 4.4a-c for storage modulus G', loss modulus G" and tan δ of Series I / II and III, respectively. Insufficient compound was available for additional measurement of the compound Mooney viscosities. Such curves are then commonly interpreted in terms of the so-called Payne effect[29]: the poorer the dispersion of the reinforcing filler, the more pronounced the difference in G' between low and high strain. One then assumes that the G' at low strain values is a measure of filler dispersion and of the degree of filler-filler interaction (filler networking): the lower the G' at low strain, the better the filler dispersion and the lower the filler-filler interaction.

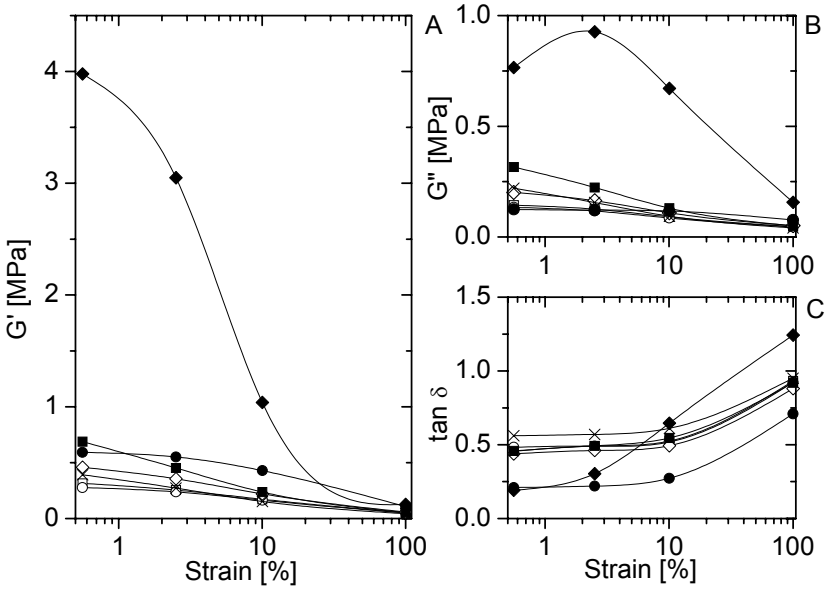

Fig.4 3: a: G' modulus against strain for Series I and II after the first mixing step;
b: G" modulus against strain for Series I and II after the first mixing step;
c: tan δ against strain for Series I and II after the first mixing step.
□ = TESPT; ○ = TESPD; ◊ = TESPM; ◆ = ETES; ■ = HTES; × = DTES; ● = MPTES.

The results in Figure 4.3a indicate that compound Ia containing TESPT shows the lowest storage modulus G' at low strain and consequently the lowest Payne effect. For TESPT this is an indication of optimal dispersion or shielding of the silica surface and therefore seems to be the reason for the low mixer torque in Figure 4.1. MPTES, TESPD, DTES and HTES all show an intermediate dispersion or relatively low filler-filler interaction, although they show great differences in Figure 4.1. Compound Id / IId (ETES) shows an exceptional Payne effect, corresponding to the highest mixer torque curve in Figure 4.1. Figures 4.3b and c (G"-modulus and tan δ) confirm this behaviour, but contribute no additional information regarding the dispersion.

The results in Figure 4.4a-c for the compounds corrected for sulphur in the mixer differ from those in Figure 4.3a-c for two compounds. Compound IIIb (TESPD) now behaves virtually as Ia (TESPT), thus confirming that the corrective quantity of sulphur causes TESPD to behave identically to TESPT, as in Figure 4.2. Compound IIIc (TESPM) does not change relative position, despite the lowering of the mixer torque curve in Figure 4.2 by the addition of the corrective quantity of sulphur. Compounds IIId (ETES), IIIe (HTES) and IIIf (DTES) also have not changed relative to the curves Id / IId, Ie / IIe and If / IIf, respectively.

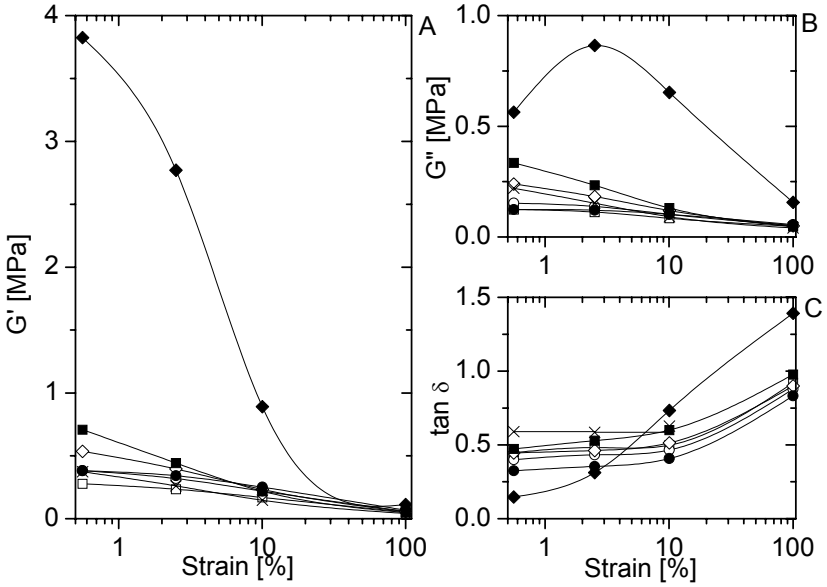

Fig. 4.4: a: G' modulus against strain for Series III after the first mixing step;
b: G" modulus against strain for Series III after the first mixing step;
c: tan δ against strain for Series III after the first mixing step.
□ = TESPT; ○ = TESPD; ◊ = TESPM; ◆ = ETES; ■ = HTES; × = DTES; ● = MPTES.

Compound IIIg (MPTES), shows a strong change with higher moduli at low and intermediate strains relative to its counterparts Ig/IIg without sulphur correction. This is an indication of scorch during the first mixing step of this coupling agent. As a result of network formation G' increases and, while G" does not change, tan δ decreases: Figure 4.4c. A closer look at Figures 4.3 and 4.4 now shows, that the G'-curves for compounds with sulphur-containing coupling agents have a convex curvature similar to the compounds containing MPTES, while concave for the compounds with sulphur-less coupling agents. TESPM and ETES take an intermediate position. This is a first indication, that all sulphur-containing coupling agents to a larger or smaller extent show scorch- or vulcanisation-reactions between the rubber polymers and the silica particles.

Temperature sweep measurements as an indicator of scorch sensitivity for Series I and II versus series III, after Brabender mixing step 1

Temperature sweep measurements (110 - 200 °C) were performed on the compounds in the RPA 2000 at 0.500 Hz and 49.94% strain (away from the Payne effect range), as an indicator of the scorch sensitivity of the various coupling agents. Results of G' vs. temperature are given in Figures 4.5 and 4.6. Compound Ia containing TESPT shows a marked increase in G' at temperatures above 160 °C. The origin of this increase has been studied in detail by Reuvekamp et

al.[30] and has been shown to result from crosslinking due to sulphur donated by TESPT in combination with the accelerator functionality of TESPT.[9] The TESPD, TESPM, ETES, HTES and DTES of Series I and II do not show this increase in G' at high temperatures, or only show it to a limited extent, apparently because no sulphur is available to be donated to the compounds. The overall high curve for the compound Id containing ETES and its gradual decrease with temperature corresponds to the high G' already seen in Figure 4.3, and the absence of scorch effects. The G' for compounds Ig / IIg containing MPTES is higher over the entire temperature range (except for the highest temperature relative to TESPT). This indicates that MPTES indeed causes scorch, even at temperatures as low as 110 °C, and even in the absence of free sulphur. This scorch effect of MPTES must therefore be responsible for the highest mixer torque occurring after dosage of the second half of the silica, silane and oil in the Brabender mixing step for compound Ig / IIg.

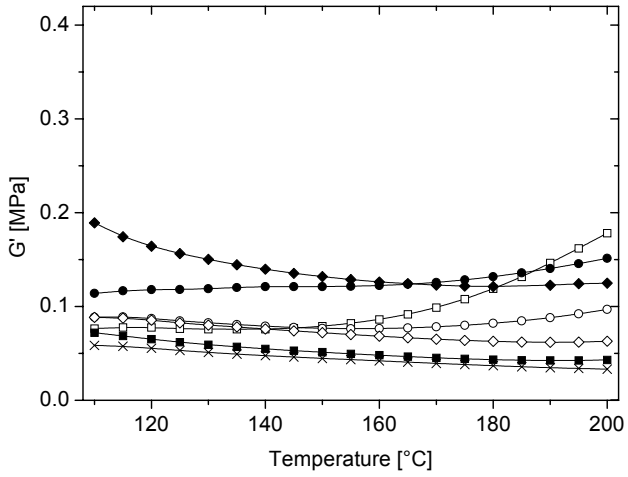

Fig. 4.5: G' modulus against temperature for Series I and II; □ = TESPT; ○ = TESPD; ◊ = TESPM; ◆ = ETES; ■ = HTES; × = DTES; ● = MPTES.

In the case of Series III the temperature-dependence of G' is distinctly different from that of Series I and II; see Fig. 4.6. In the presence of the corrective quantity of sulphur in the first Brabender mixing step, MPTES gives rise to far more scorch in the mixer even than without extra sulphur. This also has already been reflected in the strain sweep measurements (Fig. 4.4a-c). All the other compounds show similar scorch behaviour to TESPT at temperatures above 150 °C. Only for ETES, HTES and DTES it is delayed slightly until the temperature reaches 170 °C. It is surprising to see that TESPD and TESPM in the presence of corrective quantities of free sulphur behave essentially identically to the TESPT-containing reference compound.

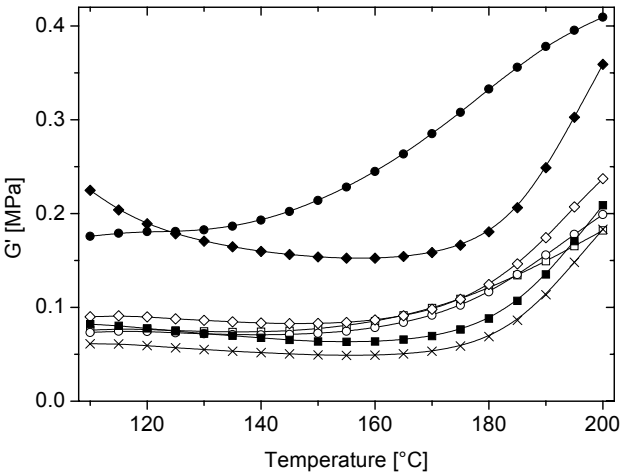

Fig.4.6: G' modulus against temperature for Series III; □ = TESPT; ○ = TESPD; ◊ = TESPM; ◆ = ETES; ■ = HTES; × = DTES; ● = MPTES.

Results of Brabender mixing step 2 for all series

The mixing energies in the second mixing step do not differ significantly between any of the compounds in Series I and II and their corresponding compounds in Series III (Table 4.4). For Series III the compounds c, e and g show a higher mixing energy when compared with compounds c, e and g in Series I / II. For compound IIIg (MPTES) this higher mixing energy in the presence of corrective amounts of sulphur is now obviously the result of its scorch effect, which is also indicated by the distinctly higher Mooney ML (1+4) 100 °C for this compound. Compounds IIIc and IIIe with TESPM and HTES, respectively, also show a significantly higher compound Mooney viscosity, which corresponds with the higher mixing energy. Although no clear signs of scorch emerged in the earlier experiments for these compounds, Fig. 4.6 shows that TESPM and HTES in the presence of free sulphur at the highest temperatures tend to show slightly more scorch behaviour than TESPT and TESPD. The extremely high mixing energies for the compounds containing ETES result in impracticably high Mooney viscosities and confirm the observations in earlier experiments.

Curing behaviour of all series

The shape of the rheometer curve of a silane coupling agent containing silica-reinforced compound differs significantly from the shape of a carbon black-reinforced compound, as can be seen in Figs. 4.7 – 4.9 for Series I – III. A "normal" rheometer torque curve passes through a minimum at the beginning of the test cycle before curing starts, owing to heating of the compound. After this minimum the rheometer torque increases with crosslinking and more or less levels off in a plateau, when vulcanisation is complete. For the silica-reinforced compounds the rheometer curve usually consists of two distinct regions, separated by a shoulder, sometimes even a second plateau. The first increase in torque is often interpreted as a sign of filler flocculation: demixing of the silica at a rate much faster than the

formation of the polymer network during vulcanisation.[31] Another explanation is that this is a sign of two different curing processes, separated in time, are at work, more in the case of TESPM, ETES, HTES and DTES than for TESPT and TESPD. All the compounds contain the same amount of curing additives and – as a first assumption – the accelerating effects of these curatives are not expected to be influenced significantly by the particular coupling agent. TESPM, ETES, HTES and DTES contain little or no sulphur in the molecule, and it therefore seems highly unlikely that this affects curing significantly.

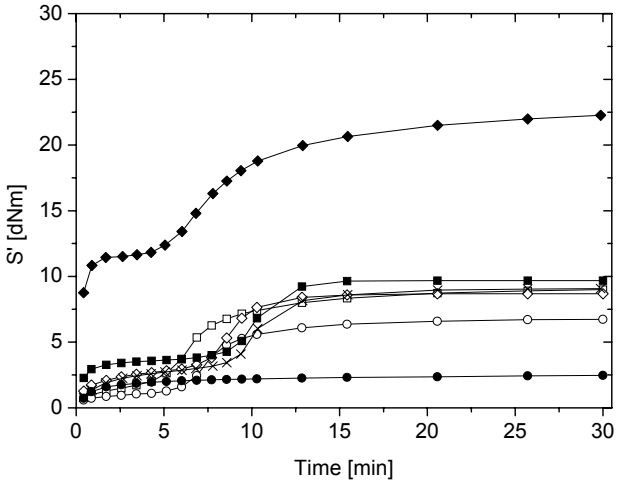

Fig .4.7: Rheometer curves for Series I; □ = TESPT; ○ = TESPD; ◊ = TESPM; ◆ = ETES; ■ = HTES; × = DTES; ● = MPTES.

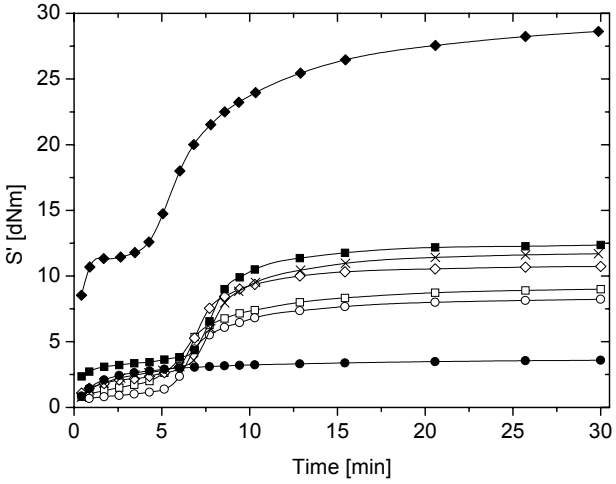

Fig .4.8: Rheometer curves for Series II; □ = TESPT; ○ = TESPD; ◊ = TESPM; ◆ = ETES; ■ = HTES; × = DTES; ● = MPTES.

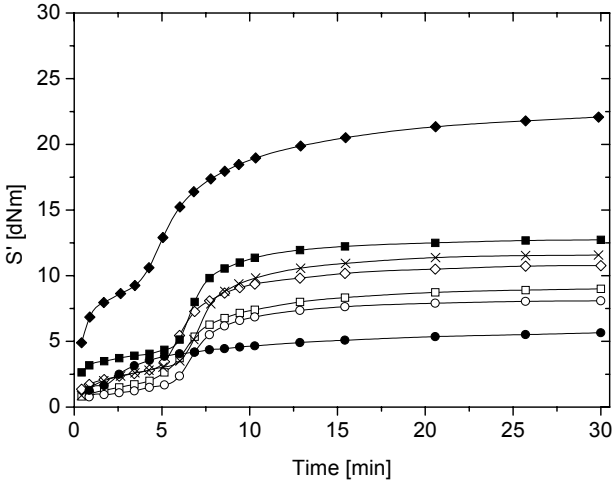

Fig. 4.9: Rheometer curves for Series III; □ = TESPT; ○ = TESPD; ◊ = TESPM; ◆ = ETES; ■ = HTES; × = DTES; ● = MPTES.

From the curing properties as derived from Figs. 4.7 – 4.9 and listed in Table 4.5 it can be seen that there is also a difference in $\Delta S' = S'_{max} - S'_{min}$ for the different compounds. When the corrective quantity of sulphur is added, the $\Delta S'$ is always higher than in the corresponding compounds of Series I where no additional sulphur was added, as might be expected. However, it is surprising that the addition of the corrective quantity of sulphur either on the two-roll mill or in the

internal mixer no longer makes a difference, while in the earlier experiments described in this paper differences between these two series were quite conspicuous. A further comparison of $\Delta S'$ between the various compounds is not feasible. $\Delta S'$ is strongly dependent on S'_{min} as determined to a large extent by the silica dispersion. The differences in S'_{min} are in good agreement with the degree of filler-filler interaction, shown in Figs. 4.3 and 4.4. The effect of crosslink formation on $\Delta S'$ cannot unequivocally be separated from the silica dispersion. The compounds containing MPTES show poor vulcanisation behaviour, which is obviously due to impairment by early scorch in the mixing operation.

Table 4.5 RPA 2000 rheometer data.

Sample	S'_{min} [dNm]	S'_{max} [dNm]	$S'_{max} - S'_{min}$ [dNm]	$t_c(02)$ [m.m]	$t_c(10)$ [m.m]	$t_c(90)$ [m.m]	$t_c(95)$ [m.m]
Ia	0.54	9.02	8.48	0.48	2.45	13.94	18.26
Ib	0.43	6.77	6.34	0.59	4.21	13.14	16.70
Ic	0.62	8.73	8.11	0.25	0.81	11.00	12.44
Id	2.46	22.26	19.8	0.13	0.19	13.82	19.40
Ie	0.84	9.72	8.88	0.18	0.37	11.99	13.08
If	0.49	9.07	8.58	0.30	0.87	13.12	15.70
Ig	0.49	2.48	1.99	0.25	0.41	12.82	18.52
IIb	0.39	8.24	7.85	0.79	4.80	13.44	17.38
IIc	0.56	10.72	10.16	0.32	1.54	11.46	14.22
IId	2.24	28.63	26.39	0.14	0.22	14.15	19.10
IIe	0.78	12.40	11.62	0.20	0.51	12.20	15.48
IIf	0.50	11.70	11.20	0.36	1.24	13.51	16.84
IIg	0.48	3.62	3.14	0.27	0.44	11.78	17.80
IIIb	0.45	8.15	7.70	0.55	3.76	12.88	16.84
IIIc	0.69	10.86	10.17	0.28	1.18	12.48	16.76
IIId	1.69	22.08	20.39	0.15	0.29	13.56	18.58
IIIe	0.97	12.79	11.82	0.18	0.42	11.10	14.64
IIIf	0.53	11.59	11.06	0.31	1.08	12.52	16.18
IIIg	1.07	5.7	4.63	0.50	1.57	17.24	22.79

Because of the abnormal rheometer curve shapes at short curing times, it is difficult to derive significant information from scorch times such as $t_c(2)$ or $t_c(10)$. Visual comparison of Figs. 4.7 – 4.9 shows that particularly the point at which the main increase in S' takes place is different for the various coupling agents but is also dependent on whether and when correcting sulphur was added. In Series I, Fig. 4.7, the main increase in S' is delayed by about 2.5 min, in the case of the compounds containing TESPD, TESPM, HTES and DTES, relative to the reference compound with TESPT. In Series II with the sulphur correction made during the addition of the other vulcanisation ingredients this delay is compensated for all silanes: the increase in S' occurs at the same moment, except for ETES which shows an earlier increase in S'. But if the sulphur correction is already made in the first mixing stage, a further shift to earlier times takes place for the compounds containing TESPM, ETES, HTES and DTES, while the compound with TESPD does not change position relative to TESPT. $t_c(90)$ varies little when corresponding compounds in the three series are compared, again with the exception of MPTES. The differences in $t_c(90)$, if any, are at their most conspicuous, but are still minor, within one series as a function of the particular coupling agent used.

Tensile properties of cured compounds

The tensile properties of the compounds were measured after curing at 160 °C for a period corresponding to $t_c(90)$ of the specific compound. The results for the Series I, II and III, respectively, are shown in Figs. 4.10 – 4.12. Corresponding values for the E-modulus, stress at 100% strain (M_{100}), stress at 300% strain (M_{300}), tensile strength and strain at break are summarised in Table 4.6.

Table 4.6 Mechanical properties of cured compounds.

Sample	E-Modulus [MPa]	σ_{break} [MPa]	ε_{break} [%]	M_{100} [MPa]	M_{300} [MPa]	$\frac{M_{300}}{M_{100}}$	tan δ 60 °C	S' 60 °C [dNm]	S" 60 °C [dNm]
Ia	9.9	14.9	426	1.7	9.2	5.4	0.15	17.0	2.9
Ib	7.4	13.9	467	1.2	7.1	5.9	0.18	14.4	2.3
Ic	11.4	13.1	614	0.9	4.3	4.8	0.23	17.7	3.2
Id	7.0	10.4	782	0.6	2.1	3.5	0.16	31.6	5.1
Ie	10.9	10.2	793	0.6	1.6	2.7	0.25	19.3	3.8
If	9.7	10.6	764	0.6	1.6	2.7	0.24	14.1	3.3
Ig	1.6	11.8	453	0.9	5.7	6.3	0.17	8.8	0.9
IIb	10.0	14.8	404	1.7	10.0	5.9	0.16	13.4	2.1
IIc	15.3	13.6	491	1.4	7.0	5.0	0.20	16.7	3.4
IId	18.0	12.1	560	1.2	5.0	4.2	0.13	32.0	4.1
IIe	15.6	10.5	585	0.9	3.3	3.7	0.22	17.7	3.9
IIf	15.5	10.3	571	0.9	3.0	3.3	0.20	17.1	3.3
IIg	2.4	13.3	347	1.4	10.3	7.4	0.14	6.6	0.9
IIIb	10.1	16.1	487	1.5	8.3	5.5	0.16	12.5	2.3
IIIc	12.8	15.3	483	1.6	8.2	5.1	0.18	15.8	3.6
IIId	12.9	12.2	417	1.4	7.4	5.3	0.13	36.0	4.7
IIIe	14.8	12.5	602	1.0	3.9	3.9	0.20	15.8	3.9
IIIf	13.5	9.8	557	0.9	3.1	3.4	0.19	16.7	3.3
IIIg	3.1	12.0	209	2.9	-	-	0.10	5.8	1.0

For Series I all the compounds show different behaviour. TESPT (Ia) and TESPD (Ib) show the highest tensile strength, with TESPD having a somewhat greater strain at break. The value for the ratio M_{300}/M_{100} is quoted as an alternative measure of coupling efficiency according to Rauline.[28] Compound Ig with MPTES shows the highest value, in spite of its scorchiness in earlier processing steps. Of the other compounds TESPD (Ib) comes out best. Looking at the overall shape of the curves, the higher elongation at break of compound Ib with TESPD makes it preferable to the reference compound Ia, despite the lower curve for TESPD compared with TESPT.

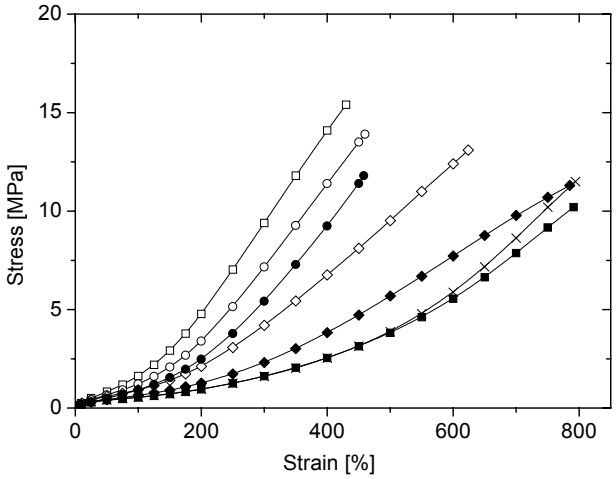

Fig. 4.10:Stress-strain curves for Series I; □ = TESPT; ○ = TESPD; ◊ = TESPM; ◆ = ETES; ■ = HTES; × = DTES; ● = MPTES.

Correction for sulphur on the two-roll mill generally leads to curves moving closer to the curves for the TESPT-containing reference compounds: TESPT, TESPD and even MPTES coincide, as seen in Fig. 4.11. MPTES (IIg) only has a somewhat lower stress at break. TESPM (IIc), ETES (IId), HTES (IIe) and DTES (IIf) also show a higher stress at break relative to their counterparts, which were not corrected for sulphur. The value for M_{300}/M_{100} also increased for all four compounds: Table 4.6.

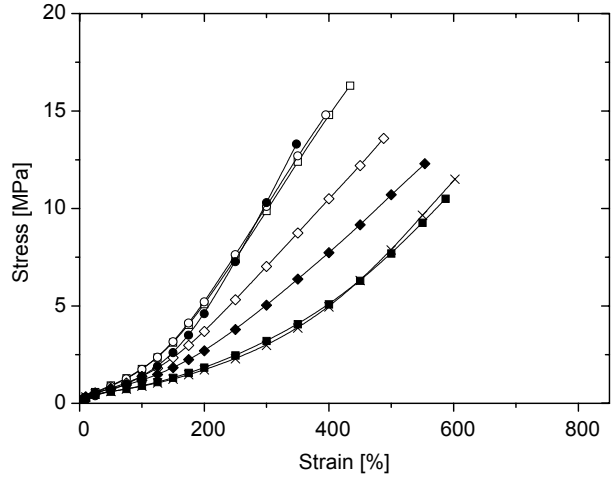

Fig. 4.11:Stress-strain curves for Series II; □ = TESPT; ○ = TESPD; ◊ = TESPM; ◆ = ETES; ■ = HTES; × = DTES; ● = MPTES.

With sulphur correction during the first mixing step in the internal mixer, Series III is even a step further in terms of the changes observed between Series II and I. The tensile properties of the compounds containing TESPT (Ia), TESPD (IIIb) and even TESPM (IIIc) and ETES (IIId) now coincide (Fig. 4.12). For ETES (IIId) this result is surprising since this compound came out worse in earlier experiments. The compound with HTES (IIIe) moved somewhat upwards, the one with DTES (IIIf) did not change. The compound with MPTES (IIIg) progressed so far upwards as to have lost most of its tensile strength and elongation at break in comparison with the corresponding compounds of Series I and II: again a result of scorch in the internal mixer, as described before.

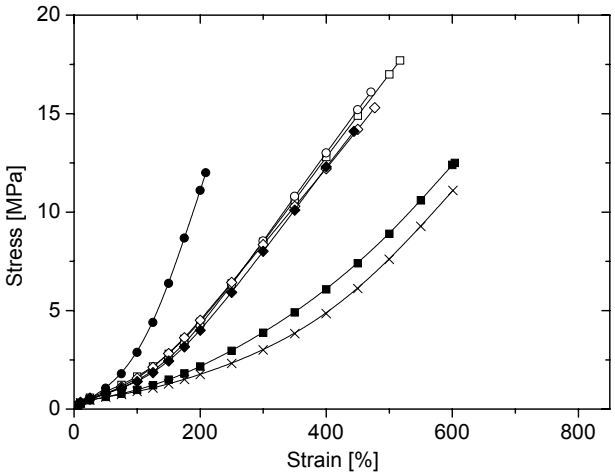

Fig. 4.12:Stress-strain curves for Series III; □ = TESPT; ○ = TESPD; ◊ = TESPM; ◆ = ETES; ■ = HTES; × = DTES; ● = MPTES.

Tan δ measurements at 60 °C as an indicator of rolling resistance

S', S" and tan δ measurements were taken on a RPA 2000 at 60 °C, 3.49% strain and 15 Hz (see Table 4.6) as an indicator of rolling resistance. For Series I tan δ increases with decreasing sulphur rank of the silane coupling agent, except for MPTES (Ig) which shows a tan δ value comparable with TESPT (Ia) but an S' and S" approximately one third of that of TESPT. This corresponds to the low E-modulus for the compound containing MPTES (Ig). Changing the carbon rank of the silane coupling agents has an opposite effect on tan δ, but less marked. Increasing from $(CH_2)_2$ (Id) to $(CH_2)_6$ (Ie) shows an increased tan δ, while the increase from $(CH_2)_6$ (Ie) to $(CH_2)_{10}$ (If) does not have an influence on tan δ anymore. Although a low tan δ is found, S' and S" for the compound containing ETES (Id) are approximately twice as high as for the TESPT (Ia) reference compound. MPTES (Ig) shows the opposite behaviour, S' and S" are roughly half the value for TESPT. It has to be remembered that not so much the tan δ by itself determines the rolling resistance of a tyre, but the S" or G" at 60 °C for a fixed value of S' or G' at 60 °C to represent the stiffness of a tyre compound. So tan δ in combination with S' are the determining properties.

For Series II and III the pattern seen is largely comparable with the shift in tensile properties. Successive corrections of sulphur on the mill and in the mixer, respectively, move the tan δ of TESPD (IIb/IIIb) to a value equal to that for TESPT (Ia), and TESPM (IIc/IIIc), HTES (IIe/IIIe) and DTES (IIf/IIIf) in the direction of TESPT. Sulphur correction leads to a tan δ value for MPTES (IIg/IIIg) and ETES (IId/IIId) that is even lower than for TESPT (Ia).

4.4 Discussion and conclusions

The previous section describes the influence of the sulphur rank and the carbon rank of the coupling agents in more or less chronological order from mixing till the final mechanical properties. A strong interaction has become apparent between the choice of the sulphur- or carbon rank of the silane and the application of corrective quantities of free sulphur during the different stages of processing, which results in major differences in the final properties.

Extensive literature has been published recently describing the reaction of free sulphur with TESPD dissolved in decalin to give sulphur rank distributions largely comparable with TESPT.[18-21] Applying this to actual compounds, TESPD and TESPT were compared on an equimolar basis with correction for the missing sulphur in the mill mixing stage: as in our Series II. Effects similar to those found in the present study are seen, particularly in the case of the curing properties. An attempt is then made to interpret these effects in terms of – more or less – independent processes taking place in these systems: silica shielding by the coupling agent and subsequent distribution in the rubber matrix, vs. the curing process by means of accelerators and sulphur. Recently, *Luginsland et al*[32,33] have modified this concept by adding the extra effect of “In Rubber Structure”: Figure 4.13. The latter represents a strain-independent contribution to the G’-modulus, which is due to chemical coupling of the filler to the rubber phase by means of the coupling agent: the filler acts like a multifunctional crosslinking agent.

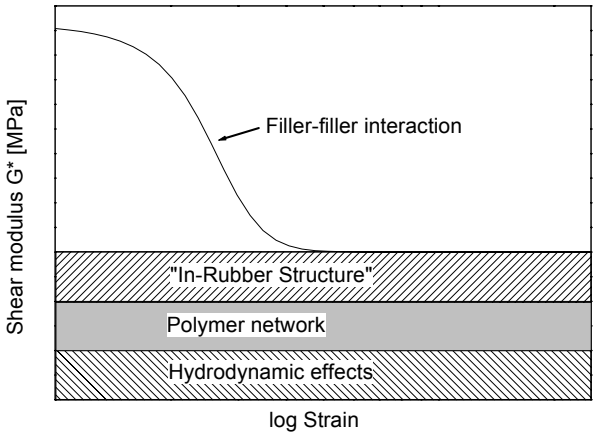

Fig. 4.13: Contributions to the complex shear modulus G vs. strain.*

The present work shows that sulphur along with the coupling agent plays a crucial role throughout the processing history of these compounds. Sulphur not only acts as a crosslinking agent between rubber molecules but is also in vigorous interaction with the coupling agent, the latter extending so far as to apply even to the coupling agents ETES, HTES and DTES, which have no built-in sulphur at all. It is hard to believe – nor are the present experiments suitable to prove – that this sulphur is somewhere built into the $(CH_2)_x$ units of these silanes. An alternative, but hardly probable explanation could be the occurrence of some reaction between the free sulphur and the silanol side of the silanes: not only do the silanol groups themselves interact and also react with the silica particle to form a hydrophobic shield around the silica, but implicitly they also could take along some rubber molecules by grafting them with the free sulphur to the silica particle. The latter would again be consistent with the older concept of e.g. TESPT being (also) a vulcanisation accelerator. It is challenging to prove this concept with more appropriate techniques, as presently pursued in our group. Still another explanation could be, that the correcting amount of sulphur added during the mixing, either in the first or in the final mix, does not fully react with the coupling agent and partially remains for the vulcanisation step.

It has become clear that the compounds with sulphur containing coupling agents are more prone to show effects of silica-rubber coupling, which may be interpreted as “In Rubber Structure”, than those containing sulphur-free coupling agents: Figs. 4.3 and 4.4. The more so, the higher the sulphur rank of the coupling agent or free sulphur added during the mixing stage.

Another point of discussion is the interpretation of the degree of dispersion of the silica in terms of the Payne effect, the tan δ or M_{300}/M_{100}. The Payne effects seen throughout this study are difficult, if not impossible, to relate to the choice of the coupling agent and/or the role of free sulphur. One might usefully ask whether the Payne effect – known from experience with carbon black and the more common precipitated silicas – is really an effect of the dispersion of the very readily dispersible silica used in the “green tyre” recipe.[34] Other projects within our group also indicate that new concepts of rubber reinforcement need to be invoked if we are to explain all the phenomena.[35]

Tan δ at 60 °C and M_{300}/M_{100} are both used as performance criteria for low hysteresis or rolling resistance of a tyre. In fact the two are interrelated, as shown in Fig. 4.14, where the values of M_{300}/M_{100} are plotted against tan δ at 60 °C for all the compounds. The two properties show a better correlation than might have been expected because of their totally different physical nature. Only the compounds containing ETES do not obey the relationship. M_{300}/M_{100} is basically related to the shape of the tensile curves as shown in Figs. 4.10 – 4.12. The greater the tendency of the stress to grow with elongation (Figs. 4.10 – 4.12), the higher the M_{300}/M_{100} ratio and, in accordance with Fig. 4.14, the lower the tan δ at 60 °C. The overall effect of progressing from Series I to Series III indicates an increase in the crosslink density, as can be seen from S’ (60 °C), the rheometer data ΔS’ and the E-modulus. This is therefore a further indication that the observed

effects are related more to the crosslink densities obtained than to Payne effects related to silica dispersion.

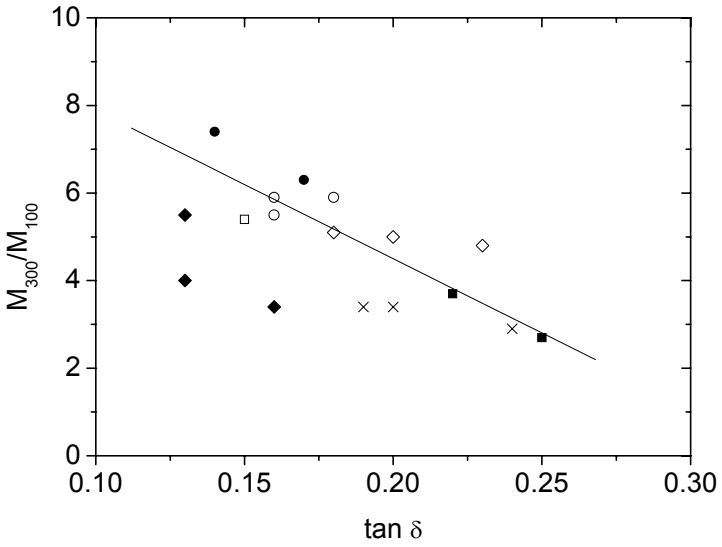

Fig. 4.14:Correlation of M_{300}/M_{100} with tan δ at 60 °C for all compounds; □ = TESPT; ○ = TESPD; ◊ = TESPM; ◆ = ETES; ■ = HTES; × = DTES; ● = MPTES.

Finally, this section seems to be an appropriate point to make an overall comparison of the different coupling agents vs. the reference, TESPT, bearing in mind the effects of correcting for the sulphur contents.

TESPD vs. TESPT

Others have reported that TESPD can function as a replacement for TESPT.[19,20,25,26] It has been shown that TESPT consists of a dynamic equilibrium of isomers with different sulphur ranks. TESPD acts in the same way if extra sulphur is supplied. Our study confirms this: TESPD requires corrective quantities of sulphur to make it behave identically to TESPT in terms of mixing, curing and physical properties, including the tan δ at 60 °C. It is, however, recommended that the corrective quantity of sulphur be added only in the third mixing step on the two-roll mill, together with the other vulcanisation ingredients. Then TESPD even has an advantage over TESPT, in that the scorch safety of the compound is greatly enhanced. This allows for a higher maximum mixing temperature and a broader temperature window. For TESPT this window is very narrow due to the need for a minimum of 140 °C in order to obtain sufficient reaction between the coupling agents and the silica, plus the risk of scorch onset at temperatures higher than 160 °C.[30] The only disadvantage of TESPD vs. TESPT is an approx. 5% increase in mixer energy consumption.

TESPM vs. TESPT

Although TESPM is commonly held[25-27] to have a very inert sulphur atom, the data in this study show that TESPM also behaves rather like TESPD if corrective quantities of sulphur are added, while not being as good overall. It must be concluded that TESPM also shows a dynamic equilibrium with free sulphur. In mechanical properties and tan δ it still comes very close to TESPT and TESPD plus sulphur, provided the corrective quantity of sulphur is added during the Brabender mixing step. The compound unexpectedly becomes more scorch-sensitive than TESPT at mixer batch temperatures above 160 °C, while without corrective sulphur (Fig. 4.5) no signs of scorch are observed. The origin of this scorch remains a point of conjecture. The present experiments cannot adequately answer this question, although we have previously postulated that the silanol groups of the silane together with the free sulphur are the root cause. Further study is required, e.g. by model vulcanisation experiments, and these our group is currently conducting.

ETES vs. TESPT

The high mixing energy and the high Payne effect indicate strong filler-filler interactions. A plausible explanation for the poor performance of ETES may be that this coupling agent is too short to fold itself with both silanol-ends towards the silica. It is not able to properly hydrophobise the silica surface, because there is a silanol-end sticking out into the rubber matrix rather than a carbon- or sulphur-moiety, like for the others. The tensile properties of the compounds containing ETES are overall worse when compared to TESPT, although sulphur correction on the two-roll mill increases the tensile strength towards the level of TESPT. The tensile properties of the ETES-containing compound corrected for sulphur during the first mixing step in the internal mixer are almost equal to the tensile properties of the TESPT-containing compound. Overall this coupling agent is impracticable because of the excessive compound Mooney viscosities.

HTES vs. TESPT

Even HTES shows a reaction with free sulphur, although less than TESPM. The Payne effect in the case of HTES is much larger than with TESPT, a finding which seems inconsistent with the same low energy consumption during mixing. The mechanical properties and tan δ at 60 °C are – together with DTES – the poorest of all the compounds, although the addition of free sulphur in the first mixing step still increases the mechanical properties in the direction of those of TESPT. But with HTES the addition of free sulphur during the first mixing step leads to increased scorch. HTES is therefore not a feasible alternative to TESPT.

DTES vs. TESPT

Using DTES, the energy consumption during mixing is even lower. The Payne effect of this compound is on a comparable low level with TESPT, which indicates a good silica dispersion. The addition of the correcting amount of sulphur during mixing does not influence the mixing behaviour or Payne effect.

This coupling agent is less sensitive to an increase in G' at higher temperatures when sulphur is added in the internal mixer: Fig. 4.4. This is of minor importance since the temperature during mixing commonly is kept below 150 °C.

Vulcanisation of the DTES-containing compound is delayed compared to TESPT if no sulphur correction is made. When sulphur correction is applied this delay is neutralised. The tensile properties of the DTES-containing compounds are lowest of all and react only very little on sulphur correction. Tan δ 60 °C, S' 60 °C and S" 60 °C are at a comparable level for the DTES-containing compound and the TESPT reference compound. Overall, this coupling agent would have been a good alternative to TESPT, if the tensile properties would have been acceptable.

MPTES vs. TESPT

Others[27] have already mentioned the pronounced scorch tendency of MPTES. Our study also demonstrates this. MPTES starts to scorch as early as during mixing, subsequently suffering from insufficient curing during the actual vulcanisation stage, either because the compound has lost much of its curing ability or because uniform dispersion of the curatives into the already scorched compounds proved impossible. When free sulphur is added in the first mixing step this effect becomes even more marked, resulting in a compound which is barely amenable to further processing. MPTES consumes about 10% more mixer energy than TESPT and shows a more pronounced Payne effect, more as a consequence of the scorch than poor dispersion of the silica. However, the high level of mechanical properties obtained with MPTES as a coupling agent is still surprising: the values for tan δ at 60 °C are the best obtained for any of the compounds studied. Processing considerations mean that overall the balance of properties obtained with TESPT is far superior to that of MPTES.

References

1. M. J. Wang, S. Wolff and J. B. Donnet, Rubber Chem. Technol., 64, 559 (1991).
2. J. B. Donnet, Kautsch. Gummi Kunstst., 47, 628 (1994).
3. S. Wolff, Tire Sci. Technol., 15, 276 (1987).
4. M. P. Wagner, Rubber Chem.Technol., 49, 703 (1976).
5. E. M. Dannenberg, Rubber Chem. Technol., 48, 410 (1975).
6. Y. Bomal, S. Touzet, R. Barruel, P. Cochet and B. Dejean, Kautsch. Gummi Kunstst., 50, 434 (1997).
7. B. T. Poh and C. C. Ng, Eur. Pol. J., 24, 975 (1998).
8. R. H. Hess, H. H. Hoekje, J. R. Creasey and F. Straim (to PPG Industries), US Pat. 3,768,537 (30-10-1973).
9. S. Wolff, Kautsch. Gummi Kunstst., 30, 516 (1977).
10. F. Thurn and S. Wolff, Kautsch. Gummi Kunstst., 28, 733 (1975).
11. S. Wolff, Kautsch. Gummi Kunstst., 34, 280 (1981).
12. S. Wolff, Rubber Chem. Technol., 55, 967 (1982).
13. S. Wolff, Kautsch. Gummi Kunstst., 36, 969 (1983).
14. S. Wolff, E. H. Tan and J. B. Donnet, Kautsch. Gummi Kunstst., 47, 485 (1994).
15. S. Wolff, U. Görl, M. J. Wang and W. Wolff, Eur. Rubber J., January, 16 (1994).

16. S. Wolff, Rubber Chem. Technol., 69, 325 (1996).
17. U. Görl and A. Parkhouse, Kautsch. Gummi Kunstst., 52, 493 (1999).
18. U. Görl and J. Muenzenberg, Paper No. 38 presented at a meeting of ACS, Rubber Division, Anaheim, California, May 6-9, 1997
19. H. D. Luginsland, Paper No. 74 presented at a meeting of ACS, Rubber Division, Chicago, Illinois, April 13-16, 1999
20. H. D. Luginsland, Kautsch. Gummi Kunstst., 53, 10 (2000).
21. H. D. Luginsland, Paper No. 34 presented at a meeting of ACS, Rubber Division, Dallas, Texas, April 4-6, 2000
22. A. Hasse and H. D. Luginsland, presented at a meeting of International Rubber Conference, Helsinki, Finland, June 12-15, 2000
23. A. Hunsche, U. Görl, H. G. Koban and T. Lehmann, Kautsch. Gummi Kunstst., 51, 525 (1998).
24. J. W. Pohl, Paper No. 100 presented at a meeting of ACS, Rubber Division, Cleveland, Ohio, October 21-24, 1997
25. R. W. Cruse, M. H. Hofstetter, L. M. Panzer and R. J. Pickwell, Paper No. 75 presented at a meeting of ACS, Rubber Division, Louisville, Kentucky, Oct. 8-11, 1996
26. R. W. Cruse, M. H. Hofstetter, L. M. Panzer and R. J. Pickwell, Rubber & Plastics News, April 21, 14 (1997).
27. P. Vondrácek, M. Hradec, V. Chvalovsky and H. D. Khanh, Rubber Chem. Technol., 57, 675 (1984).
28. R. Rauline (to Compagnie Generale des Etablissements Michelin - Michelin & Cie), Eur. Pat. 0 501 227 A1 (12-02-'92).
29. A. R. Payne, Rubber Chem. Technol., 39, 365 (1966).
30. L. A. E. M. Reuvekamp, J. W. ten Brinke, P. J. van Swaaij and J. W. M. Noordermeer, accepted for publication in Rubber Chem. Technol.,
31. C.-C. Lin, W. L. Hergenrother, E. Alexanian and G. G. A. Böhm, Paper No. 90 presented at a meeting of ACS, Rubber Division, Cleveland, Ohio, October 16-19, 2001
32. H. D. Luginsland, J. Fröhlich and A. Wehmeier, Paper No. 3 presented at a meeting of Deutsche Kautschuk Gesellschaft, Fortbildungsseminar "Soft Matter Nano-Structuring and Reinforcement", Hannover, Germany, May 22, 2001
33. H. D. Luginsland, J. Fröhlich and A. Wehmeier, Paper No. 59 presented at a meeting of ACS, Rubber Division, Providence, Rhode Island, April 24-27, 2001
34. C. Yvonnick and J. C. Morawski (to Rhone-Poulenc Chimie), Fr. Pat. 8405406
35. L. A. E. M. Reuvekamp, M. Debowski, J. Vancso and J. W. M. Noordermeer, in preparation.

Chapter 5

The effect of triethoxysilylpropyl benzothiazole disulphide as a coupling agent in a silica reinforced tyre tread compound

A combination of a silane and the accelerator MBT is investigated as a potential coupling agent for a silica reinforced tyre tread compound. In a tyre tread compound recipe, the silane is replaced by triethoxysilylpropyl benzothiazole disulphide (TESBD). Variations in the curing package are performed because of the accelerator function built-in into the coupling agent. The compound containing TESBD shows lower Mooney viscosities when compared to TESPT, which reflects in a better and smoother processability. The spontaneous "release" of MBT from TESBD for acceleration of the cure reaction is very slow. A small amount of amine, in the form of DPG is sufficient to speed up the release of benzothiazole accelerator moieties from TESBD to obtain properties grossly comparable with the TESPT reference compound, without further use of accelerator needed.

5.1 Introduction

The reaction of the silica filler with the rubber matrix via the TESPT silane coupling agent was studied by Görl et al. Model compounds were used to investigate the reaction of the tetrasulphide group, which is the rubber-reactive group of the silane, towards the rubber matrix. Modern analytical techniques were applied to analyse the reaction products. The link of the TESPT polysulphide group to the rubber was assumed to be brought about by the intermediate addition of accelerators. The authors propose the course of the reaction via an intermediate asymmetric polysulphide, formed by a reaction between the silane and accelerator, e.g. mercapto benzothiazole. In the subsequent reaction, the polysulphide is substituted into the allyl position of the rubber with release of mercapto benzthiazole: Fig. 5.1. This reaction subsequently leads to a covalent bond between rubber and filler, chemically binding the rubber to the filler.[1,2]

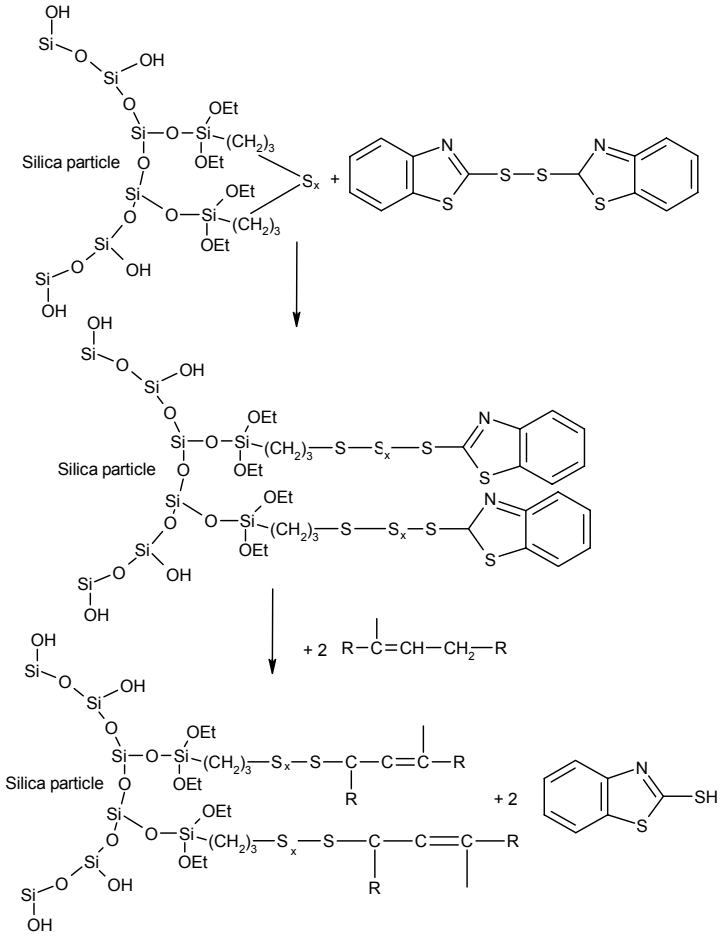

Fig.5.1: Proposed reaction mechanism of TESPT with rubber in the presence of a mercapto benzothiazole accelerator.[1,2]

By combining a silane and an accelerator into one reagent, instead of using them separately, the coupling reaction may become more efficient. For this reason, a combination of a silane and an accelerator was synthesised: Chapter 3. This silane-accelerator combination, triethoxysilylpropyl benzothiazole disulphide will be applied in the present chapter in the tyre tread compound. The silane TESPT is replaced by equimolar quantities of triethoxysilylpropyl benzothiazole disulphide. An optimisation of the mixing process will be described, as well as the effect of different amounts of sulphur and accelerator. The properties will be compared with a reference compound containing the commercially used triethoxysilylpropyl tetrasulphide (TESPT). The silane accelerator combination of the present chapter is assumed to be the intermediate asymmetric sulphide, which was proposed by Görl et al. The question must be answered, whether an additional amount of accelerator is still necessary to perform the crosslinking of the rubber, as the second reaction next to the silica-rubber coupling.

5.2 Experimental

5.2.1 Materials

Buna VSL 5025 HM, Bayer AG, solution SBR was used for the experiments. This S-SBR was composed of 75% butadiene with a vinyl content of 50% and 25% styrene, and was extended with 37.5 phr aromatic oil. The Mooney viscosity of the SBR ML (1+4) 100 °C was 65. This S-SBR was blended with Kosyn KBR 01, Korea Kumho Petrochemical Co. Ltd. BR with a cis content of >96% and a Mooney viscosity ML (1+4) 100 °C of 44. The compound further contained silica, Zeosil 1165 MP supplied by Rhodia, Enerflex 75 aromatic oil from BP Oil Europe and stearic acid and zinc oxide both supplied by Merck. The curing package consisted of sulphur (J.T. Baker), and the accelerators N-cyclohexylbenzthiazole-2-sulphenamide (CBS) and diphenyl guanidine (DPG) both supplied by Flexsys B.V. The triethoxysilylpropyl benzothiazole disulphide (TESBD) was synthesised as described in Chapter 3.

5.2.2 Optimisation of the mixing procedure

The compound compositions used for the experiments described in the current chapter are listed in Table 5.1. A comparison was made with the common TESPT-containing reference compound. Therefore, triethoxysilylpropyl benzothiazol disulphide (TESBD) was added equimolar to TESPT.

Table 5.1 Compound recipes.

Component	Reference recipe 1	Reference recipe 2	3	4	5
Brabender mixing step 1 + 2					
S-SBR	75.0			75.0	
BR	25.0			25.0	
ZnO	2.5			2.5	
Stearic acid	2.5			2.5	
Silica	80.0			80.0	
Aromatic oil	32.5			32.5	
TESPT	7.0			-	
TESBD	-			10.6	
Mill mixing step					
CBS	1.7	1.7	-	1.7	-
DPG	2.0	2.0	-	2.0	2.1
MBT	-	3.2	-	-	-
Sulphur	1.4	1.4	1.4	1.4	1.4
Total	229.6	232.8	229.5	233.2	231.6

The compounds were all mixed according to the three step mixing procedure as described in Chapter 4. For the TESPT-containing reference compound the rotor speed was set to 100 rpm, for the TESBD-containing compound 5 different rotor speeds were applied, varying from 40 till 120 rpm. The mixer fill factor was 63% and the starting mixing temperature was 50 °C. The temperature of the cooling water was kept constant at 50 °C for all the compounds during mixing.

In the first mixing step, silica, coupling agent and oil were added in two doses, each half of the required amount. The temperature of the compound was measured online during mixing, using a thermocouple embedded in the discharge door of the

mixer. As dump temperature, the temperature measured with the thermocouple at the end of the mixing step was taken, which is somewhat lower than the actual temperature of the compound. After both mixing steps in the internal mixer the compounds were sheeted out on a Schwabenthan 100 ml two roll mill. The curing system was added in a third mixing step on the same two roll mill at a temperature setting of about 40 °C.

5.2.3 Optimisation of curing system

As described in the introduction of this chapter, TESBD is similar to the intermediate product in the reaction of the coupling agent with the accelerator system: Fig. 5.1. The addition of further accelerator in the curing package therefore would seem unnecessary. However, the amount of accelerator in that case would not be equimolar to the TESPT reference compound: recipe 1. Therefore, the following changes in compound composition will be investigated:

- no extra accelerator added to the TESBD-containing compound: recipe 3;
- the same curing system added to the TESBD-containing compound, as normally applied for the TESPT reference compound: recipe 4;
- recipe 4 now contains a very high content of mercapto benzothiazole moieties included in the TESBD and CBS. To correct for that to some extent, the CBS-part of the curing system is omitted in recipe 5. However, the consequence is, that the amount of amine as included in the CBS is reduced as well, which may have a negative effect on vulcanisation speed. In order to correct for that, in turn the DPG-level is raised to the extent that the total amount of amine in the recipe is at the old level again;
- because in recipe 5, in spite of the omission of CBS, there is still much more mercapto benzothiazole present in either form to allow a proper comparison with the reference compound 1, an extra amount of MBT is added relative to recipe 1, so that the total amount of benzothiazole moieties equals that of recipe 5: recipe 2.

It will be clear, that an unequivocal comparison between all 5 recipes is not possible, because of the combined functionalities of the TESBD and the various accelerators.

In all cases the curing system was added in the final mixing step on the two roll mill.

5.2.4 Compound viscosity and cure properties

The compound Mooney viscosity ML (1+4) at 100 °C was measured by a 2000 E Mooney viscometer from Alpha Technologies. The cure properties of the compounds were determined using an RPA 2000 dynamic mechanical rheological tester from Alpha Technologies under the conditions described before in Chapter 4. Curing of the compounds was done using a WLP 1600/5*4/3 Wickert laboratory press at 160 °C and 100 bar pressure, for a time period corresponding to $t_c(90)$ of the specific compound. The dimensions of the cured specimens were 90 x 90 mm x 2 mm thick.

5.2.5 Mechanical characterisation

The uncured compounds were characterised by dynamic mechanical measurements using the RPA 2000 tester from Alpha Technologies at 100 °C and a frequency of 0.500 Hz. Tensile properties of the cured compounds were measured with a Zwick Z020 tensile tester in accordance with ISO 37.

The loss tangent in the cured state was measured with the RPA 2000 at 60 °C, 3.49% strain and a frequency of 15 Hz, after first curing the compounds in the RPA 2000 at 160 °C for $t_c(90)$ and subsequent cooling to 60 °C.

5.3 Results and Discussion

The results of the optimisation of the mixing procedure and the curing system will be the subject of the current chapter. The properties of the compounds mixed at different rotor speed and/or containing a different curing system will be compared to the TESPT-containing reference compound: recipe 1.

5.3.1 Optimisation of the mixing procedure

Brabender mixing step 1

The processing behaviour during mixing of the green tyre tread compound containing triethoxysilylpropyl benzothiazole disulphide (TESBD) was studied at different rotor speeds and compared to the TESPT containing reference compound mixed at 100 rpm. Five different rotor speeds varying from 40 till 120 rpm were applied. The influence of the rotor speed on the torque during mixing can be seen in Fig. 5.2: mixer torque vs. time for the first mixing step. The accompanying mixing energies and dump temperatures are listed in Table 5.2.

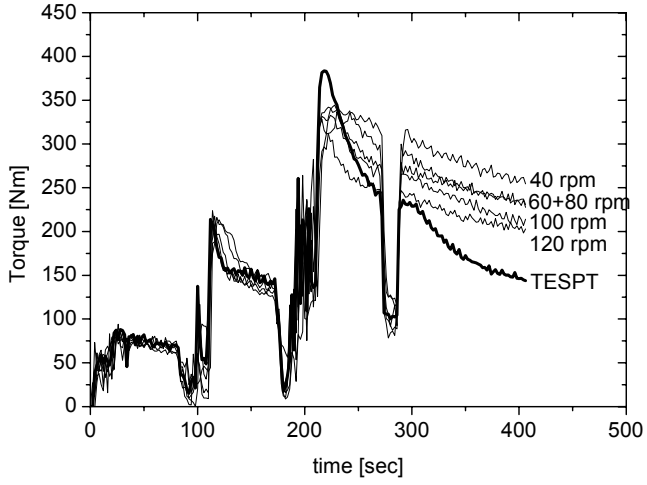

Fig. 5.2: Torque during mixing for the TESBT-containing compound mixed at different rotor speed and for the TESPT reference compound.

The thickest line in Fig. 5.2 applies to the reference compound according to recipe 1. Comparing the compounds mixed at increasing rotor speed, a decrease in torque during the later stages of the first mixing step is observed. The increase in torque after dosage of the second half of the silica, coupling agent and oil (210 sec) is less pronounced for the TESBD-containing compound when compared to the TESPT reference compound. No clear scorch-like effects are observed for the TESBD-containing compounds in the final stage of mixing. It is surprising, that the torque at the end of the first mixing step is higher for the TESBD compounds compared to TESPT, while the Mooney viscosities of the TESBD compounds mixed at 80, 100 and 120 rpm are significantly lower: Table 5.2. This is opposite to the results seen in Chapter 4. It is worth mentioning at this stage, that the compounds containing TESBD were particularly smooth and easy to process on the two roll mill: a practical confirmation of the low viscosity. The Mooney viscosity test, in spite of its high value in rubber technology, is only a one-point viscosity measurement. Admittedly, a rubber compound is a visco-elastic material for which the Mooney viscosity measurement is not the most appropriate. The results above do indicate, that for the present TESBD-containing compounds the “elastic nature” is less pronounced than for the TESPT-containing reference. It would be worth to investigate this in more detail, if possible.

Table 5.2 Mixing energies and dump temperatures for the compounds as function of mixer rotor speed.

Mixer rotor speed	Reference 100	40	60	80	100	120
Mixing energy 1st step [kJ/g]	664.3	318.3	451.0	566.3	687.4	788.3
Dump temperature 1st step [°C]	140	107	123	139	150	161
Mixing energy 2nd step [kJ/g]	448.4	207.4	262.6	332.8	437.5	489.3
dump temperature 2nd step [° C]	109	85	91	100	108	120
Mooney viscosity ML (1 + 4) 100 ° C	55.0	66.8	57.5	51.1	47.2	48.4

Strain sweep measurements as an indicator of silica dispersion

To further investigate the origin of the opposite effects seen in the previous paragraph, strain sweep measurements were taken on the compounds in the RPA 2000 at 100 °C and 0.500 Hz, as an indication of the degree of dispersion obtained in the first mixing step. Results are given in Fig. 5.3 for storage modulus G’ (a), loss modulus G” (b) and tan δ (c), respectively. As a measure of silica dispersion and of the degree of filler-filler interaction, the G’ at low strain values may be considered: the lower G’ at low strain, the better the silica dispersion and the lower the degree of filler-filler interaction.

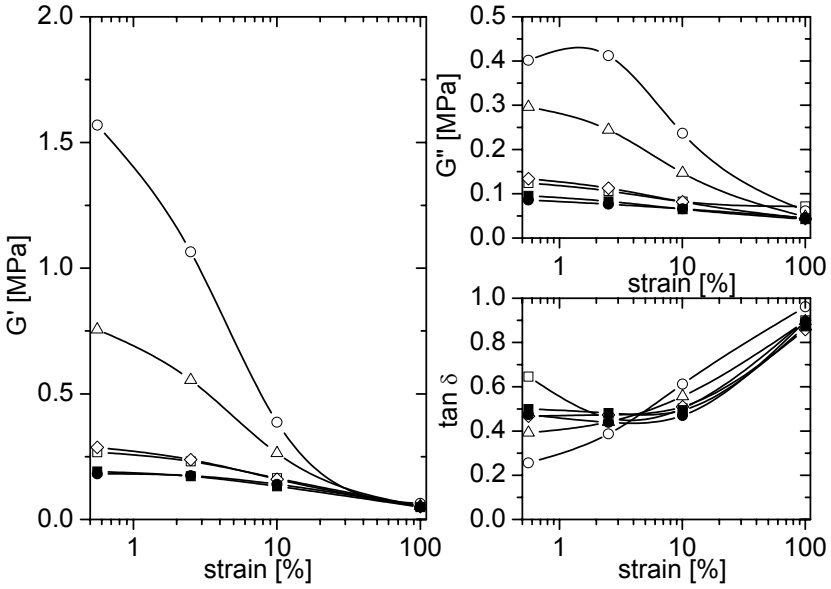

Fig. 5.3:Storage modulus G' (a), loss modulus G" (b) and tan δ (c) as a function of strain for the TESBT-containing compounds mixed at 40 (○), 60(Δ), 80(✧), 100(■) and 120(●) rpm and for the TESPT (□) reference compound 1, after the first Brabender mixing step.

The results in Fig. 5.3a indicate that the order of G' at low strain corresponds with the compound Mooney viscosities. The TESBD-containing compounds mixed at 100 rpm or higher, show a storage modulus G' at low strain which is even lower than G' at low strain for the TESPT reference compound, mixed at 100 rpm. This low Payne effect indicates an even better dispersion or shielding of the silica surface and therefore can be taken as the reason for the low compound Mooney. Increasing the rotor speed from 100 to 120 rpm has hardly any effect anymore on the Payne effect.

Temperature sweep measurements as an indicator of scorch sensitivity

A next step is to check, whether the opposite effects above are due to premature scorch during the mixing stage. The RPA 2000 was used for temperature sweep measurements, performed on the compounds at 0.500 Hz and 49.94% strain in the temperature range from 110 to 200 °C. Results of the G' vs. temperature are given in Fig. 5.4.

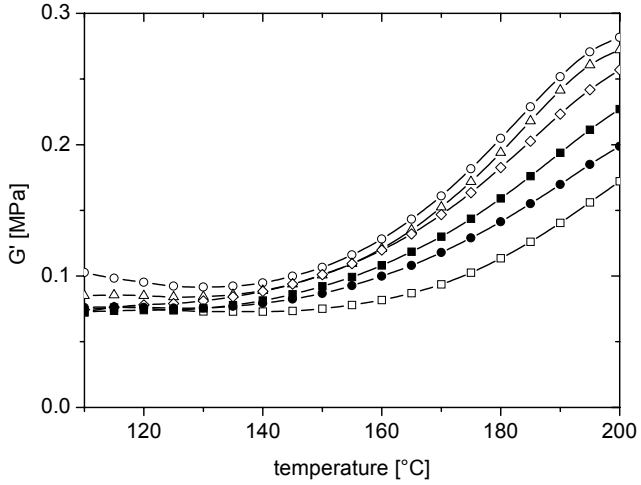

Fig 5.4: Temperature sweep measurements after the first Brabender mixing step for the TESBT-containing compounds mixed at 40 (○), 60(Δ), 80(✧), 100(■) and 120(●) rpm and for the TESPT (□) reference compound 1.

All compounds show a marked increase in G' at higher temperatures. The increase in G' for the TESBD-containing compounds starts at about 140 °C, compared to 160 °C for the TESPT reference compound. This indicates indeed, that there is the possibility of some premature scorch with the TESBD, starting at about 20 °C lower temperature than for TESPT. For TESPT this scorch was ascribed to crosslinking due to sulphur donated by TESPT, in combination with the accelerator functionality of TESPT[3,4]: Chapter 4. It is hard to believe that the increase in G' above 140 °C for the TESBD compounds is due to sulphur donated by TESBD. Early crosslinking by the accelerator functionality of TESBD is the most plausible explanation in this case.

Brabender mixing step 2

The torque curve in the second mixing step showed a similar order for the different rotor speeds as found in the first mixing step. The mixing energy and dump temperature increase with increasing rotor speed due to the higher shear generated. The Mooney viscosity decreases with increasing rotor speed, which is the result of a better breakdown of the silica network and therefore the better dispersion due to the higher friction.

Summarising the different observations in relation to the opposite effects seen in the mixing and compound Mooney viscosities, TESBD appears to be a highly effective shielding agent relative to TESPT, however with the disadvantage that it is somewhat more scorch sensitive. This apparently does not seriously damage the further processability of the compounds, as demonstrated by their smooth

behaviour on the two roll mill. As such, this coupling agent is worth further pursuing.

5.3.2 Results for the optimisation of the curing system

Curing behaviour

Curing behaviour of the compounds was investigated using the RPA 2000. The rheograms of the TESBD-containing compounds mixed at different rotor speeds, according to recipe 3 and of the TESPT reference compound are shown in Fig. 5.5.

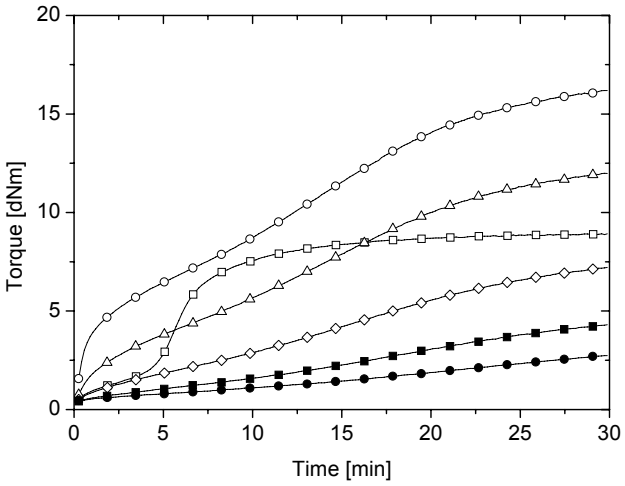

Fig. 5.5:Rheograms of TESBD-containing compound 3, mixed at 40 (○), 60(Δ), 80(✧), 100(■) and 120(●) rpm and without additional accelerator added in the curing package, compared to TESPT, recipe 1(□).

The cure behaviour of the TESBD-containing compound differs notably from the cure behaviour of the TESPT reference compound. There is a clear influence of rotor speed on the cure behaviour of the TESBD compounds. The cure curve of the compound mixed at 40 rpm starts at a higher rheometer torque value when compared to those for the higher rotor speeds, which is the result of poor silica dispersion, as seen in Chapter 4. Consequently, with increasing mixer rotor speed, the value of the rheometer torque at the beginning of cure decreases by the better filler dispersion. The TESBD-containing compounds, mixed at 100 and 120 rpm show only a slow increase in rheometer torque during vulcanisation, while the compounds mixed at lower rotor speeds show a kind of accelerating effect. This indicates that in the compounds mixed at higher rotor speeds and therefore at higher temperature the accelerator part of TESBD was already “released” during mixing. This released accelerator is then inactive in further vulcanisation. The latter corresponds with the earlier observation, that some scorch may have taken place at higher mixer rotor speeds.

The compounds mixed at lower rotor speeds show a dual increase in rheometer torque. This dual increase is slower when compared to TESPT but faster then the – still dual - increase in rheometer torque of the compounds mixed at high rotor speeds. In this case the temperature during mixing was not high enough to (fully) release the accelerator part of TESBD. This dual increase may be explained by as slow release of the benzothiazole accelerator moiety from TESBD before it can act as accelerator. It is important to note, that this would not agree with the mechanism proposed by Görl[1,2] as depicted in Fig. 5.1.

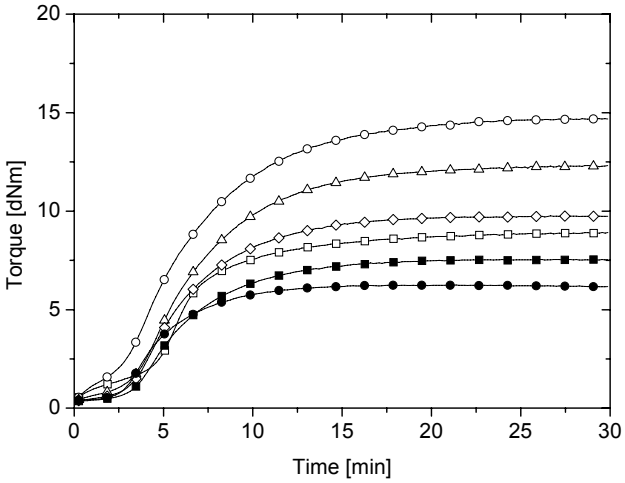

Fig. 5.6:Rheograms of TESBD-containing compounds according to recipe 4 mixed at 40 (○), 60(∆), 80(✧), 100(■) and 120(●) rpm, compared to TESPT, recipe 1(□).

In order to investigate the effect of addition of accelerators, the rheograms in Fig. 5.6 show the vulcanisation behaviour of the TESBD-containing compounds, according to recipe 4, which is now similar to the TESPT reference compound 1. Contrary to the rheograms observed for recipe 3, all compounds now show “normal” behaviour with a clear scorch time. The final cure levels reached – the maximum torques - are less sensitive to the mixer rotor speed than the ones seen in Fig. 5.5. The shoulder in the rheogram, which is usually observed for TESPT is not visible for the TESBD-containing compounds mixed at higher rotor speeds of 80, 100 and 120 rpm. Similarly, the dual increase of rheometer torque as seen for recipe 3, is also gone. This is understandable from the fact, that recipe 4 contains a substantial amount of extra accelerator CBS, which overshadows the release of the benzothiazole-moiety from TESBD. For the compound mixed at 40 rpm, a faster vulcanisation than TESPT is observed, which again can be explained by the release of the accelerator part from TESBD. It must be kept in mind that in the present case the curing systems for the TESBD-containing compound and for TESPT are different. On molar base the TESBD compound contains more accelerator then the TESPT reference compound. A fair comparison can therefore not fully be made.

A third curing system was therefore investigated. In this system the amount of benzothiazole, amine, sulphur and silanol was added in equimolar quantities for both the TESPT and the TESBD containing compounds; recipes 2 and 5. The curing curves for all recipes, TESBD- and TESPT-containing, as mixed at 100 rpm, are shown in Fig. 5.7.

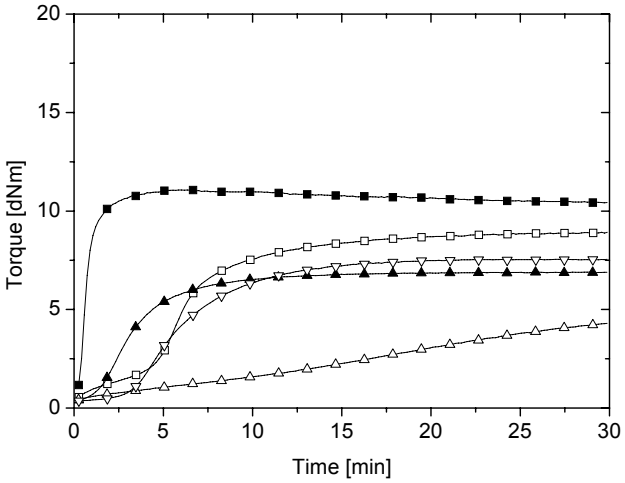

Fig. 5.7:Rheograms for TESBD and TESPT mixed at 100 rpm, according to recipe 1 (□), 2 (■), 3(Δ), 4(∇) and 5(▲).

This figure clearly shows the different effects of MBT, in free form or inserted in TESBD or CBS. The extra amount of free MBT in the curing package of the TESPT reference compound 2 results in a very fast vulcanisation, without scorch delay and resulting in a considerably higher crosslink density than recipe 1. On molar base this recipe 2 contains exactly the same curing package as the TESBD compound 5 with extra sulphur and DPG added. A similar rheogram might therefore be expected. However, Fig 5.7 shows a different rheogram for recipe 5, for which a clear scorch delay is observed. This again indicates that the benzothiazole moiety of the coupling agent reacts in a different manner compared to free MBT, added later with the curing package: the benzothiazole first has to be released from the TESBD before it can act as an accelerator. Apparently, the addition of extra amine in recipe 5 does accelerate the release of benzothiazole from the TESBD, as seen by a comparison with the very slow vulcanisation seen for recipe 3, which is the same recipe as for recipe 5, but without extra amine added. Recipe 4, providing two sources of benzothiazole: in TESBD as well as in CBS, takes an intermediate position. For CBS, being a delayed action accelerator, it is commonly understood that benzothiazole first has to be released before it can act as an accelerator. Overall these experiments show that benzothiazole must be released from TESBD before it can act as an accelerator and that this release can be regulated by the amount of amine (DPG) added to the recipe.

Mechanical properties

The mechanical properties of the cured TESBD-containing compounds are listed in Table 5.3. The stress-strain curves for recipe 3, without additional accelerator added are shown in Fig. 5.8.

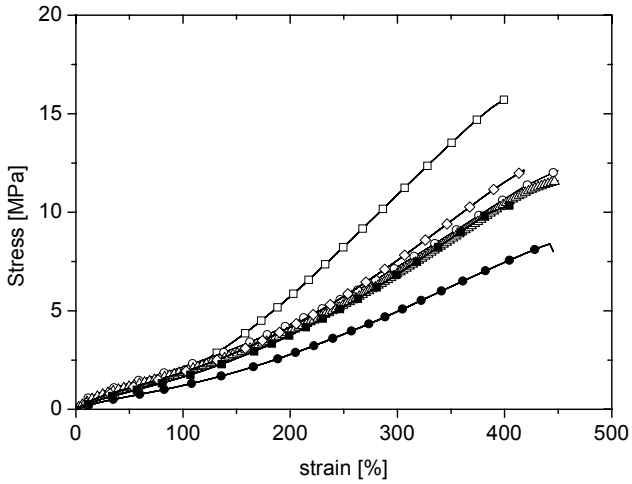

Fig 5.8: Tensile properties of the TESBD-containing compound, according to recipe 3 and mixed at 40(○), 60(Δ), 80(✧), 100(■) and 120(●) rpm, compared to TESPT, recipe 1(□), mixed at 100 rpm.

When comparing compound 3 mixed at different rotor speeds with the reference compound 1 it becomes clear, that in all cases the tensile properties of compound 3 are inferior to the reference compound. With increasing rotor speed a decrease in E-modulus, σ_{break}, ε_{break} and M_{100} is observed, while tan δ increases. Based on the breakdown of the silica network and potential degradation of the polymer chains at higher rotor speeds, these results are in accordance with the previous observations.

Table 5.3 Mechanical properties of cured compounds for the compounds according to recipes 1-5.

	E-modulus [MPa]	σ_{break} [MPa]	ε_{break} [%]	M_{100} [MPa]	M_{300} [MPa]	$\frac{M_{300}}{M_{100}}$	tan δ 60 °C	S' 60 °C [dNm]	S" 60 °C [dNm]
1-100	7.49	15.14	388	1.89	10.86	5.7	0.157	13.82	2.18
2-100	8.68	14.28	258	3.4	*17.33*	*5.1*	0.143	16.99	2.43
3-40	19.88	11.87	438	2.15	7.23	3.4	0.151	27.36	4.14
3-60	12.66	11.34	429	1.92	6.88	3.6	0.159	22.59	3.59
3-80	8.31	11.84	409	1.89	7.56	4.0	0.167	15.09	2.51
3-100	4.45	10.29	401	1.64	6.87	4.2	0.175	10.16	1.77
3-120	3.37	8.4	447	1.21	4.96	4.1	0.186	7.61	1.41
4-40	23.73	12.01	270	3.08	*12.40*	*4.0*	0.174	22.79	3.96
4-60	22.81	13.38	293	2.94	*13.72*	*4.7*	0.166	19.52	3.24
4-80	14.23	11.95	252	2.92	*14.96*	*5.1*	0.143	14.59	2.09
4-100	6.78	12.00	248	2.74	*15.59*	*5.7*	0.109	10.94	1.20
4-120	5.11	12.57	242	2.81	*16.82*	*6.0*	0.093	9.08	0.82
5-100	4.56	14.91	348	1.96	12.25	6.3	0.107	11.20	1.51

The addition of an extra amount of accelerator to the curing package of the compound containing TESBD, according to recipe 4, as depicted in Fig 5.9, results in an increase of the E-modulus, σ_{break}, M_{100} and tan δ relative to recipe 3. The stress-strain curves indicate excessive curing, which commonly results in an increased modulus, accompanied by a decrease in tensile strength and elongation at break.[5] The ε_{break} of compound 4 is even lower than 300%. As M_{300}/M_{100} is often used as a measure for rolling resistance, see Chapter 4, that value cannot be evaluated here, additional to tan δ at 60 °C. Therefore, the modulus was extrapolated to 300% strain in order to calculate a value for M_{300}/M_{100} as an indication of rolling resistance. These extrapolations are indicated in italics.

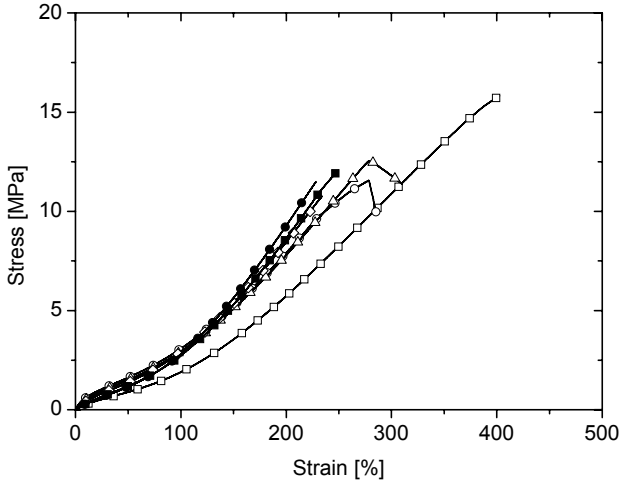

Fig 5.9: Tensile properties of the TESBD-containing compound, according to recipe 4 and mixed at 40(○), 60(Δ), 80(✧), 100(■) and 120(●) rpm, compared to TESPT, recipe 1(□), mixed at 100 rpm.

In Fig. 5.10 tensile properties of all accelerator systems investigated are compared for TESBD as well as for TESPT all mixed at 100 rpm. Comparing recipe 1 and 2 (both TESPT) shows a clear effect of the extra amount of MBT in recipe 2: again clear signs of excessive cure. When comparing the compounds according to recipe 2 (TESPT) and 5 (TESBD), containing equimolar amounts of silane, benzothiazole, amine and sulphur, the overall tensile properties are best for recipe 5 (TESBD) and come closest to those of the conventional TESPT-containing reference compound 1. Recipe 5 contains no more than sulphur and some amine in the form of DPG; all acceleration of vulcanisation has to come from benzothiazole moieties contained in TESBD. This result again shows, that the little amount of amine is sufficient to release the benzothiazole moieties for vulcanisation purposes. It is felt, that with some optimisation of the DPG-quantities, the tensile strength properties of recipe 1 can be matched.

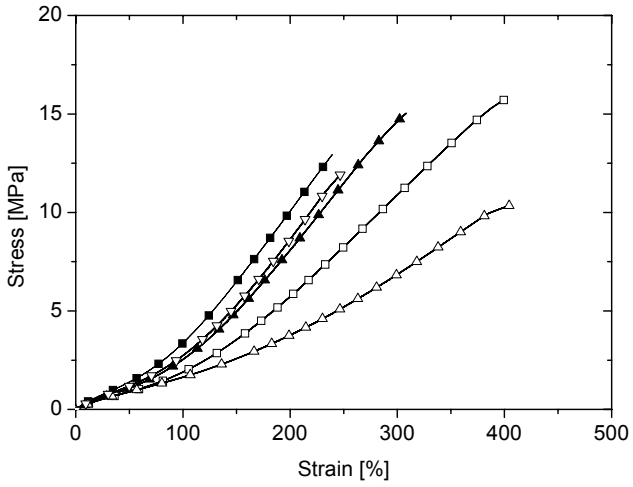

Fig 5.10:Tensile properties of the TESBT- and TESPT-containing compounds, according to recipe1 (□), 2 (■), 3(Δ), 4(▽) and 5(▲).

In Fig. 5.11 the tan δ's and M_{300}/M_{100}'s for all compounds of Table 5.3 are collected. It is clearly seen that the tan δ and M_{300}/M_{100} are much better for recipes 4 and 5 in particular, even better than for the reference compound 1. This positive result would motivate further fine-tuning of the newly described TESBD coupling agent, also showing accelerator properties in the presence of small amounts of amines and further providing better processability, than the conventional TESPT-containing green tyre compound.

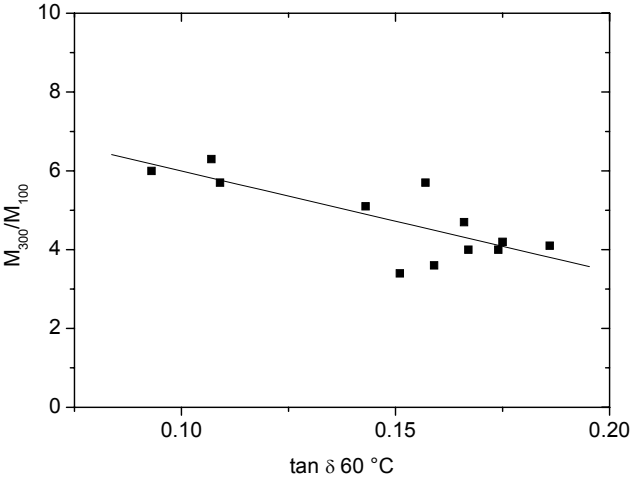

Fig 5.11: Correlation of M_{300}/M_{100} with tan δ at 60 °C for all compounds.

5.4 Conclusions

The use of triethoxysilylpropylbenzothiazole disulphide as a coupling agent in a silica reinforced tyre tread compound results in an improved dispersion of the silica filler relative to a TESPT-containing green tyre reference compound, if mixed under the same conditions of mixer rotor speed. Mixer torque remains comparatively high relative to the TESPT-compound, which could be explained by some premature scorch. However, in spite of this scorch, the compound Mooney viscosities are lower than for TESPT, which in turn reflects in a better and smoother processability on the two roll mill. In the case of TESPT mixed at higher rotor speeds, this scorch effect usually results in difficulties in further processing of the compounds.

The spontaneous “release” of MBT from TESBD for acceleration of the cure reaction is very slow, as can be seen from the rheograms and also shown in the tensile tests. An extra amount of accelerator in the curing package exceeds the optimum, if the tensile properties of the TESPT-containing reference compound are taken as the target. A small amount of amine, in the form of DPG, is sufficient to speed up the release of benzothiazole accelerator moieties from the TESBD to obtain properties grossly comparable with the TESPT reference compound, without further use of accelerator needed. This coupling agents indeed performs like a combined coupling agent and accelerator, as aimed for with the development of this product. The results of TESBD as a combined coupling agent/accelerator are very promising, although further optimisation of the vulcanisation system is necessary.

References

1. U. Görl and J. Muenzenberg, Paper No. 38 presented at a meeting of ACS, Rubber Division, Anaheim, California, May 6-9, 1997
2. U. Görl, J. Münzenberg, D. Luginsland and A. Müller, Kautsch. Gummi Kunstst., 52, 588 (1999).
3. L. A. E. M. Reuvekamp, J. W. ten Brinke, P. J. van Swaaij and J. W. M. Noordermeer, Kautsch. Gummi Kunstst., 55, 41 (2002).
4. S. Wolff, Kautsch. Gummi Kunstst., 30, 516 (1977).
5. A. Y. Coran, "Science and Technology of Rubber", Academic Press, New York, 1978.

Chapter 6

The effect of diisopropylthiophosphoryltriethoxysilylpropyl monosulphide as a coupling agent in a silica reinforced tyre tread compound

A combination of a thiophosphoryl sulphide and a silane was developed as a coupling agent to combine the function of hydrophobation of the silica surface and possibly also of curing accelerator. The processing behaviour and the dynamic mechanical properties are discussed in the current chapter. A silica reinforced tyre tread compound recipe was used, where the silane coupling agent was replaced by diisopropylthiophosphoryl triethoxysilylpropyl monosulphide. The compound was mixed at different rotor speeds in order to find the optimum mixing procedure. The sulphur and accelerator content of the recipe was changed in several ways. The accelerator content of the recipe was adjusted because of the accelerator function built-in into the coupling agent. The sulphur content was varied because of the different sulphur content and activity of diisopropylthiophosphoryl triethoxysilylpropyl monosulphide when compared to the commercially most used coupling agent triethoxysilylpropyl tetrasulphide. The optimum rotor speed for mixing the diisopropyl thiophosphoryl triethoxysilylpropyl monosulphide in the green tyre tread compound was 80 rpm. At this rotor speed the Payne effect, and therefore the filler dispersion was at its optimum. Without further accelerator added to the compound, the mechanical properties remained far inferior to those of the reference. The compound cured with the same curing package as the reference compound with TESPT, showed final properties, which reasonably match the TESPT reference compound. The conclusion must be drawn, that the thiophosphoryl accelerator moiety within the newly developed coupling agent has little effect by itself.

6.1 Introduction

The use of bis(diisopropyl)thiophosphoryl disulphide (DIPDIS) as an accelerator for cis-1,4-polyisoprene has been studied in detail by Pimblott et al.[1] During curing at 160 °C a predominantly monosulphidic network was generated. The thermal-oxidative aging behaviour of this DIPDIS vulcanisate was superior to a conventional S/CBS vulcanisate. The better aging behaviour was shown to be due to the formation of zinc diisopropyl dithiophosphate in situ, which acts as an antioxidant.

The reaction between DIPDIS and silica has been investigated by Mandal et al.[2] Silica and DIPDIS were heated at 140 °C upon which isopropyl alcohol was released. On heating DIPDIS without silica no isopropyl alcohol could be detected. Similar experiments were performed in the presence of natural rubber (NR) and again isopropyl alcohol was detected in the sample containing silica. The chemical

nature of the bond was characterised by IR analysis of the reaction products of silica and DIPDIS, both in the presence and absence of NR.

Preliminary experiments with DIPDIS as a coupling agent in a tyre tread compound were performed by mixing in a Brabender Plasticorder. When mixed in this internal mixer, DIPDIS was found to be too scorch sensitive in the silica-reinforced S-SBR/BR blend. The crosslinking reaction takes place prior to the hydrophobation of the silica surface, thereby hindering this latter reaction and making further processing impossible. For a good processing behaviour the hydrophobation of the silica surface should take place prior to the crosslinking reaction. A potential solution for this problem could be a combination of the properties of a silane, which has a higher reactivity towards the silica surface due to its ethoxy-groups, with the accelerator function of DIPDIS. Another potential advantage of this combination would be the reduction of the activity of the thiophosphoryl-group as an accelerator, and thereby reducing the scorch sentitivity. The synthesis and characterisation of such a compound: diisopropylthiophosphoryl triethoxysilylpropyl monosulphide (DIPTESM) was described in Chapter 3. In the current chapter the effect of this DIPTESM in the green tyre tread compound will be discussed.

An optimisation of the mixing process for DIPTESM by varying the rotor speed, as well as the effect of different amounts of sulphur in the presence and absence of additional accelerator, normally used in a tyre tread compound, will be described. The properties will be compared to a reference compound containing the commercially used triethoxysilylpropyl tetrasulphide (TESPT). TESPT contains 3.8 sulphur atoms per molecule on average, while DIPTESM contains only two sulphur atoms per molecule. Therefore, a correction has to be made for the difference in the amount of sulphur. It is a point of discussion how this sulphur correction should be made. Several assumptions can be made: (1) The sulphur atoms of DIPTESM do not participate in the curing reaction, (2) only one sulphur atom of DIPTESM participates or (3) both sulphur atoms of DIPTESM participate in the curing reaction.

DIPTESM potentially plays an extra role compared to TESPT, namely the accelerator function of the thiophosphoryl part. Assuming that this thiophosphoryl part really acts as an accelerator, the addition of accelerators to the compound in the curing package would not be required. Therefore, a comparison has been made between the addition and omission of accelerators in the curing package. The results will be discussed in a way similar to the discussion of the results in Chapter 5.

6.2 Experimental

6.2.1 Materials

The solution-SBR used for the experiments was Buna VSL 5025 HM, Bayer AG, composed of 75% butadiene with a vinyl content of 50% and 25% styrene, extended with 37.5 phr aromatic oil. The Mooney viscosity of the SBR ML (1+4) 100 °C was 65. The BR (Kosyn KBR 01, Korea Kumho Petrochemical Co. Ltd.) had a cis content of >96% and a Mooney viscosity ML (1+4) 100 °C of 44. The compound further contained silica, Zeosil 1165 MP supplied by Rhodia, Enerflex 75

aromatic oil from BP Oil Europe and stearic acid and zinc oxide both supplied by Merck. The curing package consisted of sulphur (J.T. Baker), and the accelerators N-cyclohexylbenzthiazole-2-sulphenamide (CBS) and diphenyl guanidine (DPG) both supplied by Flexsys B.V. The diisopropylthiophosphoryl triethoxysilylpropyl monosulphide was synthesised as described in Chapter 3.

6.2.2 Optimisation of the mixing procedure

The compound compositions for optimisation of the mixing procedure and the TESPT-containing reference compound are listed in Table 6.1. Diisopropyl thiophosphoryl triethoxysilylpropyl monosulphide was added equimolar to TESPT. The compounds were mixed using a three-steps mixing procedure as described before in Chapter 4. The starting temperature was 50 °C and the cooling water was kept constant at 50 °C. Recipes A till E are the same in the first two Brabender mixing steps. This masterbatch was mixed at five different rotor speeds, varying from 40 to 120 rpm in steps of 20 rpm. To these compounds in turn the different curing packages, as listed in the lower part of Table 6.1 were added. The rotor speed applied in the first mixing step was also used for the second remix in the internal mixer. For the TESPT reference compound the rotor speed was only set to 100 rpm. The mixer fill factor was chosen as 63%. Silica, coupling agent and oil were added in two doses, each of half the required amounts.

Table 6.1 Compound recipes of the masterbatch mixed at different rotor speeds.

Component	Reference recipe 1	A	B	C	D	E
Brabender mixing step 1 + 2						
S-SBR	75.0			75.0		
BR	25.0			25.0		
ZnO	2.5			2.5		
Stearic acid	2.5			2.5		
Silica	80.0			80.0		
Aromatic oil	32.5			32.5		
TESPT	7.0			-		
DIPTESM	-			5.6		
Mill mixing step						
CBS	1.7	-	-	-	-	1.7
DPG	2.0	-	-	-	-	2.0
Sulphur	1.4	1.4	3.0	2.6	2.2	1.4
Total	229.6	224.5	225.9	225.5	225.1	228.2

During mixing the temperature was measured online, using the thermocouple embedded in the discharge door of the mixer. The temperature measured at the end of the mixing step was taken as the dump temperature. As mentioned before, it must be kept in mind that this temperature is somewhat lower than the actual temperature of the compound.

After both mixing steps the compounds were sheeted out on a Schwabenthan 100 ml two roll mill. Accelerators and sulphur were added in a third mixing step on the same two roll mill at a temperature of about 40 °C, according to the scheme, detailed in the next paragraph.

6.2.3 Optimisation of curing system

The thiophosphoryl group in DIPTESM is known to act as an accelerator.[1,2] Therefore the question rises whether it is necessary to add the same curing system as normally applied for TESPT. Another difference compared to TESPT is the amount of sulphur atoms and the activity of these sulphur atoms in the curing reaction. Based on the curing system normally used for a green tyre tread compound, several variations have been included in Table 6.1:

- Compound A: no accelerators added and the same amount of sulphur as in the green tyre tread recipe
- Compound B: no accelerators added but an extra amount of sulphur compared to the green tyre tread compound. This extra amount is based on the assumption that no sulphur atoms in the coupling agent are active in the curing, compared to four active sulphur atoms in the TESPT-reference compound.
- Compound C: no accelerators added but an extra amount of sulphur compared to the green tyre tread compound. This extra amount is based on the assumption that one sulphur atom in the coupling agent is active in the curing, compared to the four active sulphur atoms in the TESPT-reference compound.
- Compound D: no accelerator added but an extra amount of sulphur compared to the green tyre tread compound. This extra amount is based on the assumption that two sulphur atoms in the coupling agent are active in the curing, compared to four active sulphur atoms in the TESPT-reference compound.
- Compound E: the same amounts of sulphur and accelerators as in the green tyre tread compound recipe.

In all cases the curing system was added in the final mixing step on the two roll mill.

6.2.4 Compound viscosity and cure properties

The compound Mooney viscosity ML (1+4) at 100 °C was measured with a 2000 E Mooney viscometer from Alpha Technologies. The cure properties of the compounds were determined using an RPA 2000 dynamic mechanical rheological tester from Alpha Technologies under the conditions described before in Chapter 4. Curing of the compounds was done using a WLP 1600/5*4/3 Wickert laboratory press at 160 °C and 100 bar pressure, for a time period corresponding to $t_c(90)$ of the specific compounds. The dimensions of the cured specimens were 90 x 90 mm x 2 mm thick.

6.2.5 Mechanical characterisation

The uncured compounds were characterised by dynamic mechanical measurements using the RPA 2000 tester from Alpha Technologies at 100 °C and at a frequency of 0.500 Hz. Tensile properties of the cured compounds were measured with a Zwick Z020 tensile tester in accordance with ISO 37.

The loss tangent was measured with the RPA 2000 at 60 °C, 3.49% strain and a frequency of 15 Hz, after first curing the compounds in the RPA 2000 at 160 °C for $t_c(90)$ and subsequent cooling to 60 °C.

6.3 Results and Discussion

The behaviour of the masterbatch during mixing at different rotor speeds will be discussed and compared to the TESPT reference compound. The effect of different amounts of sulphur in the curing package and the effect of the accelerator on dynamic mechanical properties and cure behaviour will be described later.

6.3.1 Optimisation of the mixing procedure

Brabender mixing step 1

The processing behaviour during mixing of a green tyre tread compound containing DIPTESM was studied at different rotor speeds and compared to a TESPT containing reference compound mixed at 100 rpm. The influence of the rotor speed on the torque during mixing is shown in Fig. 6.1: mixer torque vs. time for the first mixing step. The corresponding mixing energies and dump temperatures are listed in Table 6.2.

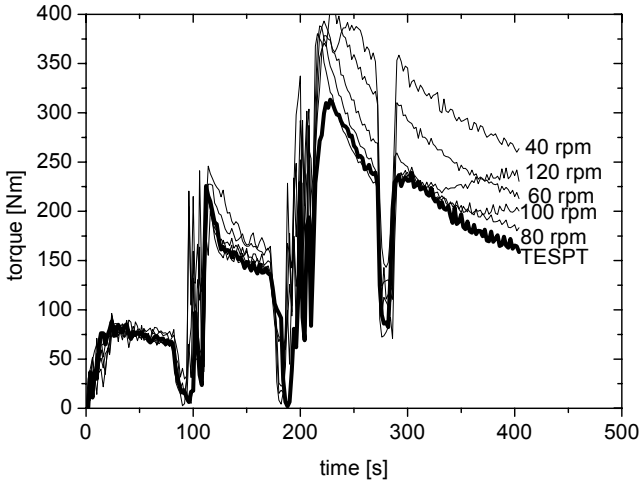

Fig. 6.1: Mixer torque vs. time for the first mixing step of the masterbatch in the Brabender Plasticorder at different rotor speeds as indicated and of the TESPT reference compound at 100 rpm.

The thickest line in Fig. 6.1 applies to the reference compound according to reference recipe 1. Comparing the compounds mixed at rotor speeds of 40 – 120 rpm, a decrease in torque during the latter stages of the first mixing step was observed for an increase in rotor speed from 40 to 80 rpm. At a rotor speed of 80 rpm the mixer torque coincides with the curve for the TESPT reference compound within experimental scatter. At rotor speeds of 100 and 120 rpm a scorch-like increase in torque in the final stage is seen similar to the effect observed for 3-mercaptopropyltriethoxy silane as discussed in Chapter 4.

Table 6.2 Mixing energies and dump temperatures for the reference compound and the masterbatch, mixed at different rotor speeds.

rotor speeds	100 (TESPT)	40	60	80	100	120
mixing energy 1st step [kJ/g]	1.78	0.95	1.35	1.61	1.95	2.35
dump temperature 1st step [°C]	143	111	131	146	163	180
mixing energy 2nd step [kJ/g]	1.33	0.75	0.93	1.04	1.47	1.56
dump temperature 2nd step [° C]	109	92	103	114	127	129
Mooney viscosity ML (1 + 4) 100 ° C	49.7	67.5	56.1	53.9	58.2	52.1

At the same mixing conditions of 100 rpm the energy consumed during the first mixing step and the dump temperature of the DIPTESM-containing compound are higher when compared to the TESPT reference compound. This higher energy consumption and dump temperature causes a scorch-like increase in torque at the final stage of mixing. As might be expected an increase in rotor speed results in an increase in energy consumption and dump temperature. At 80 rpm the dump temperature and the energy consumed during the first mixing step are more or less comparable to the dump temperature and the energy consumed in the first mixing step by the TESPT reference compound at 100 rpm. Apparently, DIPTESM tends to premature scorch at about the same mixing/dump temperatures as TESPT. The reason for the higher energy consumption during mixing of the DIPTESM-containing compound at the same rotor speed of 100 rpm as the reference compound, must be an indication for a higher viscosity of the DIPTESM-containing compounds: see after the second Brabender mixing step.

Strain sweep measurements as an indicator of silica dispersion

Strain sweep measurements were taken on the masterbatch in the RPA 2000 at 100 °C and 0.500 Hz, as an initial indicator of the degree of dispersion obtained in the first mixing step. Results are given in Fig. 6.2a-c for storage modulus G', loss modulus G" and tan δ respectively. A better dispersion of the silica filler leads to a smaller difference in G' at low strain and G' at high strain.

The results in Fig. 6.2a show the lowest storage modulus G' at low strain for the reference compound containing TESPT. This low Payne effect indicates an optimal dispersion or shielding of the silica surface and therefore seems to be the reason for the lower mixer torque in Fig. 6.1. The masterbatch, mixed at the lowest rotor speed of 40 rpm shows the highest Payne effect. With increasing rotor speed the Payne effect decreases, indicating an improvement in filler dispersion or shielding of the surface with an increased rotor speed.

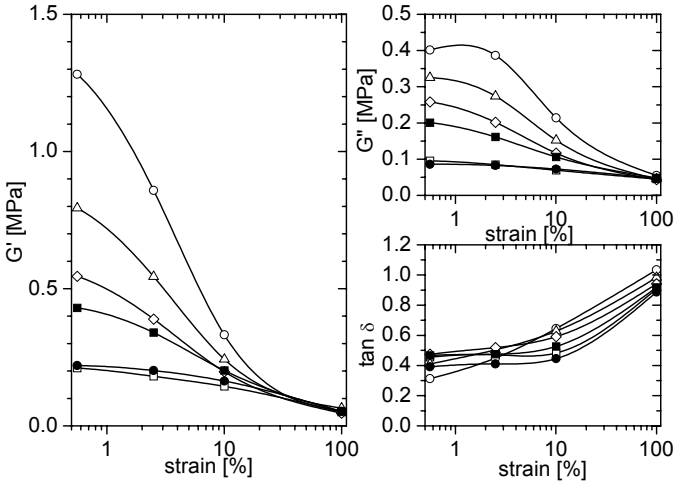

Fig. 6.2: G'-modulus (a), G"-modulus (b) and tan δ (c) as a function of strain for the masterbatch mixed at 40 (○), 60 (Δ), 80 (◊), 100 (■) and 120 (●) rpm and compared to TESPT (□) mixed at 100 rpm.

The compound containing 3-mercaptopropyltriethoxy silane (MPTES), as discussed in Chapter 4, showed a higher G'-modulus at 100% strain in the strain sweep curve. Together with the higher mixing torque in the final stage of mixing, this was taken as an indication of scorch during the first mixing step of that coupling agent. Although a similar scorch-like effect was seen in the mixer torque vs. time curves for the present masterbatch mixed at 100 and 120 rpm, the higher G'-modulus at intermediate strain in the strain sweep measurements is absent. The scorch-effect, as indicated by the increase in mixer torque in the final stage of the first mixing step is not confirmed by an increase of the G' at intermediate strains, contrary to experiences with MPTES in Chapter 4.

The loss-modulus G" curves are shown in Fig. 6.2b. The higher the rotor speed during the first mixing step for the compounds containing DIPTESM, the more the curve of G" against strain shows a course similar to the curve for MPTES as described in Chapter 4. A parabolic shape of the G" curve was shown for the compounds mixed at 40 and 60 rpm. For MPTES this behaviour was the result of premature scorch during the first mixing step. For the compounds containing DIPTESM and mixed at 100 and 120 rpm this therefore can be an indication of scorch in the first mixing step. At this higher rotor speed, the temperature during mixing increases faster and results in an early initiation of the crosslinking reaction. This crosslinking reaction can only be initiated by the thiophosphoryl part of the coupling agent, since no other curing agents are present in the compound during this first mixing stage.

Temperature sweep measurements as an indicator of scorch sensitivity

The RPA 2000 was used for temperature sweep measurements, performed on the compounds at 0.500 Hz and 49.94% strain in the temperature range from 110 to 200 °C. Results of the G' vs. temperature are given in Fig. 6.3.

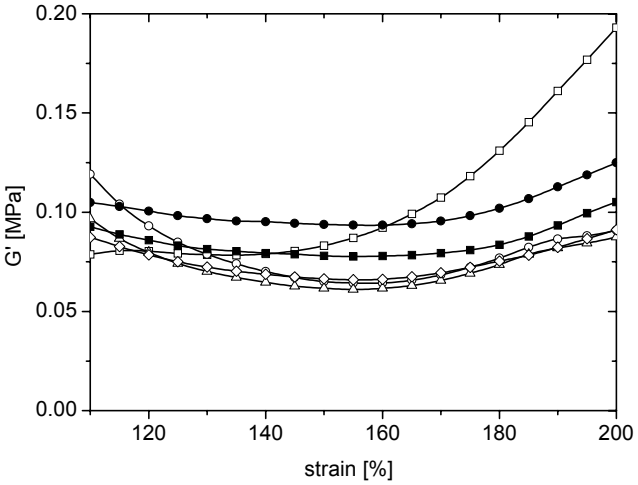

Fig. 6.3: G'-modulus at 50% strain as a function of temperature for the masterbatch mixed at mixed at 40 (○), 60 (△), 80 (◊), 100 (■) and 120 (●) rpm and compared to TESPT (□) mixed at 100 rpm.

The reference compound, containing TESPT shows a marked increase in G' at temperatures above 160 °C, as seen before (Chapter 4 and 5). Reuvekamp et al. [3,4] showed this increase to be the result of crosslinking due to activated sulphur moieties in TESPT. DIPTESM shows this increase in G' at higher temperatures only to a limited extent. The increase in G' for the DIPTESM containing compounds starts at approximately 160 °C, while the increase for the TESPT reference compound already starts at 140 °C. The temperature sweep indicates a better scorch safety for the DIPTESM containing compound. The shielding reaction of the silica surface on the other hand seems to be slower compared to the TESPT reference compound, resulting in more heat generation during mixing, which in turn causes the scorch effect at the final stage of the first mixing step.

The masterbatch mixed at 120 rpm shows a higher G' over the whole temperature range, except for the highest temperature relative to TESPT. This higher G'-modulus again is an indication of scorch in the first mixing step. This scorch effect must be responsible for the increase in torque at the final stage of mixing for this compound.

Brabender mixing step 2

The torque curve in the second mixing step showed a similar order for the different rotor speeds as found in the first mixing step. The mixer torque is highest at a rotor speed of 40 rpm, while at 120 rpm the mixer torque is lowest. At low rotor speeds

of 40 and 60 rpm this high mixer torque, is also reflected in a higher Mooney ML (1+4) 100 °C. The rotor speed seems to be too low to result in a good dispersion of the silica, as indicated by the G'-modulus at low strain. At these low rotor speeds the friction is not strong enough to properly break down the silica network, respectively the temperature remains too low to achieve proper hydrophobation of the silica surface by the coupling agent.

6.3.2 Results for the optimisation of the curing system

Curing behaviour

Different curing systems were applied to the compounds containing DIPTESM, as listed in Table 6.1. The cure properties for the compounds A-D as measured with the RPA 2000 are shown in Fig. 6.4. The differences for these compounds are due to the different amounts of sulphur added.

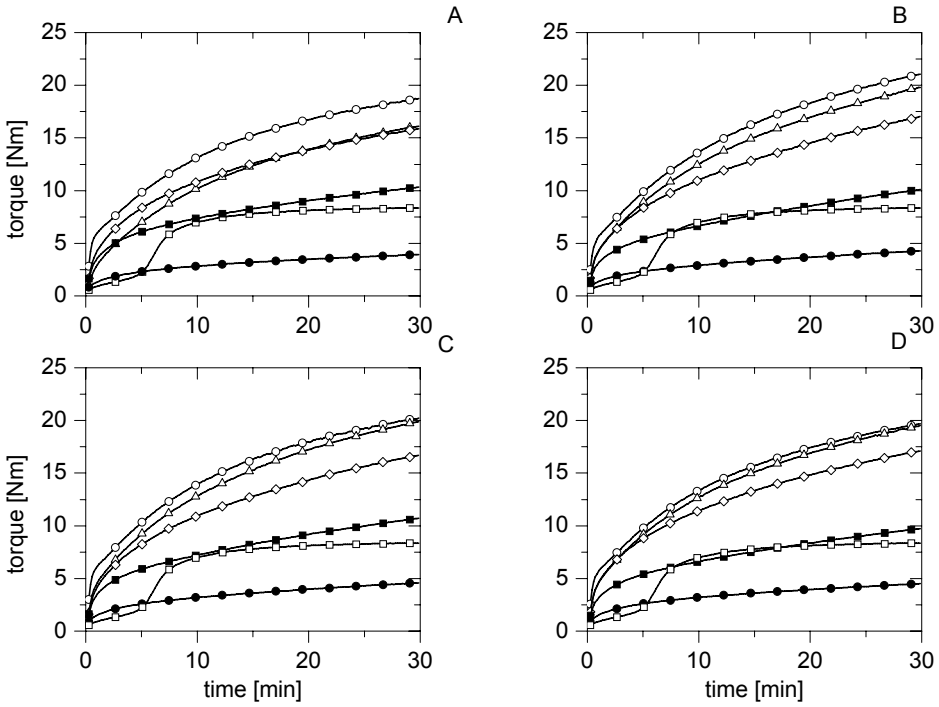

Fig. 6.4: The cure behaviour of compounds for recipes A-D mixed at 40 (○), 60 (Δ), 80 (◊), 100 (■) and 120 (●) rpm and compared to TESPT (□) mixed at 100 rpm.

Comparing the cure curves for the DIPTESM containing compounds to the TESPT reference compound, it becomes clear that the DIPTESM compounds do not properly cure. The torques increase fast at the beginning of cure and keep on increasing, resulting in a marching modulus. The compounds mixed at lower rotor speed show a stronger delta torque when compared to the compounds mixed at higher rotor speeds. This must be the effect of the poorer filler dispersion, as

already seen in Fig 6.2a. Due to a better filler dispersion reached with a high rotor speed of 120 rpm the G'-modulus of that compound is lower, resulting in a significantly lower torque value at the beginning of cure. With increasing crosslink density the torque increases, dependent on crosslink density, but also on minimum torque. The higher the minimum torque to start with, the stronger the increase in torque due to crosslinking. The different shape of the cure-curve compared to that for the TESPT reference compound is very conspicuous and more indicative for the cure characteristics than the absolute value of the torque increase. The accelerator part of the coupling agent seems to be hindered by the coupling to the silica surface, which results in a slower cure reaction and a less developed network.

The cure behaviour of the compounds with the composition corresponding to recipe E is shown in Fig. 6.5. The difference of these compounds compared to the compounds A-D is the extra amount of accelerator added. The same curing system as used for the TESPT-containing reference compound was added.

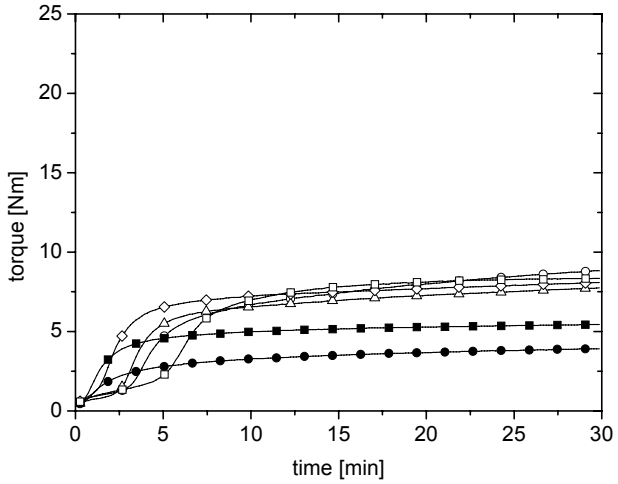

Figure 6.5: Cure behaviour for the compound according to recipe E, mixed at 40 (○), 60 (Δ), 80 (◊), 100 (■) and 120 (●) rpm and compared to TESPT (□) mixed at 100 rpm.

At rotor speeds of 40 and 60 rpm the curing properties show a behaviour similar to the TESPT reference compound, except for a shorter scorch time and a somewhat marching modulus. At higher rotor speeds of 80, 100 and 120 rpm the scorch time becomes much shorter. For the compounds mixed at 100 and 120 rpm the difference between minimum and maximum torque (ΔS') becomes smaller, when compared to the TESPT reference compound. Similar behaviour was found for the MPTES containing compound as described in Chapter 4. For MPTES this lower ΔS' was the result of premature scorch in the first mixing step. At 100 and 120 rpm the compound containing DIPTESM showed scorch in the first mixing step as well. Scorch therefore also seems to be the reason for the lower ΔS' in the current case.

Tensile properties of cured compounds

The results of the measurements of the tensile properties for the compounds mixed at different rotor speeds and cured with different curing packages are shown in Fig. 6.6a – Fig. 6.6e. Fig. 6.6f shows the tensile properties of the compounds A-E mixed at 80 rpm and of the TESPT reference compound mixed at 100 rpm. In Table 6.3 the corresponding values for the E-modulus, stress at 100% strain (M_{100}), stress at 300% strain (M_{300}), tensile strength and strain at break are listed.

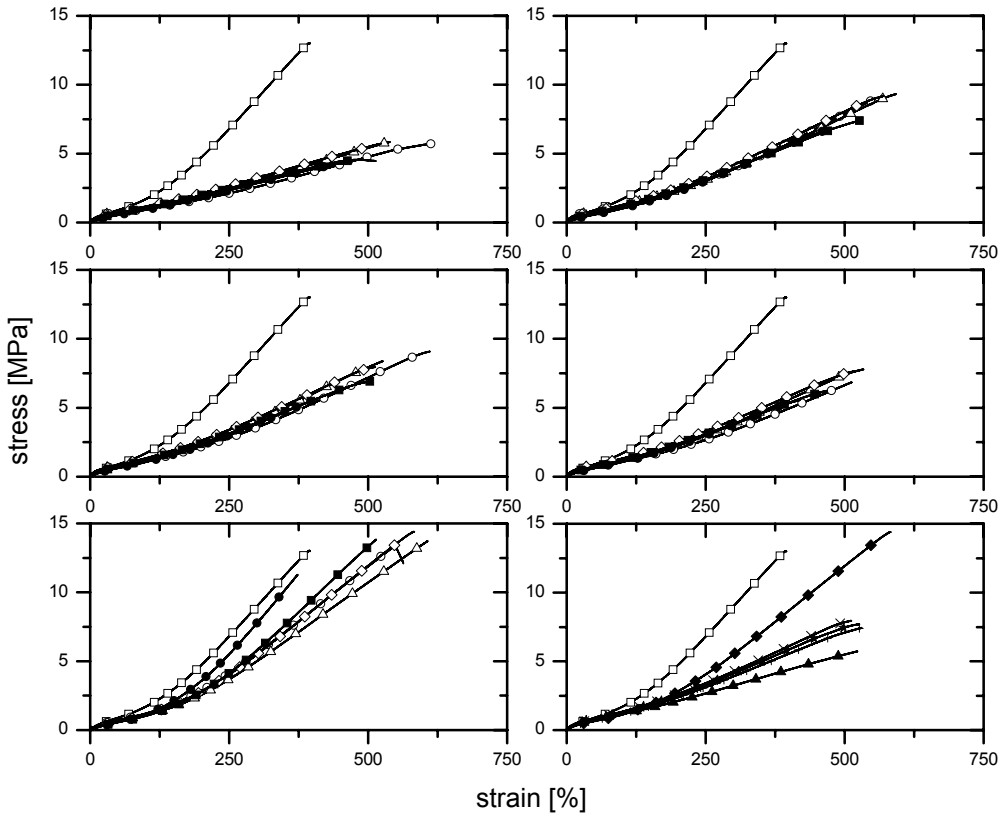

Figure 6.6: Tensile properties for compounds, according to recipes A-E, mixed at 40 (○), 60 (∆), 80 (◊), 100 (■) and 120 (●) rpm and compared to TESPT (□) mixed at 100 rpm and tensile properties for compounds according to recipes A (▲), B (★), C (✚), D (×) and E (◆), mixed at 80 rpm, compared to TESPT (□).

Table 6.3 Mechanical properties of cured compounds, containing different curing packages (recipes A-E) and mixed at different rotor speeds (40-120 rpm).

	E-modulus [MPa]	σ_{break} [MPa]	ε_{break} [%]	M_{100} [MPa]	M_{300} [MPa]	$\frac{M_{300}}{M_{100}}$	tan δ 60 °C	S' 60 °C [dNm]	S" 60 °C [dNm]
1	9.9	13.3	403	1.7	9.0	5.3	0.16	14.7	2.3
40 A	14.7	6.2	648	1.0	2.6	2.6	0.18	30.3	5.4
60 A	14.9	6.4	598	1.2	3.1	2.6	0.19	30.4	5.8
80 A	13.3	6.0	551	1.2	3.2	2.7	0.20	29.3	5.7
100 A	5.0	4.4	513	0.91	2.6	2.9	0.20	22.2	4.4
120 A	2.59	4.5	473	0.92	2.9	3.2	0.20	15.3	3.0
40 B	17.0	9.8	606	1.2	3.9	3.3	0.16	30.2	4.9
60 B	16.0	9.4	598	1.2	3.9	3.3	0.17	29.6	5.0
80 B	13.1	9.0	559	1.3	4.2	3.2	0.18	29.0	5.1
100 B	6.5	7.4	524	1.2	3.9	3.3	0.19	21.6	4.0
120 B	2.5	6.9	478	1.0	3.9	3.9	0.20	15.3	3.0
40 C	16.5	9.0	604	1.1	3.6	3.3	0.16	30.0	4.8
60 C	17.1	8.7	541	1.3	4.1	3.2	0.17	29.3	5.0
80 C	14.2	8.0	508	1.3	4.3	3.3	0.19	29.1	5.4
100 C	7.1	6.9	498	1.2	3.9	3.3	0.20	22.6	4.4
120 C	2.7	6.1	445	1.1	3.8	3.5	0.20	14.8	3.0
40 D	16.1	7.9	583	1.1	3.4	3.1	0.17	29.6	5.1
60 D	17.8	7.9	534	1.3	3.9	3.0	0.18	29.6	5.2
80 D	14.7	7.6	506	1.3	4.1	3.2	0.18	29.6	5.2
100 D	7.3	6.4	489	1.2	3.8	3.2	0.18	21.7	3.8
120 D	3.2	5.6	428	1.1	3.8	3.5	0.19	14.8	2.9
40 E	13.3	14.0	572	1.2	5.6	4.7	0.22	15.8	3.4
60 E	12.1	14.0	621	1.1	5.0	4.5	0.22	14.2	3.2
80 E	6.6	14.4	580	1.1	5.5	5.0	0.20	14.6	2.9
100 E	4.1	14.5	532	1.0	5.8	5.8	0.20	11.1	2.2
120 E	2.1	12.4	396	1.1	7.8	7.1	0.17	7.9	1.4

The tensile properties of the compounds mixed at 100 and 120 rpm are generally inferior to the compounds mixed at 40, 60 and 80 rpm. Especially the E-modulus, tensile strength and strain at break values of the compounds mixed at 100 and 120 rpm are much lower compared to the values for the compounds mixed at 40, 60 and 80 rpm. This must again be a consequence of premature scorch in the first mixing step at a rotor speed of 100 rpm or higher.

Sulphur correction only hardly influences the tensile properties (compounds A-D). The compounds with the highest amount of extra free sulphur added in the curing package show slightly better properties. This is most probably the result of a higher crosslink density due to this extra sulphur. The properties of the compounds A-D are all far inferior to the properties of the TESPT-containing reference compound. For compound E with the accelerator added in the curing package, the tensile properties come closer to the tensile properties of the TESPT reference compound. The increase in tensile stress with strain however is less pronounced when compared to the reference compound. The phenomena described above already indicated an inferior silica dispersion and no optimal shielding of the silica surface for the compounds containing DIPTESM. This is also an explanation for the difference in properties between DIPTESM and the TESPT reference compound. A better silica dispersion and a better shielding of the silica surface must be the

reason for the overall best properties of the TESPT-containing reference compound.

Tan δ measurements at 60 °C as an indicator of rolling resistance
As an indicator of rolling resistance S', S", and tan δ measurements were performed on the cured compounds using an RPA 2000 at 60 °C, 3.49% strain and 15 Hz. The values for tan δ are almost the same for all compounds mixed at the same rotor speed. However, the tan δ at low rotor speed is lower for the compounds without accelerator added: A-D, compared to higher rotor speed. Although tan δ differs somewhat for the compounds mixed at different rotor speeds, much larger differences are seen for the values of S' and S". With increasing rotor speed S' and S" decrease in all cases, which corresponds to the decrease in E-modulus. The rolling resistance of a tyre is not only represented by the tan δ at 60 °C but more by the value of S" at 60 °C for a fixed value of S' at 60 °C, the latter being a measure for the tyre stiffness. When comparing all three values, tan δ, S' and S", the values for the compounds without accelerator mixed at 120 rpm are closest to the values of the reference compound 1. However, other properties show that at this high rotor speed premature scorch takes place in the first mixing step in the internal mixer, overall resulting in inferior properties.

When accelerator is added in the curing package: compound E, tan δ, S' and S" are comparable to the values found for TESPT, for the compounds mixed at 40, 60 and 80 rpm. Contrary to what was seen in the compounds A-D, surprisingly the tan δ now decreases with increasing rotor speed, while S' and S" again slightly decrease. At 100 and 120 rpm the decrease in S' and S" is somewhat stronger for the compounds E. At 80 rpm the values are best comparable to the TESPT reference compound.

6.4 Discussion and Conclusions
Extensive literature has been published describing the reaction of DIPDIS with NR[2,5] as well as with silica.[6,7] The application of DIPDIS in a silica-reinforced NR compound showed that DIPDIS can simultaneously combine with NR and silica during cure and is therefore likely to influence the physical properties of the vulcanisate like silane coupling agents. However it must be noticed that those compounds were prepared by mill mixing. When mixed using an internal mixer, DIPDIS was found to be too scorch sensitive to properly process. The reaction of the isopropyl-group with the silica surface seemed to be much slower than the cleavage of the labile disulphide linkage. Therefore a combination of a silane and DIPDIS was synthesised in the present work, in order to create a coupling agent, which reacts with silica faster or at least with the same reaction rate as the reaction with rubber: diisopropyl triethoxysilylpropyl monosulphide (DIPTESM).
Mixing this DIPTESM into the green tyre rubber compound at different rotor speeds showed an optimum combination of properties at a rotor speed of 80 rpm. Although at this rotor speed the filler dispersion, as represented by the Payne effect, was not the best compared to the higher rotor speeds, no scorch effects were observed. At higher rotor speed the results indicated scorch effects in the first mixing step in the internal mixer, resulting in worse final properties of the compound.

The effect of different amounts of sulphur, added in the third mill mixing step to correct for the lower intrinsic sulphur content of DIPTESM vs. TESPT, on the tensile properties is little pronounced. With increasing sulphur content of the curing package the tensile properties slightly increase, due to a higher crosslink density. However the properties remain far inferior to the TESPT reference compound. The accelerator part of the silane seems to be hindered too much to properly accelerate the curing reaction. This hindering most likely is due to a limited reactivity of the S-S bond. Similar results were found by Mandal and Basu[7] in their study of various diisopropylthiophosphoryl compounds. They studied monosulphidic as well as disulphidic combinations of DIPDIS and other accelerators. The monosulphides in their case showed lower modulus and tensile strength than the disulphides, which was ascribed to the nonavailability of the labile S-S bonds in the case of monosulphides. In earlier work[2] the authors studied the cure synergism of DIPDIS with thiazole based accelerators, concluding that a combination with N-oxydiethylene-2-benzothiazole sulphenamide was a very useful combination of accelerators. Therefore, although in DIPTESM, the thiophosphoryl part was expected to act as an accelerator, an extra amount of accelerator turned out to be necessary to obtain good properties. The addition of accelerator results in a clear increase of the modulus in the tensile properties. The stress at break is doubled compared to the compounds without accelerator added. For the compound mixed at 80 rpm and with accelerator added later in the curing package, the tensile properties are at about the same level as for the TESPT reference compound. Thus, extra accelerator is still needed, but the overall properties of the TESPT-containing reference compound can reasonably be matched. Therefore, a further fine-tuning to find the optimum amount of DIPTESM, accelerator, sulphur, and all in combination with the proper mixer conditions is recommended.

References

1. J. G. Pimblott, G. Scott and J. E. Stuckey, J. Appl. Polym. Sci., 23, 3621 (1979).
2. S. K. Mandal, R. N. Datta and D. K. Basu, Rubber Chem. Technol., 62, 569 (1989).
3. L. A. E. M. Reuvekamp, J. W. ten Brinke, P. J. van Swaaij and J. W. M. Noordermeer, Kautsch. Gummi Kunstst., 55, 41 (2002).
4. L. A. E. M. Reuvekamp, J. W. ten Brinke, P. J. van Swaaij and J. W. M. Noordermeer, submitted to Rubber Chem. Technol.
5. J. G. Pimblott, G. Scott and J. E. Stuckey, J. Appl. Polym. Sci., 19, 865 (1975).
6. S. K. Mandal, R. N. Datta, P. K. Das and D. K. Basu, J. Appl. Polym. Sci., 35, 987 (1988).
7. S. K. Mandal and D. K. Basu, Rubber Chem. Technol., 67, 672 (1994).

Chapter 7

Interactions of Stöber silica with natural rubber under the influence of coupling agents, studied by ^{1}H NMR T_2 relaxation analysis[#]

^{1}H NMR T_2 relaxation has proved to be a successful technique for the study of rubber-filler interactions in carbon black-filled rubbers. For the present study the interactions between NR and pure silica as well as silicas grafted with various coupling agents were investigated using ^{1}H NMR T_2 relaxation. Monodisperse spherical silica particles were used, prepared according to a method by Stöber, and afterwards treated with the coupling agents prior to mixing into NR. Depending on the type of coupling agent and the degree of condensation, grafting densities of coupling agent on the silica range from minimum 62% till 100%. NMR shows that the highest amount of immobilised rubber chains on the silica surface occurs for pure silica: about 15%. Grafting of the silica leads to a decrease of the fraction of immobilised rubber chains, dependent on the chemical structure of the coupling agent and its ability to physically or chemically interact with NR: 13% immobilised rubber for a mercapto-functional coupling agent, which is expected to react with the NR-unsaturation; till about 1% for a coupling agent with only a propyl group extending into the rubber matrix, unable to react. The immobilisation of rubber chains to the silica surface corresponds to the formation of a physical network, which is strong enough to remain intact at 100 °C, even when swollen in a good solvent.

7.1 Introduction

The use of silica for reinforcing rubbers is attracting increasing attention on account of specific properties exhibited by such composites, especially for use in tyres. In comparison with carbon black, silica reduces the rolling resistance of tyres, thus leading to lower fuel consumption. In combination with this lower rolling resistance, silica provides greater wear resistance and superior wet traction.[1,2]

In the case of silica, hydrogen bond interactions between surface silanol groups in agglomerates are very strong in comparison with the interactions between the polar siloxane groups or silanol groups of the silica and the commonly non-polar olefinic hydrocarbon rubbers. This causes great difficulty when mixing silica with rubber.[3,4] Since an optimal reinforcing power can be achieved only if the filler is well-dispersed in the rubber matrix, improving the mixing quality is of major importance. Another factor important to the reinforcing effect of the filler is the chemical or physical interaction between the filler and the rubber. Chemical modification of the

[#] The work described in this Chapter has been accepted for publication in Macromolecules.

silica surface using bifunctional organosilanes enhances the compatibility between hydrocarbon rubber and the silica and leads to remarkable improvements in the mechanical properties of silica-reinforced rubber vulcanisates. Despite numerous studies devoted to these materials,[5-9] the reinforcement mechanism of the silica-filled rubbers has not been clarified to such an extent as that of carbon black-filled rubbers.

Low resolution proton (^{1}H) NMR is one of the few techniques successfully used in the study of rubber-filler interactions in carbon black and silica-filled rubbers.[10-16] In all these studies physical adsorption of rubber chains onto the surface of the filler is observed, causing significant immobilisation of the rubber chains in the vicinity of the filler surface. This immobilisation is in most cases interpreted as bound rubber resulting from interactions between the filler and the rubber. This immobilised bound rubber consists of two micro-regions with strongly differing local chain mobilities: a tightly bound, low-mobility, almost rigid phase, which directly covers the filler surface, and a loosely bound, highly mobile rubber phase remote from this interface. A physical network exists due to absorption of rubber chains to the silica surface. Grafting of silica in particular with methanol or hexadecanol was shown to decrease the ability of the filler to exchange strong interactions with the surrounding rubber.[14] Modification of the surface activity by grafting was associated with a change in the proportion of tightly to loosely bound rubber. Less active sites remaining after the grafting with either alcohol resulted in a smaller tightly bound rubber component. If the filler, with or without grafting with coupling agent, is compounded into the rubber matrix, a third phase comes into play with an even higher mobility than the other two.

In previous studies, as mentioned above, generally silica and/or carbon black were modified with alcohols. Each alcohol molecule can react with only one silanol group in the silica. In the case of silica-reinforced compounds silanes containing three alkoxy groups per silicon atom are commonly used as grafting agents, allowing for a maximum of three reactions with silanols on the silica. With the aim of achieving a better understanding of the typical silica performance in tyre applications, ^{1}H NMR T_2 relaxation experiments are used in the present study to investigate the modification of the silica surface with various silane coupling agents and the consequent effect of this on natural rubber (NR) – silica interactions. Silica-reinforced passenger car tyre treads normally consist of a solution styrenebutadiene rubber/ butadiene rubber (S-SBR/BR) blend.[17] Truck tyres are commonly composed of NR. NR was chosen for this study, because the relaxation of the styrene moieties in S-SBR tends to interfere with the relaxation of the interface between the rubber and the silica filler. Further, monodisperse spherical silica particles were used for this study in order to avoid the effect of irregularities in the surface roughness of the silica, which could result from peculiarities of the various production processes employed for the synthesis of silica.[1] Using these monodisperse silica particles, complication of data as a result of surface roughness could be avoided.

7.2 Experimental section

Materials

Ethanol (Lamers & Pleuger, technical grade) and tetraethoxy silane (TES) (Fluka, purity ≥ 98%) were freshly distilled. Ammonium hydroxide (Merck, 25%) was of analytical reagent quality and contained 15.6 mol/l ammonia (NH_3) as indicated by titration. Monodisperse silica particles were synthesised in accordance with the method described by Stöber.[18] The reaction temperature was set at 20 °C. Spherical particles (average diameter 40 nm) were prepared in a mixture of ethanol and ammonia (25%) by the polymerisation of silicic acid, formed by the hydrolysis of TES. The final particle size can be pre-determined by the initial concentration of the reactants.[18] Concentrations of the reactants were set at 0.17 M TES and 0.65 M NH_3. The preparation and properties of non-aqueous model dispersions of chemically modified, charged silica spheres, has further been described in detail by Philipse and Vrij.[19]

Surface silanol groups on these silica particles are claimed to react readily with silane coupling agents.[19] The silica particles were grafted with, respectively, propyltriethoxy silane (PTES) [Gelest Inc., ABCR GmbH & Co.], 3-mercaptopropyltriethoxy silane (MPTES) [Gelest Inc., ABCR GmbH & Co.], bis(triethoxysilylpropyl) tetrasulphide (TESPT) [OSi Specialties, Crompton Corporation, Silquest® A-1289 silane] and 2-benzothiazyl-(3-triethoxysilyl)propyl disulphide (triethoxysilylpropyl benzothiazole disulphide, TESBD) by hydrolysis and subsequent silanisation under reflux conditions in the silica/ethanol dispersion. Structures of the coupling agents are listed in Fig. 7.1.

PTES:

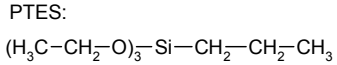

MPTES:

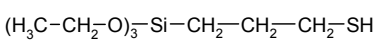

TESBD:

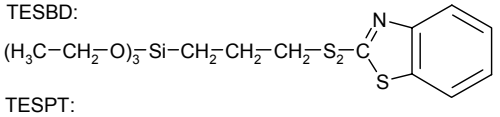

TESPT:

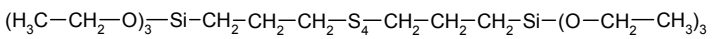

Fig. 7.1:Chemical structures of the silane coupling agents.

TESBD was synthesised from MPTES and dibenzothiazole disulphide (MBTS) [Merck, >98%]. MBTS (16.63 g) was dissolved in 210 ml toluene by heating at reflux temperature. 11.92 g 3-mercaptopropyltriethoxy silane was added dropwise to the clear yellow solution. After 2 hours 90.6 mol.% of the product and 9.4 mol.% of tetraethoxysilylpropyl disulphide (TESPD) was formed. Impurities in the product were removed by washing with diethyl ether. The TESPD by-product could not be removed by washing with diethyl ether and remained in the TESBD as an impurity. ^{1}H NMR spectra recorded at 300 MHz in deuterated chloroform, $CDCl_3$, were used to confirm the structure of the product: δ0.78 (t, 2H); δ 1.22 (m, 9H); δ 1.96 (m, 2H);

δ 2.72 (t, 2H), due to impurity of TESPD; δ 3.02 (t, 2H); δ 3.84 (q, 6H); δ 7.18-7.58 (m, 2H); δ 7.80-7.96 (m, 2H).

Natural rubber [SIR 20] was purified by dissolving in 1,1,2,2-tetrachloroethane [Aldrich, 98%] and filtering over a glass filter. Samples were dried in a vacuum oven at 60 °C.

Sample preparation for the NMR experiments

In order to obtain a quantitative measure of the influence of network junctions – of a chemical and/or physical nature – on the T_2 relaxation, a vulcanised gum stock of 100 phr pure NR was studied. For this purpose, pure NR was mixed on a two-roll mill with 3.05 phr CBS, 1.75 phr S, 5 phr ZnO and 2.5 phr stearic acid and subsequently vulcanised in a hydraulic press at 145 °C for a duration corresponding to $t_c(90)$, determined by cure meter testing.

To prepare NR-silica mixes containing approximately 160 phr silica, NR dissolved in 1,1,2,2-tetrachloroethane was mixed with the various silica samples dispersed in ethanol. The ethanol and 1,1,2,2-tetrachloroethane were evaporated, while the mixes were continuously stirred to improve dispersion of silica. The samples were subsequently dried in a vacuum oven under N_2 flow at 100 °C for 72 hrs. Approximately 0.2 g of the pure NR and of the mixtures of NR with silicas was introduced into a 9 mm diameter NMR tube of 180 mm length. The sample mass was about the same for all the samples: 0.2022 ± 0.0033 g. For purposes of comparison, experiments were also performed on pure silica samples. The quantity of silica taken for these experiments was equal to the quantity of silica present in the silica-filled NR. This allowed determination of the contribution of the silica protons to the transverse magnetisation of silica-filled NR.

7.2.1 Solid state NMR experiments and data analysis

Equipment

^{29}Si MAS and CP/MAS NMR spectra were recorded on a Varian Unity - 200 MHz wide-bore NMR spectrometer operating at an ^{29}Si frequency of 38.73 MHz. The experiments were performed using a 7 mm CP/MAS probe. The ^{29}Si 90° pulse width was approx. 6.5 μs.

Proton NMR T_2 relaxation experiments were performed on a Bruker Minispec NMS-120 spectrometer. This spectrometer operates at a proton resonance frequency of 20 MHz. The length of the 90° pulse and the dead time were 2.8 μs and 7 μs, respectively. A BVT-3000 temperature controller was used for temperature regulation. The temperature gradient and stability were better than 1 °C.

^{29}Si NMR experiments

^{29}Si NMR experiments were performed on pure and grafted silicas, as well as on the original coupling agents in order to characterise the grafted silicas. The experiments were carried out with magic angle spinning (MAS), using high-power proton decoupling and a spinning frequency of 2.2 kHz and 6 kHz for the coupling agent and silicas, respectively. The cubic octamer silicic acid trimethylsilyl ester

(Q_8M_8)[20] was used to optimise the Hartmann-Hahn condition for the ^{29}Si cross-polarisation CP/MAS experiments. ^{29}Si spectra were referred to the methyl resonance of Q_8M_8 at 11.7 ppm relative to the internal standard tetramethyl silane (TMS). ^{29}Si CP/MAS spectra were recorded with a cross-polarisation time of 8 ms. A recycle time of 1.5 sec and 30 sec was used for the CP/MAS and single-pulse excitation MAS experiments, respectively. The number of scans was 200 for the MAS and 150000 – 200000 for the CP/MAS experiments.

^{1}H NMR T_2 relaxation experiments

Two different pulse sequences were used to record the decay of the transverse magnetisation (T_2 decay) for both the almost rigid (1) and the mobile (2) fractions of the samples described previously[12]. (1): A solid echo pulse sequence (SEPS), $90°_x$ - t_{se} - $90°_y$ - t_{se} - [acquisition of the amplitude of the transverse magnetisation A*(t)*], with t_{se} = 9 μs was used to measure the T_2 free induction decay. The point in time after the first pulse $t = 2t_{se} - t_{90}/2$ was taken as zero, where $t_{90}/2$ is the half time of the 90° pulse. (2): a Hahn echo pulse sequence (HEPS), $90°_x$ - t_{He} - $180°_x$ - t_{He} - [acquisition *A(t)* of the amplitude of an echo maximum], was used to record the slow part of the T_2 relaxation decay for the mobile fraction of the samples, where t_{He} was varied between 35 μs – 400 ms. The second pulse in the HEPS inverts nuclear spins of mobile molecules only, and an echo signal is formed with a maximum at time $t = 2t_{He} - t_{180}/2$ after the first pulse, where $t_{180}/2$ is the half time of the 180° pulse. By varying the pulse spacing in the HEPS, the amplitude of the transverse magnetisation A(*t*) is measured as a function of time *t*. HEPS makes it possible to eliminate the magnetic field and chemical shift inhomogeneities, and to measure the T_2 relaxation time for mobile materials accurately.

Measurements on samples swollen in 1,1,2,2-deuterated tetrachloroethane ($C_2D_2Cl_4$) were performed in order to gain insight into the strength of interactions between (grafted) silica and NR and the heterogeneity of the NR-silica physical network.

The time constants (T_2 relaxation time) characteristic of different rates of the magnetisation decay curve were obtained by performing a least squares fit of the data with the Weibull function, or a linear combination of the Weibull function and exponential functions. Depending on the system studied, one, two or three components were used for the fit. It was not statistically significant to use a series of more than three components fit for these purposes. The different fitting functions used will be detailed in the relevant paragraphs with the results.

The relaxation component and its relative amplitude, originating from almost rigid material on the silica surface and from tightly bound rubber in the mixtures was determined by fitting SEPS data for pure as well as grafted silica-filled NR. Only the initial part of the decay ($t < 400\mu s$) was fitted. In this fit, the base line was fixed to the value that was measured under the same conditions after the sample was removed from the NMR probe. The relaxation component arising from the relaxation of loosely bound rubber and free, extractable rubber $(T_2^{in})^{NR}$, and $(T_2^{l})^{NR}$, respectively, and their respective fractional amplitudes $A(0)^{in}$ and $A(0)^{l}$ were determined from the fit of the HEPS data. The HEPS was also used for the

measurement of the T_2 decay for non-vulcanised and vulcanised NR non-reinforced gum stock. Details of the fitting functions and the corresponding symbols for the various systems investigated are shown in Figs. 7.2a-c and Table 7.1.

Table 7.1 The fitting functions used for the least squares fit of the data for the various systems studied, designation of relaxation components, α-parameter in the fitting functions and pulse sequences used.

Sample	T_2^{short}	$T_2^{intermediate}$	T_2^{long}
Silica	-	-	$(T_2^l)^{OH}$/SEPS
Silica + $C_2D_2Cl_4$	-	-	$(T_2^l)^{OH}$/SEPS
Grafted silica	$(T_2^s)^{sil}$/SEPS/α=1.34	-	$(T_2^l)^{OH}$/SEPS
Grafted silica + $C_2D_2Cl_4$	$(T_2^s)^{sil}$/SEPS/α=1.34	-	$(T_2^l)^{OH}$/SEPS
NR	-	-	$(T_2^l)^{NR}$/HEPS
NR + $C_2D_2Cl_4$	-	-	$(T_2^l)^{NR}$/HEPS
NR + silica	$(T_2^s)^{sil+NR}$/SEPS/α=1.34	$(T_2^{in})^{NR}$/HEPS	$(T_2^l)^{NR}$/HEPS
NR + silica + $C_2D_2Cl_4$	$(T_2^s)^{sil+NR}$/SEPS/α=1.34	$(T_2^{in})^{NR}$/HEPS	$(T_2^l)^{NR}$/HEPS

Fitting function for hydrophilic silica:

$$A(t) = A(0)^{OH}\ e^{[-t/(T_2^l)^{OH}]^{\alpha}} \qquad (7.1a)$$

Fitting function for grafted silicas:

$$A(t) = A(0)^{sil}\ e^{[-t/(T_2^s)^{sil}]^{\alpha}} + A(0)^{OH}\ e^{[-t/(T_2^l)^{OH}]} \qquad (7.1b)$$

Fitting function for NR filled with (grafted) silica:

$$A(t) = A(0)^{sil+NR}\ e^{[-t/(T_2^s)^{sil+NR}]^{\alpha}} + A(0)^{in}\ e^{[-t/(T_2^{in})^{NR}]} + A(0)^{l}\ e^{[-t/(T_2^l)^{NR}]} \qquad (7.1c)$$

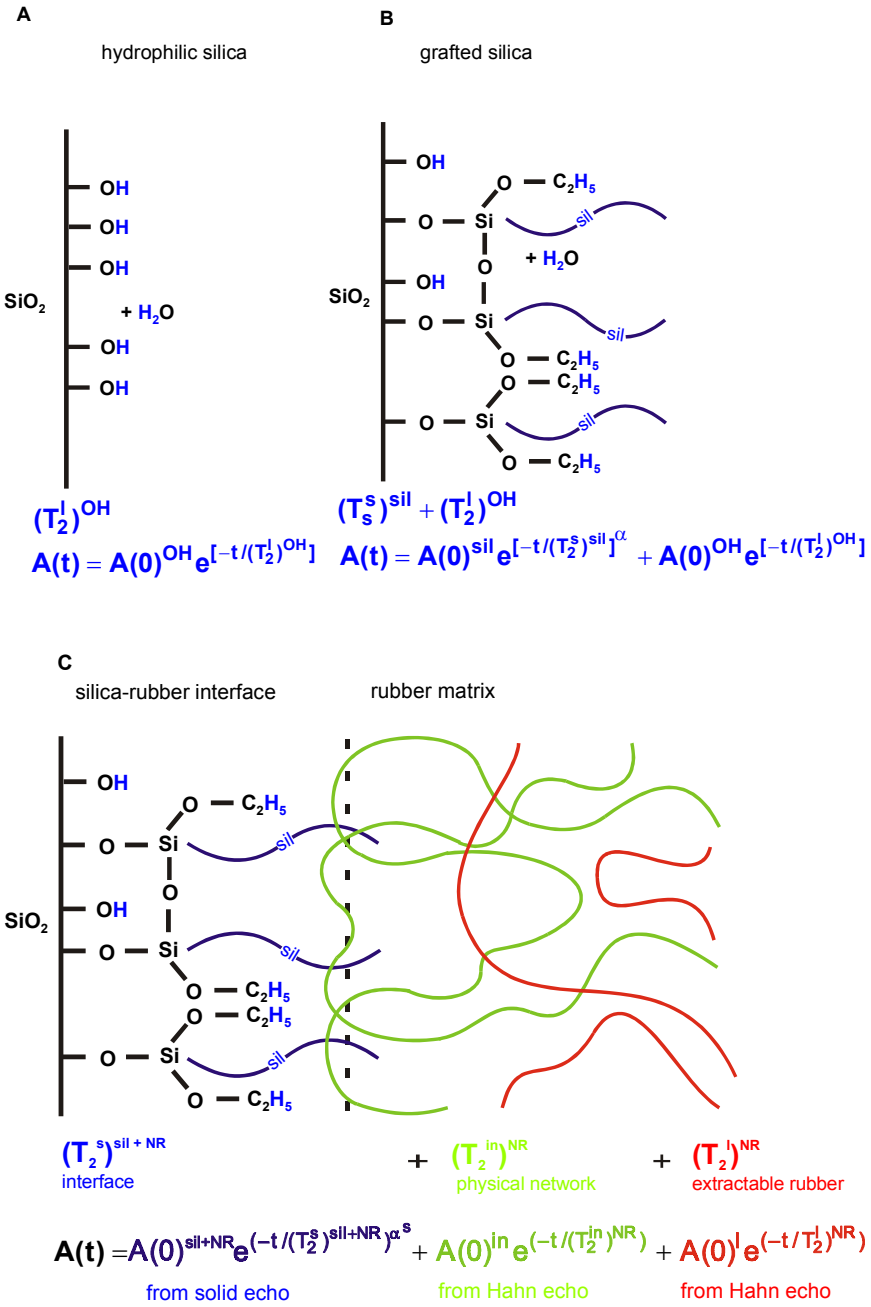

Fig. 7.2: The molecular origin of the different relaxation components for hydrophilic silica (A), grafted silicas (B) and silica-filled NR in the swollen state (C) and the fitting functions used.

7.4 Results and discussion

7.4.1 Characterisation of the silica samples

The particle diameter of the silica particles obtained from the Stöber synthesis, as determined using transmission electron microscopy, was 44 ± 6 nm: Fig. 7.3. The

water content of the pure and silane-grafted silica samples was determined using the Karl-Fisher method (200 °C) and is listed in Table 7.2. The water content is slightly lower for the grafted silicas, as might be expected on account of the decrease in the silanol group content, these being the sites of water adsorption.

Table 7.2 Results of elemental analysis (percentages by weight) of hydrophilic and grafted silica particles[a)] and the minimum possible grafting density estimated in % of reacted silanol groups.

Sample	C (%)	H (%)	N (%)	S (%)	H_2O (%)	Min. grafting density (%)
SiO_2	0.59 ± 0.06	1.16 ± 0.08	-	-	4.88 ± 0.02	-
SiO_2-PTES	4.35 ± 0.04	1.75 ± 0.05	-	-	4.56 ± 0.02	91.6
SiO_2-MPTES	5.13 ± 0.02	1.75 ± 0.07	-	0.57 ± 0.04	4.64 ± 0.07	90.7
SiO_2-TESBD	6.50 ± 0.01	1.89 ± 0.07	0.18 ± 0.02	1.03 ± 0.09	4.06 ± 0.10	75.0
SiO_2-TESPT	5.69 ± 0.03	1.81 ± 0.14	-	1.15 ± 0.04	4.65 ± 0.08	62.2

[a)] Errors correspond to differences in duplicate results.

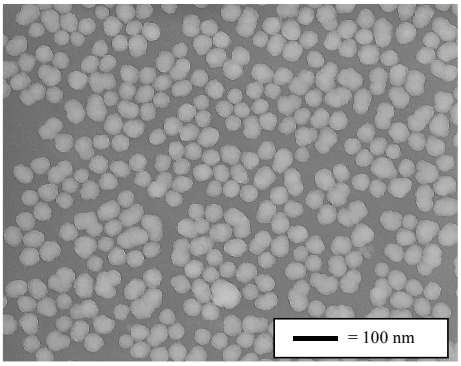

Fig.7.3: Transmission electron micrograph of the hydrophilic Stöber silica particles.

^{29}Si and ^{13}C NMR spectroscopy has been used in the past to study grafting of coupling agents to silica surfaces. It was shown by Caravajal *et al.*[21], Pursh *et al.*[22], Derouet *et al.*[23], Simonutti *et al.*[24] and Hunsche *et al.*[25] that the method provides quantitative information about the reactivity of different types of silanol groups on the silica surface facing the coupling agent, as well as on the fraction of various grafted structures formed at the silica surface. ^{29}Si CP/MAS spectra for the pure SiO_2 and MPTES-grafted SiO_2 are shown in Fig. 7.4 as examples. The spectra reveal a broad signal with overlapping peaks at –91, –100 and –109 ppm that originate from, respectively, $SiO(OH)_2$ (Q^2), $SiO_{3/2}(OH)$ (Q^3) and SiO_2 (Q^4) atoms of the silica. A second group of very small peaks in the range from –48 ppm to –66 ppm results from resonances of the reaction products of alkenyltriethoxy silanes with silanol groups on the silica surface. A resonance for pure, unreacted coupling agents is observed at approx. 46.5 ppm. The silicon atoms of mono-, bi- and tri-

substituted alkenyltriethoxy silanes have chemical shifts of approx. –49, –58 and –66 ppm, respectively. It must be noted that these resonances may originate not only from silane-grafted SiO_2 material but also from hydrolysed alkenyltriethoxy silanes and condensation products of the coupling agents.[26] The presence of resonances in the range from –48 to –66 ppm for MPTES-, TESPT- and TESBD-grafted silica proves that the silica surface is modified by the chemical reaction of the coupling agents and/or by physical adsorption of alkenyltriethoxy silanes and their condensation products. Due to the low intensity of these resonances, no accurate information can be obtained about the fraction of mono-, bi- and tri-substituted silicon atoms. For the PTES-grafted silica no resonance was measured in the range from –48 to –66 ppm. The coupling agent content on the silica surface seems to be below the detection limit of the recorded NMR spectrum.

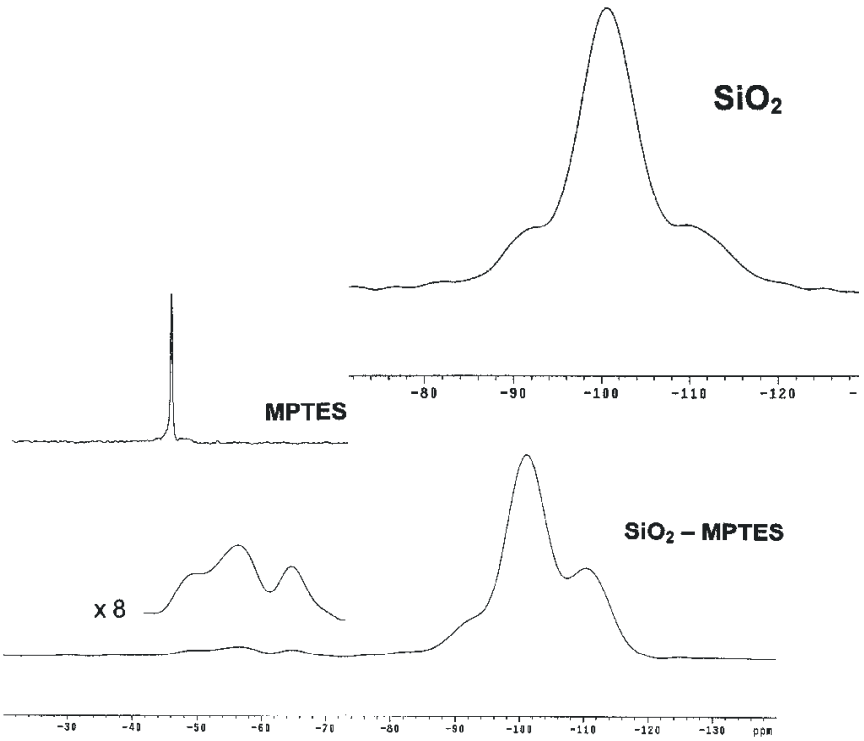

Fig.7.4: ^{29}Si CPMAS spectra for hydrophilic silica and silica-MPTES. The ^{29}Si MAS spectrum for liquid MPTES is shown on the insert.

Additional information about the grafting density could be obtained from the ^{29}Si resonances at –91 till –109 ppm. It has been established by Sindorf and Maciel[27] that the fraction of Q^2, Q^3 and Q^4 silicon atoms can be determined at a cross-polarisation time (τ_{cp}) of approx. 10 ms, which is similar to the 8 ms employed in the present study. The high intensities of the resonances at –91 and –100 ppm indicate the presence of significant quantities of unreacted hydroxyl groups on the

surface and in the pores of the silica particles, which have not reacted with a coupling agent. But as stated before, NMR is not able to provide quantitative information about the grafting density of coupling agents on the silica, owing to the presence of condensation products of the coupling agents.

Elemental analysis was therefore used to obtain additional information about this surface coverage. Results are also listed in Table 7.2. It is important to note, that elemental analysis also does not fully answer the question about grafting density: it does not discriminate between chemically grafted coupling agent and physically adsorbed material; it depends on the way the coupling agent is condensed on the silica surface. For sake of clarity, the word “grafting density”, will be used throughout the text, with the understanding that not only chemical but also physical surface coverage is included. The carbon content found for the grafted silicas is greater than for the corresponding non-grafted silica particles, confirming the presence of silane grafted to the silica surface. The carbon content of the pure, non-grafted silica must be due to C_2H_5 groups, since no other organic groups are involved in their synthesis. A range of possible grafting densities can now be derived from these elemental analyses as shown below for SiO_2-PTES, as an example. For that purpose one has to realise that the calculated surface coverage depends on the degree of condensation. Zhuravlev and other authors[28-30](and references in the publications of these authors) measured the OH group concentration of 100 different amorphous precipitated silicas and concluded that irrespective of their preparation method and their structural characteristics the number of silanols per unit surface area is a physico-chemical constant equal to approx. 5 groups/nm^2 SiO_2. Assuming that only one ethoxy group of PTES has reacted with one silanol group on the silica surface and that no mutual condensation of the other two ethoxy silane groups has taken place, a grafting density of 91.6% of the silanol groups on the silica surface can be derived from the carbon content. This value corresponds to the minimum grafting density, since the grafting density becomes even higher (till > 100%) if more than one ethoxy group of PTES has reacted either with silanol groups on the silica surface or by condensation between adjacent grafted silanes. Although peaks in the range –48 ppm to –66 ppm in the ^{29}Si-NMR spectra indicated the presence of such condensation products and of grafting, they were insufficiently quantitative to determine the relative contribution of either way of condensation. It can merely be concluded that the grafting density is at least 91.6%. In a similar manner minimum grafting densities for MPTES, TESBD and TESPT of 90.7%, 75.0% and 62.2% are estimated, respectively. One reason for the grafting density being lower than 100% may, as been noted before by Chung, Kinney and Maciel,[31] be that some of the silanol groups on the porous silica surface, presumably those occluded in the porous particle, are barely accessible for silylation.

It further appears from the ^{29}Si-NMR data that the number of ethoxy silane groups, which remain unreacted is greatest for the silica-TESPT sample, compared to the other silane-grafted silica samples. This may be due to a lower grafting density, but may also be because TESPT has double the quantity of ethoxy groups compared with the other silanes, leading to a greater quantity of possibly unreacted ethoxy

groups. Another explanation can be the larger sterical hindrances involved with TESPT.

7.4.2 Identification of a temperature to analyse network density

In order to reveal the influence of network junctions on the relaxation behaviour of NR, the temperature-dependence of ^{1}H NMR T_2 relaxation was measured for non-vulcanised and vulcanised NR non-reinforced gum stock: Fig. 7.5. The T_2 relaxation time for non-vulcanised NR increases continuously with rising temperature in the range studied. This behaviour is commonly attributed to an increase in the amplitude and the frequency of large spatial-scale chain motions. By contrast with the non-vulcanised sample, the vulcanisate exhibits only a moderate increase in T_2 when the temperature increases. The difference in T_2 values for the samples is therefore related to the effect of crosslinking. It must be noted, however, that the temperature-dependence of the T_2 relaxation for the present NR vulcanisate does not show a well-defined high temperature "rubber plateau", unlike well-cured rubbers.[32-34] This suggests that the vulcanisate still contains a significant fraction of network defects, such as chain loops, dangling chain ends, loosely crosslinked moieties and residues of non-vulcanised material. It appears from the results in Fig. 7.5 that a difference in T_2 values above 80 °C between non-vulcanised and vulcanised NR can be used as a quantitative measure of the density of network chains.

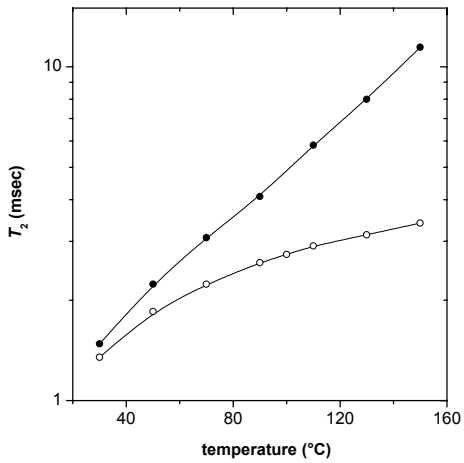

Fig.7.5: Temperature-dependence of the T_2 relaxation time for non-vulcanised (●) and vulcanised NR (○).

7.4.3 Immobilisation of rubber chains at the silica surface and the nature of the physical rubber-filler network for non-vulcanised samples

T_2 relaxation experiments for all unmodified and grafted silicas and silica-filled NR compounds were performed at 100 °C. At this temperature the results can to a greater or lesser extent be related quantitatively to the volume-average density of physical junctions in the silica-filled NR. The amount of silica taken for the experiment was equal to that in the silica-filled NR compounds. Since the

experimental set-up used for the experiments with the silicas and silica-filled NR compounds was the same, this enables the contribution made by the silica protons to the relaxation of the silica-filled NR to be determined.

7.4.4 Molecular mobility at the surface of hydrophilic and grafted silicas

The decay of the transverse magnetisation, the T_2 decay, for pure silica can be described with a single exponential function with the characteristic decay time $(T_2^I)^{OH}$ of 0.1 ms (Fig. 7.2a, Fig. 7.6a and Table 7.3). Hydrogen atoms of adsorbed water, silanol hydrogen on the silica surface and protons of residual ethanol apparently cause this relaxation.

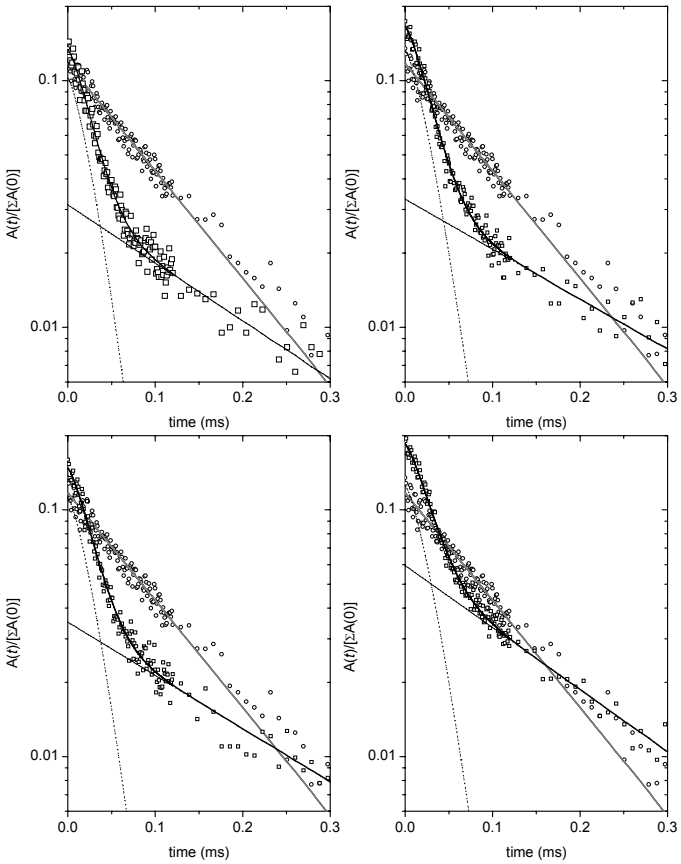

Fig.7.6: Decay of the transverse magnetisation at 100 °C for hydrophilic silica (○ and grey line), (Fig. 7.6a – d) and for silica grafted with PTES (□), (Fig. 7.6a), MPTES, (Fig. 7.6b), TESBD, (Fig. 7.6c) and TESPT, (Fig. 7.6d). The decays are measured with the SEPS and normalised to the total amplitude of the transverse magnetisation [ΣA(0)] measured for silica filled NR containing the same amount of silica. Solid, black lines represent the result of a least squares fit of the decay. For the grafted silica the separate components are represented by dotted lines. Fitting functions and the relaxation parameters are given in Tables 7.2 and 7.3, respectively.

The T_2 decay for the non-compounded grafted silicas can be fitted by two distinct components, which are characterised by a $(T_2^s)^{sil}$ of approximately 0.03 ms, and a $(T_2^l)^{OH}$ of 0.16 - 0.19 ms (Fig. 7.2b, Figs. 7.6b-e and Table 7.3). The relative fractions of these components are represented by $A(0)^{sil}$ and $A(0)^{OH}$, respectively. These fractions are proportional to the hydrogen content of the material responsible for this relaxation. The short relaxation time $(T_2^s)^{sil}$ in grafted silicas is most probably caused by relaxation of the grafted chains. This relaxation time is only slightly longer than that for glassy materials (≈0.01 – 0.02 ms), suggesting a strong immobilisation of the grafted chains on the silica surface. The long relaxation time $(T_2^l)^{OH}$ for grafted silicas is most probably caused by adsorbed water and possibly also by mobile free chain ends of the grafted and/or adsorbed material. The amplitude of this component, $A(0)^{OH}$, represents 20 – 32% compared to that observed for pure silica. This indicates that grafting of coupling agents is accompanied by a decrease in the amount of adsorbed water on the silica surface. A small decrease in the amount of adsorbed water had already been found previously (part 7.3.1) by the Karl-Fisher determination.

Table 7.3 ^{1}H NMR T_2 relaxation times and the fractional amplitude of the relaxation components, as measured at 100 °C for silica samples.

Sample	$(T_2^s)^{sil}$ (ms)	$(T_2^l)^{OH}$ (ms)	$A(0)^{sil}$	$A(0)^{OH}$
SiO_2	-	0.100 ± 0.002	-	100
SiO_2-PTES	0.032 ± 0.001	0.17 ± 0.02	68 ± 3	32 ± 7
SiO_2-MPTES	0.029 ± 0.001	0.18 ± 0.03	77 ± 3	23 ± 9
SiO_2-TESBD	0.031 ± 0.001	0.21 ± 0.03	80 ± 2	20 ± 8
SiO_2-TESPT	0.030 ± 0.001	0.20 ± 0.03	76 ± 3	24 ± 9

7.4.5 Rubber-filler interface in non-swollen silica-filled NR

The situation for rubber filled with grafted silica is represented in Fig. 7.2c. Two main micro-regions can be distinguished, the rubber-silica interface, which is almost glassy (black, measured with SEPS) and the rubber matrix (dark + light grey, measured with HEPS). The network region in the rubber matrix gives rise to two different relaxation times, one originating from rubber loosely bound to the silica (light grey), which forms a physical network, and one arising from free, extractable rubber (dark grey). No statistically relevant data can be obtained by fitting of the relaxation of almost rigid material with two components. In consequence, the relaxation of the –OH, the grafted silanes and immobilised NR is represented by one relaxation time.

The normalised amplitude of the relaxation component with the short decay time, $A(0)^{sil+NR}$, is larger by about a few percent than that of the pure initial silicas, $A(0)^{OH}$ + $A(0)^{sil}$: Fig. 7.7. This indicates that a small fraction of chain units of NR is strongly immobilised by interactions with the silica surface. Since direct chemical attachment of rubber chains to the silica surface is improbable, the immobilisation must be caused by physical adsorption of NR on the silica surface. An exception is the MPTES-grafted silica, for which there is evidence that the –SH- group of the MPTES is highly reactive towards rubber.[35,36] The value of $(T_2^s)^{sil+NR}$ is comparable to that of pure NR in the glassy state: 0.0101 ± 0.0001 ms. Apparently, a shell of glass-like adsorbed NR is formed on the silica surface.

The relaxation component with the longer decay time has a rather complex shape. This component originates from the relaxation of the rubber matrix outside the interfacial layer: Fig. 7.2c. A single exponential does not suffice in this case. The significant deviation from a single exponential relaxation is due to the complex origin of the relaxation itself[37] and an apparent heterogeneity of the samples studied. Due to filler aggregation, which results in a heterogeneous distribution of physical rubber-filler junctions, analysis of the heterogeneous distribution of adsorption network junctions in the compounds is made more difficult by the effect of chain entanglements. Due to these reasons quantitative analysis of the relaxation components with respect to network structure in samples as a whole is complicated. On the time scale of the NMR experiment – of the order of milliseconds – the chain entanglements restrict the long spatial-scale chain dynamics in the same way as do chemical or physical adsorption junctions.[34] It has been demonstrated that valuable information concerning the structure of heterogeneous networks can be obtained by means of ^{1}H NMR T_2 relaxation experiments for swollen rubbers.[12]

7.4.6 Rubber-filler interactions and the structure of physical networks in swollen samples

The T_2 for swollen silica-filled NR consists of three components with short, $(T_2^s)^{sil+NR}$, intermediate, $(T_2^{in})^{NR}$, and long, $(T_2^l)^{NR}$, decay times (Table 7.4 and Fig. 7.2c and 7.7). Again the normalised amplitude, $A(0)^{sil+NR}$, is a few percent larger than that of pure initial silicas, $A(0)^{sil}$: Table 7.5. The values of $(T_2^s)^{sil+NR}$ and $A(0)^{sil+NR}$ are barely affected by swelling, suggesting rubber-filler interactions so strong that they remain even in the presence of a good solvent at 100 °C. Table 7.6 gives estimated fractions of NR immobilised on the silica surface. For swollen samples a significant distinction can now be made in relaxation times of loosely bound and free rubber in the rubber matrix. $(T_2^{in})^{NR}$ is in a range that is typical of network chains. This relaxation component has been assigned to a bound fraction of NR, similar to that in carbon black-filled EPDM[12]. The longest decay time $(T_2^l)^{NR}$ of 16 – 50 ms is comparable to that of swollen non-vulcanised NR (39 ms). This component must therefore be assigned to the relaxation of free rubber chains, which have hardly any attachment to the silica surface.

Table 7.4 ^{1}H NMR T_2 relaxation times and the fractional amplitude of the relaxation components of pure NR and silica-filled NR swollen in 40 vol.% 1,1,2,2-$C_2D_2Cl_4$, as measured at 100 °C. The volume fraction of the solvent for silica filled NR corresponds to the solvent content in the rubber matrix.

Sample	$(T_2^s)^{sil+NR}$ (ms)	$(T_2^{in})^{NR}$ (ms)	$(T_2^l)^{NR}$ (ms)	$A(0)^{sil+NR}$	$A(0)^{in}$	$A(0)^l$
NR	-	-	39.3 ± 0.2	-	-	100
NR + SiO_2	0.027 ± 0.003	0.57 ± 0.02	25.6 ± 0.5	11 ± 6	32 ± 2	57 ± 1
NR + SiO_2-PTES	0.029 ± 0.002	0.73 ± 0.06	16.0 ± 0.4	13 ± 4	23 ± 4	64 ± 2
NR + SiO_2-MPTES	0.027 ± 0.002	0.55 ± 0.03	50.2 ± 0.9	19 ± 3	31 ± 2	50 ± 1
NR + SiO_2-TESBD	0.028 ± 0.002	0.83 ± 0.05	17.8 ± 0.9	17 ± 3	46 ± 2	36 ± 3
NR + SiO_2-TESPT	0.028 ± 0.002	0.90 ± 0.07	27.0 ± 0.7	18 ± 3	25 ± 3	57 ± 2

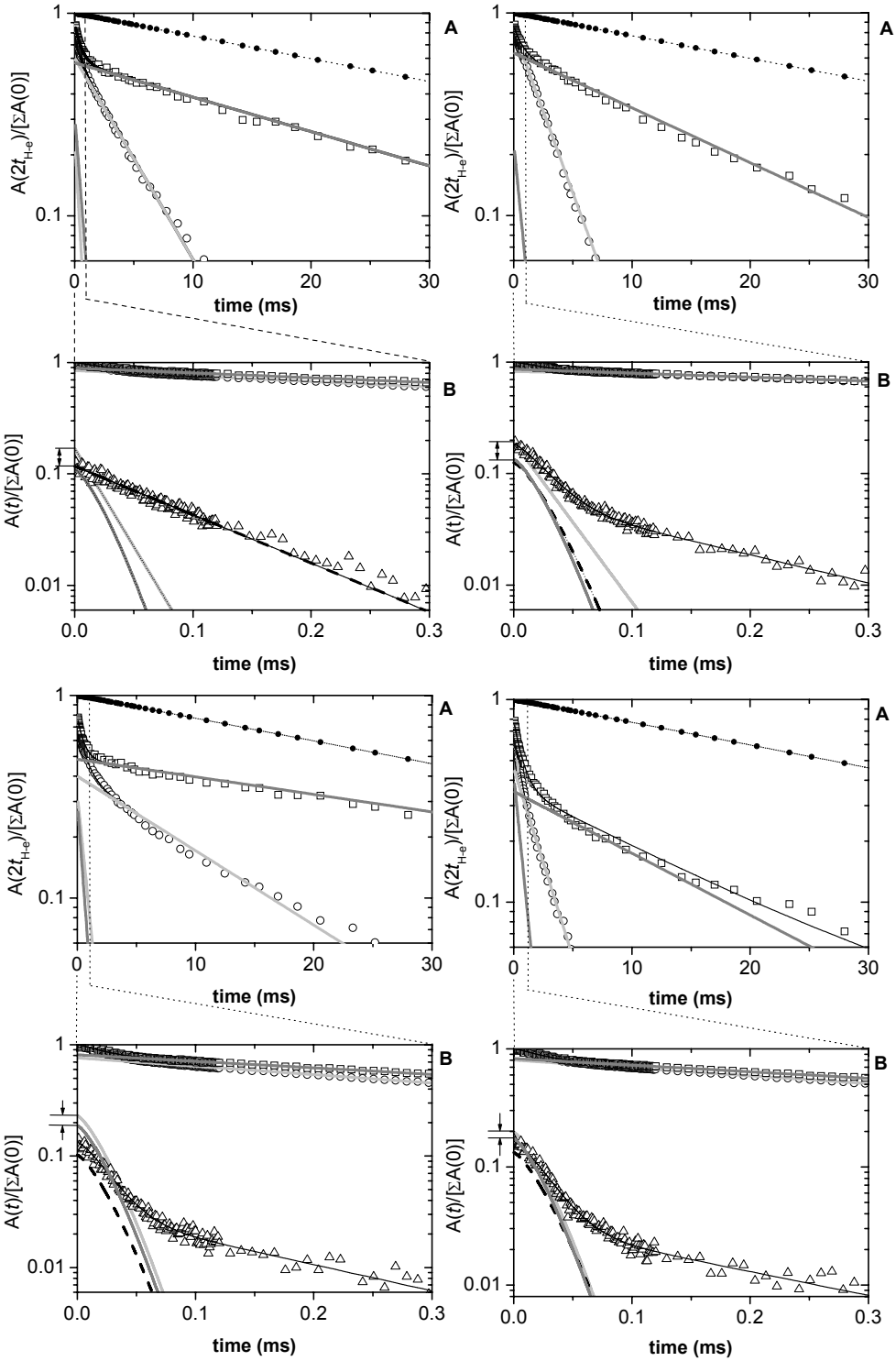
A
B
A(2t_H-e)/[ΣA(0)]
A(t)/[ΣA(0)]
time (ms)

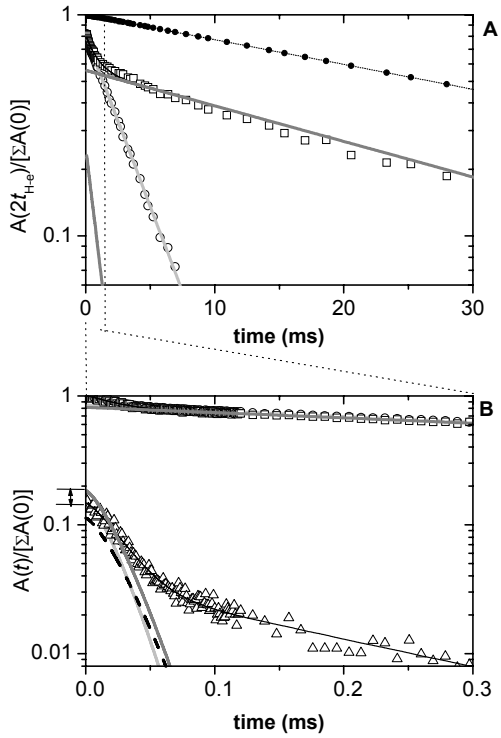

Fig.7.7: [A]: Decay of the transverse magnetisation at 100 °C for unswollen (○) and swollen (□) NR filled with hydrophilic and grafted silicas. The decay for swollen pure NR is shown by (●). The volume fraction of 1,1,2,2-$C_2D_2Cl_4$ was 40%, relative to the rubber phase. The decay is measured with HEPS and normalised to the total amplitude of the transverse magnetisation [ΣA(0)].
[B]: Initial part of the decay as measured with the SEPS for hydrophilic (Δ) (Fig. 7a) and grafted silica (Δ) (Fig. 7b – e) and unswollen (○) and swollen (□) NR filled with the same silica. Solid, black lines represent the result of a least-squares fit of the decay. The separate components for filled NR are shown by light grey lines for the non-swollen and dark grey lines for the swollen sample. $(T_2^s)^{sil}$ relaxation components for hydrophilic and grafted silicas are shown with dashed and dotted lines, respectively. Fitting functions are given in Table 2. Fig. 7a-7e represent the results for hydrophilic silica and PTES-, MPTES-, TESBD- and TESPT-grafted silicas and NR filled with the same silica, respectively. The increase in the amplitude of the relaxation component with short decay time $(T_2^s)^{sil+NR}$ is highlighted by arrows.

Table 7.5 The fractional amplitude A(0) of the relaxation component $(T_2^s)^{sil}$ for silicas, and $(T_2^s)^{sil+NR}$ for swollen silica-filled NR containing 40 vol.% 1,1,2,2-$C_2D_2Cl_4$ in the rubber matrix. The amplitudes $A(0)^{sil}$ and $A(0)^{sil+NR}$ are normalised to the total amplitude of the decay of the transverse magnetisation, $\sum A(0)^i$, as measured with the SEPS for silica-filled NR at 100 °C.

Sample	$A(0)^{sil}$	$A(0)^{sil+NR}$
SiO_2	0	0.147 ± 0.003
SiO_2-PTES	0.125 ± 0.004	0.138 ± 0.002
SiO_2-MPTES	0.103 ± 0.003	0.230 ± 0.002
SiO_2-TESBD	0.132 ± 0.003	0.197 ± 0.003
SiO_2-TESPT	0.113 ± 0.003	0.155 ± 0.002

Fig. 7.8 shows the effect of variation in the solvent content on T_2 in the rubber phase for pure NR, and NR filled with MPTES. At volume solvent contents, V_s, of below 20%, both $(T_2^{in})^{NR}$ and $(T_2^{l})^{NR}$ increase slightly with increasing solvent content (Fig. 7.8). This is mainly the result of chain disentanglement[12,34]. At V_s > 20%, $(T_2^{in})^{NR}$ (a) and $A(0)^{in}$ (b) are hardly affected any more by the degree of swelling, whereas $(T_2^{l})^{NR}$ increases continuously upon swelling, similar to that for unfilled NR (Fig. 7.8a). This is again an indication that the $(T_2^{l})^{NR}$ component is related to the relaxation of free rubber chains, which are hardly attached to the silica surface.

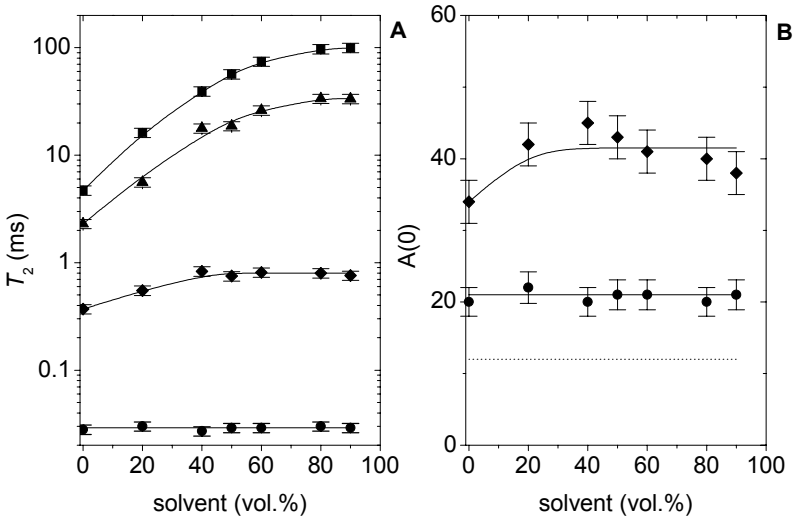

Fig. 7.8 [A]: Influence of the solvent content (vol.%), relative to the rubber phase, on the T_2 relaxation time of pure NR (■), and relaxation times (●) $(T_2^s)^{sil+NR}$, (◆) $(T_2^{in})^{NR}$ and (▲) $(T_2^{l})^{NR}$ of NR filled with MPTES-coated silica.
[B]: Influence of the solvent concentration, relative to the rubber phase on the fraction of $A(0)^{sil+NR}$ (●) and $A(0)^{in}$ (◆). The dotted horizontal line represents the initial amplitude of the T_2 decay for silica coated with MPTES, with the amount of the silica used equal to that in the silica-filled NR.

7.4.7 The mean molar mass between physical junctions

The entire collection of data indicates that a quasi-permanent rubber-silica network is formed in the samples owing to physical adsorption of chain units at the silica surface: a value of $\%NR_{immobilised}$ (Table 7.6) represents the fraction of NR bound so tightly that even in swollen samples it behaves in an almost rigid, glassy manner. The $A(0)^{in}$ represents the fraction of the network material known as bound rubber. Similar behaviour has been observed for the bound fraction of both carbon black and silica-filled rubbers[11,13-16,34] of different nature.

Table 7.6 The mean molar mass $<M_{ad}>_w$ (g/mol) and the number of monomer units $<N_{ad}>$ between adjacent adsorption junctions along a chain, the estimated mean number of the main chain carbon bonds that form a single adsorption junction, $N_{C\text{-}C\ bonds\ adsorbed}$, and the fraction of immobilised NR: $\%NR_{immobilised}$.

Sample	$<M_{ad}>_w$	N_{ad}	$N_{C\text{-}C\ bonds\ adsorbed}$	$\%NR_{immobilised}$
NR+SiO_2	710	11	8	14.7
NR+SiO_2-PTES	910	13	1	1.3
NR+SiO_2-MPTES	690	10	6	12.7
NR+SiO_2-TESBD	1040	15	4	6.5
NR+SiO_2-TESPT	1120	17	3	4.2

The distinguishing feature of the T_2 relaxation for viscoelastic networks is the plateau observed at temperatures that are well above T_g. The temperature-independence of T_2 in that plateau (T_2^{pl}) is attributed to constraints, which limit the number of possible conformations of a network chain relative to those of a free chain. For Gaussian chains the theory of transverse relaxation in elastomeric networks relates T_2^{pl} to the number of statistical segments in the network chains, Z, between chemical and physical network junctions[32,33]:

$$Z = (T_2^{pl})/[a(T_2^{rl})] \tag{7.2}$$

where a is a theoretical coefficient which depends on the angle between the segment axis and the internuclear vector for the nearest nuclear spins at the main chains. For polymers containing aliphatic protons in the main chain, this coefficient a is close to 6.2 ± 0.7.[32] T_2^{rl} is the relaxation time measured below T_g for the polymer swollen in a deuterated solvent. T_2^{rl} for NR as measured at –160 °C is 0.0101 ± 0.0001 ms. Using the number of backbone bonds in one statistical segment, designated as C_∞, the weight-average molar mass of chains between adsorption junctions and trapped chain entanglements, $<M_{ad+en}>$, can be calculated from $(T_2^{in})^{NR}$:

$$<M_{ad+en}> = ZC_\infty M_u/n \tag{7.3}$$

where M_u is the molar mass of one monomer unit of NR and n is the number of backbone bonds per monomer unit. A C_∞ of approximately 4.6 ± 0.8 rotatable bonds of the backbone of NR[38-41] was used for the calculations. The results are listed in Table 7.6. Since no chemical crosslinks are present in the samples studied the $<M_{ad+en}>$ value for swollen samples is determined by the density of physical junctions such as trapped chain entanglements and adsorption junctions at the

filler surface.[12,34] It will be shown below that adsorption junctions make the greatest contribution to the $<M_{ad+en}>$ value. The mean molar mass of NR chains between adjacent adsorption junctions along a chain can now be calculated from $(T_2^{in})^{NR}$ at V_s = 40%. At this solvent content temporary chain entanglements barely contribute to the $<M_{ad+en}>$ value.[12,34] Values obtained are given in Table 7.6. According to different authors, the molar mass between apparent chain entanglements in unfilled and unvulcanised NR, ($<M_{en}>$), as derived from equilibrium moduli in rheological measurements, equals 4700 ± 800 g/mol.[38-41] The $<M_{ad+en}>$ values calculated for the present silica-reinforced samples are all lower than $<M_{en}>$ by a factor of approximately 5. This much lower $<M_{ad+en}>$ is not surprising, because it is an indication of a significant proportion of physical junctions formed by immobilised chain units at the filler surface. The stronger the interaction between the rubber and the silica, the more pronounced the quantity of immobilised NR. The samples with the largest quantity of immobilised NR of about 12 – 15% of the total rubber: Table 7.6 – the hydrophilic silica-filled NR and the MPTES-grafted silica-filled NR – show the lowest $<M_{ad+en}>$, of 710 and 690 g/mol, respectively.

7.4.8 The effect of coupling agents on the silica-NR interface

The mean number of carbon-carbon bonds per adsorption junction, $N_{C\text{-}C\ bonds\ adsorbed}$, can be estimated from:

$$\%NR_{immobilised} = N_{C\text{-}C\ bonds\ adsorbed}/(N_{C\text{-}C\ bonds\ adsorbed} + N_{phys}) \quad (7.4)$$

The fraction of immobilised rubber and the length of the adsorbed chain at a single junction is largest for NR filled with pure silica and NR filled with MPTES-grafted silica, compared to the other samples (see Table 7.6). For pure silica as well as for the MPTES-grafted silica, the fraction of adsorbed NR chains is between 10 and 15%: Table 7.6. This is 2-10 times higher than with the other grafted silicas.

Several reasons can cause the differences in the fraction of immobilised NR, the number of C-C bonds per single adsorption junction and consequently, on the structure of the physical, rubber-silica network, i.e. (1) the chemical affinity, or the physical compatibility, of the silica surface with NR; (2) the grafting density of the coupling agent at the silica surface, which can be different for the silica samples; (3) the bulkiness of the grafted chains, which causes steric hindrance for the chain adsorption; and (4) dispersion of silica particles in the rubber matrix.

The fraction of immobilised NR chain units decreases upon treatment of the silica with a coupling agent. In the case of pure silica the large amount of immobilised rubber on the silica surface is somewhat surprising. However, Legrand et al.[14] also found that surface grafting of silica was associated with a decrease in the strength of adsorption of polybutadiene, similar conclusions follow from the results of the present study of silica-filled NR. Bound rubber experiments of hydrophilic and surface grafted silicas in SBR/BR blends similarly showed a relatively high percentage of bound rubber on the sample without silane grafting.[42]

Results described above imply that there is no major difference in the grafting density or loosely grafted areas on the silica surface. On the other hand, grafting of

the silica is expected to enhance dispersion of the silica particles. At low grafting density more aggregation of the silica remains, resulting in a smaller surface area accessible for rubber chains and hence a smaller fraction of immobilised material. However, this is in disagreement with the results found for the mixture of NR with hydrophilic silica, which showed a relatively high proportion of immobilised NR for this sample. It is therefore suggested that Si–OH-groups are the active sites for chain adsorption. Surface roughness of aggregates can also increase the strength of the adsorption.[43,44]

Within the range of grafted silicas a more or less logical order is obtained for the proportion of immobilised NR. For the MPTES-grafted silica, the high fraction of immobilised rubber can be explained by the high affinity of the –SH-group of the silane for the rubber and the possibility of the formation of a chemical bond between the silane and the NR. The affinity of the –SH-group towards 1,2-vinyl, 1,4-cis and 1,4-trans double bonds in polybutadiene, for example, was shown by Klemm and Gorski.[35,36] The 1,2-vinyl group turned out to have a very high reactivity towards the –SH-group, followed by the 1,4-cis double bond. A complex structure between the –SH-group and the 1,4-cis double bond is proposed to explain the reactivity of the 1,4-cis double bond. As before, comparison of the cis-polybutadiene and the cis-polyisoprene (NR) appears to be a logical step. The other extreme, PTES-grafted silica, shows hardly any adsorbed NR chains. In view of the aforegoing, this is to be expected because PTES has no rubber-reactive group, as well as the strength of the physical adsorption is weak.

7.5 Conclusions

^{1}H NMR T_2 Relaxation is a technique, which is very useful to get information about interactions and network structure. By measuring relaxation times of silica-filled, non-vulcanised NR samples three separate regions with a strongly different mobility were detected.

The region with the lowest mobility originates from a layer of rubber chains and coupling agent molecules, tightly bound to the silica surface. The fraction of immobilised chains depends on the nature of the silica surface and is the largest for NR mixtures with hydrophilic silica without coupling agent. Grafting of the silica surface by coupling agent leads to a decrease in the amount of immobilised chains. This corresponds to earlier similar observations for silica-polybutadiene combinations. The immobilisation of chains seems to be due to very strong physical adsorption, since the fraction of immobilised chains is not affected by the presence of a good solvent or by a high temperature of 100 °C. In case of grafted silicas, the chemical structure of the coupling agent seems to have an influence on the fraction of immobilised rubber chains. NR filled with MPTES-grafted silica shows the highest proportion of immobilised chains. This can be explained by the great affinity of the –SH-group of MPTES for the C=C-bond in NR. PTES on the other hand, cannot react with NR and only shields the silica surface, thereby making it inaccessible to physical adsorption with the NR, leading to the lowest fraction of immobilised chains.

A region with intermediate mobility can be related to network chains, with physically adsorbed chain portions acting as network junctions. In the case of MPTES-grafted silica some chemical bonds between NR and the silica by means of the coupling agent may be involved as well. The presence of a good solvent influences the mobility of these network chains to some extent mainly due to chain disentanglements.

The region with a high mobility originates from free, extractable rubber chains and is strongly influenced by the presence of a good solvent. The mobility of this rubber portion changes nearly as much as the mobility of pure NR in the presence of a good solvent.

In terms of physical interactions and the structure of the physical network, there is a marked similarity between NR filled with carbon black and NR filled with silicas. The concept of rubber chains immobilised on a carbon black surface, as represented by several authors, also appears to be applicable to silica-filled NR.

References

1. M. P. Wagner, Rubber Chem.Technol., 49, 703 (1976).
2. S. Wolff, Tire Sci. Technol., 15, 276 (1987).
3. R. W. Cruse, M. H. Hofstetter, L. M. Panzer and R. J. Pickwell, Paper No. 75 presented at a meeting of ACS, Rubber Division, Louisville, Kentucky, Oct. 8-11, 1996
4. R. W. Cruse, M. H. Hofstetter, L. M. Panzer and R. J. Pickwell, Rubber & Plastics News, April 21, 14 (1997).
5. S. Wolff and M. J. Wang, Rubber Chem. Technol., 65, 329 (1992).
6. M. J. Wang, Rubber Chem. Technol., 71, 520 (1998).
7. H. D. Luginsland, Kautsch. Gummi Kunstst., 53, 10 (2000).
8. A. Hunsche, U. Görl, H. G. Koban and T. Lehmann, Kautsch. Gummi Kunstst., 51, 525 (1998).
9. U. Görl and A. Parkhouse, Kautsch. Gummi Kunstst., 52, 493 (1999).
10. V. M. Litvinov, "Organosilicon Chemistry: From Molecules to Materials II", VCH, Weinheim, 1996.
11. V. J. McBrierty and J. C. Kenny, Kautsch. Gummi Kunstst., 47, 342 (1994).
12. V. M. Litvinov and P. A. M. Steeman, Macromolecules, 32, 8476 (1999).
13. H. Serizawa, M. Ito, T. Kanamoto, K. Tanaka and A. Nomura, Polym. J., 14, 149 (1982).
14. A. P. Legrand, N. Lecomte, A. Vidal, B. Haidr and E. Papirer, J. Appl. Polym. Sci., 46, 2223 (1992).
15. S. Ono, M. Ito, H. Tokumitsu and K. Seki, J. Appl. Polym. Sci., 74, 2529 (1999).
16. J. O'Brien, E. Cashell, G. E. Wardell and V. J. McBrierty, Macromolecules, 9, 653 (1976).
17. R. Rauline (to Compagnie Generale des Etablissements Michelin - Michelin & Cie), Eur. Pat. 0 501 227 A1 (12-02-'92).
18. W. Stöber, A. Fink and E. Bohn, J. Colloid Interf. Sci., 26, 62 (1968).
19. A. P. Philipse and A. Vrij, J. Colloid Interf. Sci., 128, 121 (1989).

20. G. Engelhardt and D. Michel, "High Resolution Solid State NMR of Silicates and Zeolites", New York, 1987.
21. G. S. Caravajal, D. E. Leyden, G. R. Quinting and G. E. Maciel, Anal. Chem., 60, 1776 (1988).
22. M. Pursh, R. Brindle, A. Ellwanger, L. C. Sander, C. M. Bell, H. Händel and K. Albert, Solid State Nuclear Magn. Res., 9, 191 (1997).
23. D. Derouet, S. Forgeard, J. C. Brosse, J. Emery and J. Y. Buzare, J. Polym. Sci.: Part A: Polym. Chem., 36, 437 (1998).
24. R. Simonutti, A. Comotti, F. Negroni and P. Sozzani, Chem. Mater., 11, 822 (1999).
25. A. Hunsche, U. Görl, A. Müller, M. Knaack and T. Göbel, Kautsch. Gummi Kunstst., 50, 881 (1997).
26. D. W. Sindorf and G. E. Maciel, J. Am. Chem. Soc., 3767 (1983).
27. D. W. Sindorf and G. E. Maciel, J. Phys. Chem., 86, 5208 (1982).
28. M. Zaborski, A. Vidal, G. Ligner, H. Balard, E. Papirer and A. Burneau, Langmuir, 5, 447 (1989).
29. L. T. Zhuravlev, Langmuir, 3, 316 (1987).
30. R. K. Iler, "The Chemistry of Silica", New York, Wiley Interscience, 1979.
31. I. S. Chung, D. R. Kinney and G. E. Maciel, J. Am. Chem. Soc., 115, 8695 (1993).
32. C. G. Fry and A. C. Lind, Macromolecules, 21, 1292 (1988).
33. Y. Y. Gotlib, M. I. Lifshits, V. A. Shevelev, I. A. Lishanskii and I. V. Balanina, Polym. Sci. USSR, 18, 2630 (1976).
34. V. M. Litvinov, W. Barendswaard and M. v. Duin, Rubber Chem. Technol., 71, 105 (1998).
35. E. Klemm and U. Gorski, Angew. Makromol. Chem., 207, 187 (1993).
36. U. Gorski and E. Klemm, Angew. Makromol. Chem., 254, 11 (1998).
37. J. P. Cohen-Addad, Progr. NMR Spectrosc., 25, 1 (1993).
38. W. W. Graessley and S. F. Edwards, Polymer, 22, 1329 (1981).
39. S. M. Aharoni, Macromolecules, 16, 1722 (1983).
40. E. A. Sidorovich, Polym. Sci., 37, 1233 (1995).
41. N. Heymans, Macromolecules, 33, 4226 (2000).
42. OSi Specialties Crompton Corporation (Europe) S.A. Meyrin Laboratories, Silane coupling agents in silica-filled rubber and their role in the filler surface interactions, 2001, private communication.
43. G. Heinrich and T. A. Vilgis, Rubber Chem. Technol., 68, 26 (1995).
44. G. Wu, S. Asai and M. Sumita, Macromolecules, 35, 945 (2002).

Appendix I

The Rubber Process Analyser

I.1 Introduction

In the study described in this thesis dynamic mechanical measurements using the Rubber Process Analyser (RPA) 2000 proved to be a valuable aid to understanding the effects of different coupling agents. The RPA is a torsional dynamic rheometer, with an advanced temperature control and fully automated operation modes. The RPA is controlled through an external computer, is easy to handle and has numerous testing capabilities in terms of frequency and strain and temperature sweeps. The RPA is specially designed to test very stiff materials, which rubber compounds usually are, in dynamic conditions within relevant strain, frequency and temperature ranges.

I.2 Technical information

Essentially the RPA consists of two main parts: the test instrument itself and an outside computer for test monitoring, data recording and treatment. The testing part consists of a biconical test chamber with grooved dies to avoid slippage, a problem often encountered with rubber testing. The advantage of this test geometry is that the strain rate is constant in the gap. The cavity is closed through the action of a ram operated with a pressure of 4 MPa and a slight excess of test material is needed for reliable torque reading to be made. Two hard fluoroelastomer seals provide the peripheral closure of the cavity. The excess material flows in a circular sew channel and further contributes to the sealing of the cavity. Tests are thus made under pressurised conditions, and therefore porosity does not develop in the sample when the instrument is operated as a curemeter. The lower die can be oscillated at controlled strain and frequency. The torque measuring system is attached to the upper die and calibrated with a torsion spring mounted between the two dies. The heart of the instrument is a special direct drive motor, which can move the lower die sinusoidally over a wide range of strains and frequencies. A harmonic torsional strain is exerted on the sample by the lower (oscillating) die and the transmitted torque is measured on the upper (fixed) wall. The sample periphery is neither free, nor spherical and its shape is imposed by the design of the seals.

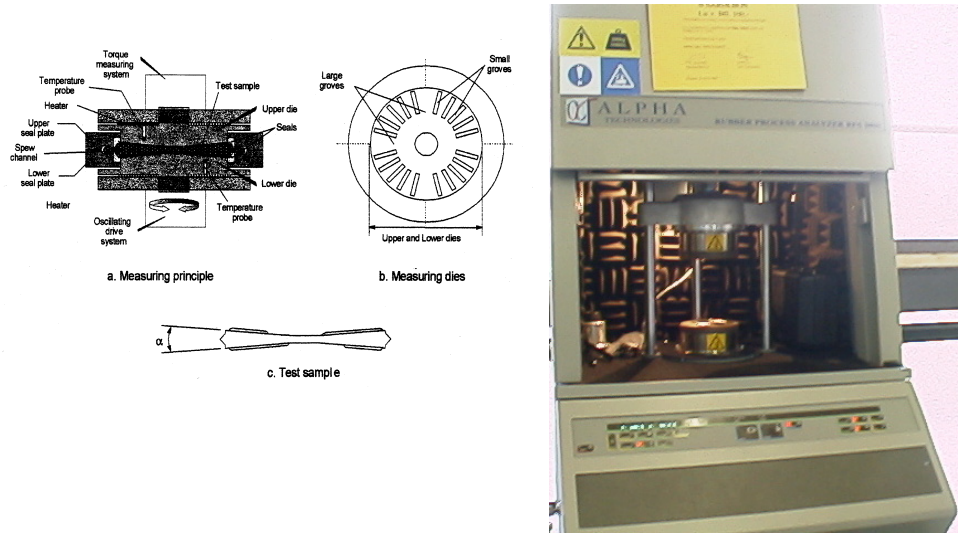

Fig I.1: Design of the Rubber Process Analyser 2000.

The temperature control system of the RPA has a resolution to the nearest 0.1 °C which, combined with the thinness of the sample, allows near isothermal tests to be performed in the 50-200 °C range. Temperature changes are very quick and monitored by the controlling computer.

Once loaded and closed, the lower part of the biconical cavity is oscillated at controlled frequency and strain. In dynamic testing, a sinusoidal harmonic strain is applied and, providing the tested viscoelastic material responds in a linear manner, the recorded torque is also sinusoidal but out-of-phase by an angle δ, depending on the visco-elastic character of the tested material. In the RPA, the phase angle is actually not measured but the assumption is made that the sinusoidal strain produces a sinusoidal torque response. The complex torque signal S* is first treated in such a manner that during one cycle several discrete values are read with respect to equal periods on the time scale. By applying a Fourier transform to the S* signal, this is divided into an elastic component S' (in phase with the strain) and a viscous component S" (90° out of phase with the strain). The phase angle δ can then be calculated. Using a shape factor for the considered test gap, the dynamic shear moduli can be obtained. Test data are automatically recorded and stored in the computer memory.

Whilst not all combinations are possible, the testing capabilities of the RPA are very broad:

- frequency range: 0.05 to 209.44 rad/s
- strain angle range: 0.01° to 90 ° (0.145 to 1256% strain)
- temperature range: 40-200 °C

Owing to technical limitations of the strain gauge and the other transducers, the lower the frequency or the strain, the larger the experimental errors. The maximum

strain is limited by the applied frequency, for instance from 7% strain at ω = 200 rad/s up to 1256% strain at 0.1 rad/s.

There are several built-in testing modes, for instance: frequency and temperature sweeps, curing test, stress relaxation and dwell time, that can be combined by the operator in various manners. For example, one of the built-in tests can be easily repeated at various temperatures by taking advantage of the RPA capability of fast temperature change within the cavity. Frequency sweep tests repeated at various increasing temperatures provide all the data necessary to build mastercurves by applying the time-temperature superposition principle.

I.3 Test programs

For the study described in this thesis several test programs of the RPA have been used. In the current paragraph these test programs will be described separately.

I.3.1 Strain sweep

The difference in G' at low and intermediate strain, the so-called Payne effect is often used as a measure for filler dispersion. To study the filler-filler interactions of the uncured compounds, the storage modulus G' was measured as a function of strain (figure I.1). During the strain sweep the temperature and frequency were kept constant at 100 °C and 0.500 Hz, respectively. G' was measured in a strain range of 0.56 – 100.04 % as well as a range of 0.56 – 900.05%. The results of the latter strain range did not show additional information concerning filler dispersion and/or filler-filler interactions. Therefore most of the strain sweeps were restricted to the range of 0.56 – 100.04 %.

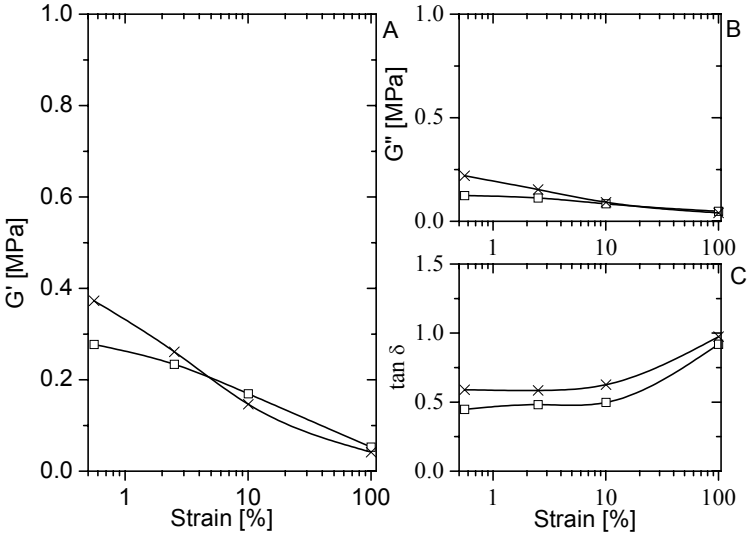

Fig. I.2: G'-modulus as a function of strain for a compound with a sulphur containing (□) and a sulphur free (X) coupling agent.

The compounds in Fig I.1 show a different Payne effect. The sulphur containing compound has a marked lower G'-modulus at low strain. This lower G'-modulus at low strain is an indication of less filler-filler interactions, and consequently a better dispersion of the silica filler in the rubber matrix. The decrease in the G'-modulus at higher strain levels is the result of break down of the filler network at higher strain.

I.3.2 Temperature sweep

The effect of increasing temperature on the G'-modulus of the uncured compounds was used as an indication of scorch. Several sulphur-containing coupling agents are known as scorch sensitive. During mixing, especially at high temperatures, the G'-modulus of the compound increases strongly for those coupling agents. Therefore temperature sweep measurements were performed at 49.94% strain and a frequency of 0.500 Hz in a temperature range 110 – 200 °C (figure I.2).

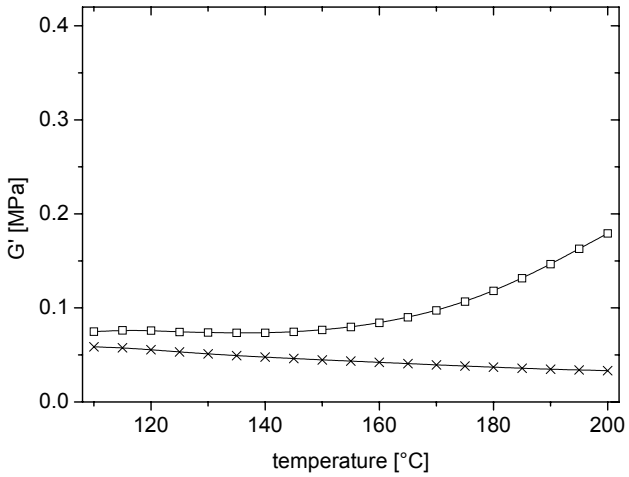

Fig. I.3: G'-modulus as a function of temperature for a compound with a sulphur containing (□) and a sulphur free (X) coupling agent.

The compound with the sulphur containing coupling agent shows a strong increase in G'-modulus at 160 °C. This increase in G'-modulus was interpreted as the result of a reaction of the coupling agent with the rubber matrix. The compound with the sulphur free coupling agent on the other hand shows a normal temperature dependence of G' for a reinforced compound, since this coupling agent is not able to react with the rubber matrix.

I.3.3 Vulcanisation rheogram

Rheograms were made to study the vulcanisation behaviour of the compounds after the addition of vulcanising agents: Figure I.3. The increase in torque at 160 °C, 0.833 Hz and 2.79% strain was measured over a time period of 30 minutes. The optimal vulcanisation times, $t_c(90)$ and scorch times $t_c(02)$ of the compounds are determined from the rheogram.

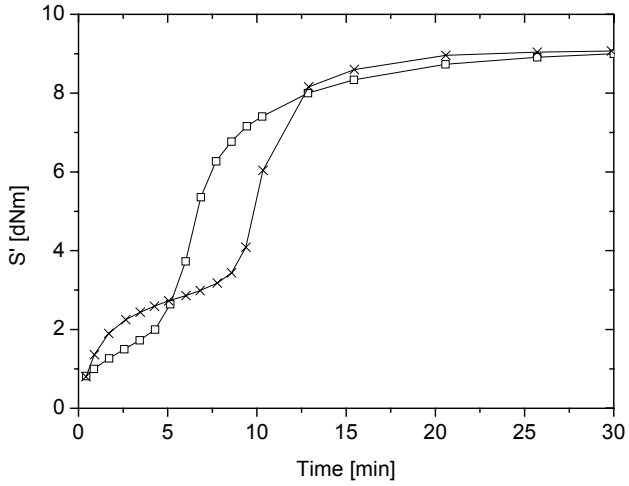

Fig. I.4: Vulcanisation behaviour of a compound with a sulphur containing (□) and a sulphur free (X) coupling agent.

I.3.4 Frequency sweep

Frequency sweeps were performed to measure tan δ at 60 °C as a measure of rolling resistance. For this measurement a new, uncured sample was vulcanised for a time period corresponding to the optimum vulcanisation time. After optimum vulcanisation the sample was cooled down to 60 °C and tan δ measured at different frequencies. The tan δ at 15 Hz was taken as a measure for the rolling resistance.

Glossary

a	a theoretical coefficient	
$A(0)^{in}$	relative amplitude of $(T_2^{in})^{NR}$ relaxation component	
$A(0)^{l}$	relative amplitude of $(T_2^{l})^{NR}$ relaxation component	
$A(0)^{OH}$	relative amplitude of $(T_2^{l})^{OH}$ relaxation component	
$A(0)^{sil}$	relative amplitude of $(T_2^{s})^{sil}$ relaxation component	
$A(0)^{sil+NR}$	relative amplitude of $(T_2^{s})^{sil+NR}$ relaxation component	
C_∞	number of backbone bonds in one statistical segment	
δ	chemical shift	[ppm]
dH	converted energy	[J]
dl	distance travelled	[m]
dt	time taken for a distance dl	[s]
ε_{break}	strain at break	[%]
E-modulus	Young's modulus for small strains of the stress-strain curve	[MPa]
F_R	rolling resistance	[N]
ϕ	volume fraction of the filler	
G	modulus of filled compound	[MPa]
G'	storage modulus	[MPa]
G"	loss modulus	[MPa]
G_0	modulus of unfilled compound	[MPa]
$\dot{H}$	rate of heat development	
m	multiplet	
M_{100}	stress at 100 % strain	[MPa]
M_{300}	stress at 300 % strain	[MPa]
$<M_{ad+en}>$	weight-average molar mass of chains between adsorption junctions and entanglements	[g/mol]
$<M_{en}>$	weight-average molar mass of chains between entanglements	[g/mol]
M_u	molar mass of one monomer unit of NR	[g/mol]
n	number of backbone bonds per monomer unit	
$N_{C\text{-}C\ bonds\ adsorbed}$	number of carbon-carbon bonds per adsorption junction	
N_{en}	mean number of monomer units between adjacent adsorption junctions along the chain	
$\%NR_{immobilised}$	fraction of immobilised rubber	
ν	number of moles of elastically effective network chains per unit volume	
P_{in}	tyre input power	[W]
P_{out}	tyre output power	[W]
P_R	power loss	[W]
q	quartet	
R	gas constante	
$\Delta S'$	difference between minimum and maximum torque	
S'_{max}	maximum torque	[dNm]
S'_{min}	minimum torque	[dNm]

σ	sinusoidal stress	[MPa]
σ_{break}	stress at break	[MPa]
t	triplet	
T	temperature	[°C]
T_2	spin-spin (transverse) relaxation time	[μs]
$(T_2^{in})^{NR}$	T_2 relaxation time of NR network chains	[μs]
$(T_2^{l})^{NR}$	T_2 relaxation time of free NR	[μs]
$(T_2^{l})^{OH}$	T_2 relaxation time of silanol groups and water molecules on the surface of hydrophilic silica	[μs]
$(T_2^{s})^{sil}$	T_2 relaxation time of the grafted chains	[μs]
$(T_2^{s})^{sil+NR}$	T_2 relaxation time of silica-NR interface	[μs]
(T_2^{pl})	T_2 relaxation time in the rubber plateau	[μs]
(T_2^{rl})	T_2 relaxation time below the glass transition temperature	[μs]
tan δ	loss tangent	
$t_c(2)$	scorch time	[min]
$t_c(90)$	optimum cure time	[min]
T_g	glass transition temperature	[°C]
τ_{cp}	cross-polarization time	[μs]
v	road speed of the tyre	[m/s]
V_s	solvent content as vol.%	[%]
ω	angular frequency	[rad/s]
γ	shear strain	
Z	number of statistical segments in the network chains	

BR	butadiene rubber
CBS	N-cyclohexyl-2-benzothiazole sulphenamide
$CDCl_3$	deuterated chloroform
$C_2D_2Cl_4$	1,1,2,2-deuterated tetrachloroethane
CP	cross-polarization
DEPDIS	bis(diethoxtythiophosphoryl) disulphide
DIPDIS	bis(diisopropyl)thiophosphoryl disulphide
DIPMBT	diisopropylthiophosphoryl-2-benzothiazole
DIPTESM	diisopropylthiophosphoryltriethoxysilylpropyl monosulphide
DIPTOS	diisopropylthiophosphoryl-N-oxydiethylene sulphenamide
DMPDIS	bis(dimethoxythiophosphoryl) disulphide
DPG	diphenyl guanidine
DTES	bis(triethoxysilyl) decane
ETES	bis(triethoxysilyl) ethane
EtO	ethoxy
EtOH	ethanol
HEPS	Hahn-echo pulse sequence
^{1}H NMR	proton nuclear magnetic resonance
HTES	bis(triethoxysilyl) hexane
IR	Infrared
MAS	magic angle spinning
MBT	mercaptobenzothiazole
MBTS	dibenzothiazole disulphide
MPTES	3-mercaptopropyltriethoxy silane

NR	natural rubber
phr	parts per hundred rubber
ppm	parts per million
PTES	propyltriethoxy silane
RPA	rubber process analyser
S	sulphur
SEPS	solid-echo pulse sequence
(S-)SBR	(solution) Styrene Butadiene Rubber
TES	tetraethoxy silane
TESBD	triethoxysilylpropyl benzothiazole disulphide (2-benzothiazyl-(3-triethoxysilyl)propyl disulphide
TESPD	tetraethoxysilylpropyl disulphide
TESPT	bis(triethoxysilylpropyl) tetrasulphide
TCPTS	3-thiocyanatopropyltriethoxy silane
TESPD	bis(triethoxysilylpropyl) disulphide
TESPM	bis(triethoxysilylpropyl) monosulphide
TMS	tetramethyl silane
TMTD	tetramethylthiuram disulphide
ZnO	zinc oxide

Summary

Since the introduction of the “green” tyre, silica is more and more used as a reinforcing filler in tyre applications. Silica when compared to carbon black, strongly reduces the rolling resistance of a tyre, which in turn leads to a lower fuel consumption of the car. The disadvantage of the use of silica is the mixing problem it introduces. Due to its polar surface, silica is difficult to mix with a hydrocarbon rubber. The solution for this problem lies in the use of a coupling agent, which shields the polar silica surface on one hand and reacts with the rubber matrix on the other hand.

The coupling agent most commonly used for these applications in industry is bis(triethoxy-silylpropyl) tetrasulphide (TESPT). The reaction of this coupling agent with the silica surface has been extensively studied by different authors. It is now widely accepted, that one silanol group of the coupling agent after hydrolysis reacts with a silanol group on the silica surface in a primary reaction. This primary reaction is followed by a secondary reaction in which the remaining silanol groups of the coupling agent react with silanol groups of neighbouring coupling agents. The reaction of the coupling agent with the rubber matrix however, has not been studied to such an extent as the reaction with the silica surface and is still not completely understood.

The objective of the research described in this thesis was to investigate the reaction of the coupling agent with the rubber matrix, in an attempt to better understand the reinforcement mechanism for silica-filled rubbers. The interaction between silica and rubber via the coupling agent was studied using three different coupling agent systems: variations on TESPT, silane-accelerator combinations and thiophosphoryl compounds. Their effects on processing as well as on dynamic mechanical properties were investigated. ^{1}H NMR relaxation measurements were used to obtain additional information concerning the interaction between rubber and silica filler in presence and absence of a coupling agent.

After a short general introduction in Chapter 1, the advantages of silica over carbon black as reinforcing fillers for rubber and the effect of coupling agents are reviewed in Chapter 2. The influence of reinforcing fillers as well as rubber polymers on tyre performance, mainly rolling resistance is discussed. The development of several types of silica as well as of different coupling agents is reviewed.

Chapter 3 describes the syntheses and characterisation of the coupling agent systems selected for investigation. Variations on TESPT were easy to synthesise, while the synthesis of silane-accelerator combinations and of thiophosphoryl compounds was more complicated. Fortunately, at least one coupling agent for each selected system could be synthesised. In the Chapters 4 – 6 the influence of these different coupling agent systems on properties of a silica reinforced tyre tread compound is discussed.

The importance of the existence of a rubber-reactive functional group in a coupling agent is shown in Chapter 4, by comparing the effect of the sulphur- and carbon chain length of silane coupling agents. The length of the sulphur chain of a silane coupling agent like TESPT has a strong influence on the processing behaviour of a silica reinforced tyre tread compound, especially on scorch safety. Decreasing the sulphur rank of TESPT from four to two, results in a better scorch safety and therefore a broader processing window, while final properties are comparable to a TESPT reference compound when correction for the reduced amount of sulphur is applied in the curing package. For a sulphur free silane coupling agent an increase in the length of the carbon chain improves the processing behaviour. Less energy is consumed during mixing when the length of the carbon chain is increased. The Payne effect, which is commonly interpreted as a measure for filler dispersion, is lower for a sulphur free silane, indicating a better filler dispersion. Mechanical properties however, fail when compared to a TESPT reference compound. When sulphur correction is applied in the curing package the tensile properties improve due to an increase in crosslink density, but remain inferior to TESPT. The fact that a sulphur free silane with an equimolar amount of sulphur added to the curing package, still shows inferior tensile properties, compared to TESPT, can be interpreted as the effect of the absence of a chemical link between silica filler and rubber via the coupling agent. In the presence of a rubber-reactive group in the form of sulphur built-in into the coupling agent, there is a strong indication of the formation of a rubber-to-filler link via the coupling agent.

Triethoxysilylpropylbenzothiazole disulphide (TESBD) is investigated in Chapter 5 as a compound containing a silane and an accelerator functionality. A silica reinforced tyre tread compound containing TESBD shows a lower Payne effect, thus indicating a better filler dispersion. The accelerator built into TESBD turns out to be too slow to act as an accelerator for the curing reaction, which is also reflected in inferior mechanical properties of the compound containing TESBD when compared to TESPT. A small amount of amine in the form of DPG turns out to be sufficient to release the accelerator part of TESBD, resulting in properties grossly comparable to TESPT.

The effect of diisopropylthiophosphoryltriethoxysilylpropyl monosulphide (DIPTESM) as a coupling agent is described in Chapter 6. The Payne-effect of DIPTESM-containing silica-reinforced tyre tread compound is far inferior to the TESPT reference compound. This high Payne-effect indicates a less pronounced shielding of the silica surface for DIPTESM, resulting in an inferior silica dispersion compared to the TESPT reference, which is also reflected in the mechanical properties. The release of the thiophosphoryl accelerator part turns out to be not effective enough to result in an appreciable crosslinking density. Addition of an extra amount of accelerator is still necessary in order to obtain properties comparable to the TESPT reference.

The indication above that a rubber-to-filler link is formed via the coupling agent is based on differences in mechanical properties, but could still not be convincingly proven with the techniques applied there. ^{1}H-NMR T_2 relaxation, which has proved to be a successful technique for the study of rubber-filler interactions, was therefore

used to investigate interactions between Natural Rubber (NR) and pure as well as grafted silica: Chapter 7. Different amounts of immobilised NR were found, depending on grafting material on the silica and grafting density. Based on the results in Chapter 4 a lower amount of immobilised NR was expected for a grafting material without a rubber-reactive group, propyltriethoxy silane (PTES). Indeed, using ^{1}H NMR relaxation measurements, a lower proportion of immobilised NR is found for the PTES-grafted silica. A higher proportion of immobilised NR is measured for the silane-accelerator combination TESBD when compared to TESPT, by ^{1}H-NMR relaxation. The better overall properties of the silane-accelerator combination TESBD compared to TESPT, as investigated in Chapter 5, can be interpreted as the result of a higher affinity of TESBD towards the rubber matrix when compared to TESPT. This then explains the higher amount of immobilised NR found for TESBD-grafted silica, when compared to the TESPT-grafted silica.

The results of ^{1}H NMR relaxation point towards the formation of a strong physical or chemical network around the silica surface. Based on the measurements discussed in Chapter 7 no conclusion can be drawn either whether the network is physical or chemical in nature. The results in Chapter 4 and 5 indicate the formation of a chemical network. Admittedly, all techniques add more or less evidence and none of them is fully conclusive. Combining all results gathered in the various chapters it may be stated that they all point to a chemical rather than a physical bond of the coupling agent to the rubber molecule, whereby it forms a chemical bridge between the polar silica and apolar rubber.

Samenvatting

Na de introductie van de zogenaamde “groene” autoband is het gebruik van silica als versterkende vulstof in bandentoepassingen sterk toegenomen. Het voordeel van silica ten opzichte van roet is dat het tot een lagere rolweerstand van de band leidt en daarmee tot een vermindering van het brandstofverbruik van een auto. Helaas kan roet niet zondermeer vervangen worden door silica, omdat het polaire silica moeilijk is in te mengen in de apolaire rubber. De mengproblemen kunnen worden overkomen door gebruik te maken van een “coupling agent”. Deze “coupling agent” schermt aan de ene kant het polaire oppervlak van het silica af en reageert aan de andere kant met de rubber.

Een voor deze toepassing veelgebruikte “coupling agent” is bis(triethoxysilylpropyl) tetrasulfide (TESPT). Verschillende auteurs hebben de reactie van deze “coupling agent” met het silica oppervlak uitgebreid bestudeerd. Het wordt tegenwoordig algemeen aangenomen dat eerst één silanolgroep van de “coupling agent” hydrolyseert en vervolgens reageert met een silanolgroep op het silica oppervlak tijdens de primaire reactie. Deze primaire reactie wordt direct gevolgd door een secondaire reactie waarbij de overgebleven silanolgroepen van de “coupling agent” reageren met de silanolgroepen van naastliggende “coupling agents”. Op deze manier wordt als het ware een apolaire laag om het silica oppervlak gevormd. De reactie van de “coupling agent” met de rubber matrix is nog niet zo uitgebreid onderzocht en wordt nog steeds niet volledig begrepen.

Het doel van het onderzoek beschreven in dit proefschrift was om de reactie van de “coupling agent” met de rubber matrix te onderzoeken, om een beter begrip te krijgen van het versterkingsmechanisme voor silica gevulde rubbers. Drie verschillende “coupling agent”-systemen zijn onderzocht om de interactie tussen silica en rubber via de “coupling agent” te bestuderen. Deze drie systemen zijn: variaties op TESPT, silaan-versneller combinaties en thiophosphoryl verbindingen. De invloeden van deze systemen op zowel de verwerking als de dynamisch mechanische eigenschappen werden onderzocht. Voor het verkrijgen van extra informatie omtrent de interactie tussen rubber en silica zowel in de aanwezigheid als in de afwezigheid van een “coupling agent” is gebruik gemaakt van ^{1}H NMR relaxatie metingen.

Hoofdstuk 1 bevat een korte algemene introductie. De voordelen van silica als versterkende vulstof ten opzichte van roet en het gebruik van “coupling agents” wordt beschreven in hoofdstuk 2. De invloed van beide versterkende vulstoffen en rubber polymeren op banden “performance”, met name rolweerstand wordt besproken. Er wordt tevens een overzicht gegeven van de verschillende types silica en “coupling agent” die de laatste jaren zijn ontwikkeld.

De syntheses en karakteriseringen van de verschillende “coupling agent” systemen worden beschreven in hoofdstuk 3 van dit proefschrift. De synthese van de variaties op TESPT leverde weinig problemen op. De silaan-versneller combinaties en de thiophosphorylverbindingen waren lastiger te synthetiseren. Ondanks de

problemen bij synthese en zuivering van deze systemen kon toch voor elk systeem tenminste één verbinding worden gemaakt. Het effect van deze verschillende “coupling agent” systemen op de eigenschappen van een compound voor een silica versterkt bandenloopvlak wordt beschreven in de hoofdstukken 4 tot 6.

De in hoofdstuk 4 beschreven effecten van de zwavel- en koolstofketenlengte van silaan “coupling agents” tonen het belang van de aanwezigheid van een rubber-reactieve functionele groep in een “coupling agent” aan. Het verwerkingsgedrag van een compound voor een silica versterkt bandenloopvlak wordt sterk beïnvloed door de lengte van de zwavelketen van de “coupling agent”, met name de gevoeligheid voor aanvulkanisatie (scorch). De scorchgevoeligheid van een compound wordt sterk verminderd bij reductie van de lengte van de zwavelketen van 4 naar 2 zwavelatomen waardoor het temperatuursbereik waarbinnen de compound goed verwerkbaar is, (“processing window”) breder wordt. Wanneer gecorrigeerd wordt voor dit lagere zwavelgehalte door toevoeging van extra zwavel tegelijk met de vulkanisatiechemicaliën, zijn de eindeigenschappen van de compound vergelijkbaar met die van de TESPT referentie compound. Door de lengte van de koolstofketen van een silaan coupling agent, zonder zwavel in het molecuul zelf, te vergroten kan het verwerkingsgedrag verbeterd worden. Er wordt minder energie verbruikt tijdens het mengen als de lengte van de koolstofketen toeneemt. Het Payne effect, dat meestal als een maat voor de dispersie van de vulstof in de rubber matrix wordt gebruikt, is lager voor de zwavelvrije silaan coupling agent met de langste koolstofketen. Dit lagere Payne effect, indiceert een betere dispersie van de vulstof. De mechanische eigenschappen van deze coupling agent zijn minder goed dan die van de TESPT referentie compound. De trek-rek eigenschappen verbeteren wanneer de corrigerende hoeveelheid zwavel wordt toegevoegd tegelijk met de vulcanisatie ingrediënten, hoofdzakelijk door een toename van de crosslink-dichtheid, maar blijven slechter dan die van TESPT. Het feit dat een zwavelvrij silaan, zelfs wanneer een corrigerende hoeveelheid zwavel wordt toegevoegd, slechtere eigenschappen geeft dan TESPT, kan worden verklaard als het gevolg van de afwezigheid van een chemische binding tussen silica vulstof en de rubber matrix met behulp van de “coupling agent”. Wanneer er zwavel als rubber-reactieve groep in de coupling agent aanwezig is, is er een sterke aanwijzing dat er een vulstof-rubber verbinding gevormd wordt via de coupling agent.

Triethoxysilylpropylbenzothiazole disulphide (TESBD) is onderzocht in hoofdstuk 5 als een compound die zowel een silaan als een versneller functie bevat. Het Payne effect van een silica versterkte loopvlak compound dat TESBD bevat is lager en is dus een indicatie voor een betere vulstof dispersie. De TESBD bevattende compound heeft slechtere mechanische eigenschappen dan TESPT. Dit is een indicatie dat het vrijmaken van de versneller ingebouwd in TESBD te langzaam is om als een versneller te werken. Het toevoegen van een kleine hoeveelheid amine in de vorm van difenylguanidine is voldoende om het versneller-deel van TESBD vrij te maken, waardoor de eigenschappen nagenoeg vergelijkbaar zijn met die van TESPT.

De invloed van diisopropylthiophosphoryltriethoxysilylpropyl monosulphide (DIPTESM) als een “coupling agent” wordt beschreven in hoofdstuk 6. De DIPTESM-bevattende silica versterkte loopvlak compound vertoont een veel hoger Payne effect dan de TESPT referentie compound. Dit hoge Payne effect duidt erop dat het silica oppervlak minder goed is afgeschermd voor de DIPTESM-bevattende compound, wat resulteert in een slechtere dispersie van het silica in de compound dan voor de TESPT referentie compound. Deze slechtere dispersie is ook terug te zien in de slechtere mechanische eigenschappen. Het vrijmaken van het thiophosphoryl versneller deel blijkt niet effectief genoeg te zijn om een voldoende hoge netwerk-dichtheid te creëren. Een extra hoeveelheid versneller moet nog worden toegevoegd om eigenschappen te krijgen die vergelijkbaar zijn met de TESPT referentie.

De aanname dat een rubber-vulstof verbinding wordt gevormd via de coupling agent is gebaseerd op de verschillen in mechanische eigenschappen, maar kan niet bewezen worden met de gebruikte technieken. ^{1}H-NMR T_2 relaxatie metingen zijn gebruikt om de interacties tussen natuurrubber (NR) en pure of met “coupling agent” behandelde silica te bestuderen, omdat is gebleken dat deze techniek succesvol kan worden toegepast voor het bestuderen van interacties tussen rubber en vulstof. De resultaten van deze metingen zijn beschreven in hoofdstuk 7. Afhankelijk van het type “coupling agent” en de dichtheid van de coupling agent op het silica oppervlak zijn verschillende hoeveelheden geïmmobiliseerd natuurrubber op het silica oppervlak gevonden. Uitgaande van de resultaten uit hoofdstuk 4 kan verwacht worden dat de hoeveelheid geïmmobiliseerd NR minder is voor een ”coupling agent” zonder rubber-reactieve groep, propyltriethoxysilaan (PTES). Met behulp van ^{1}H NMR relaxatie metingen werd ook inderdaad minder geïmmobiliseerde NR op het silica oppervlak gevonden. De silaan-versneller combinatie geeft een groter deel geïmmobiliseerd NR op het silica oppervlak dan de TESPT referentie, zoals gemeten met ^{1}H-NMR relaxatie. De resultaten uit hoofdstuk 5 waarbij TESBD betere overall eigenschappen gaf dan TESPT, kunnen nu worden geïnterpreteerd als het resultaat van een betere affiniteit van TESBD voor de rubber matrix in vergelijking tot TESPT. Dit verklaart dan weer de grotere hoeveelheid geïmmobiliseerd NR op het silica oppervlak voor de TESBD-behandelde silica.

De ^{1}H NMR relaxatie metingen duiden op de vorming van een sterk fysisch of chemisch netwerk rond het silica oppervlak. Met de resultaten uit hoofdstuk 7 kan geen uitsluitsel gegeven worden of dit netwerk fysisch of chemisch van aard is. De resultaten in hoofdstuk 4 en 5 duiden op de vorming van een chemisch netwerk. Alle gebruikte technieken geven min of meer een bewijs, maar geen van de technieken geeft echt uitsluitsel over de aard van het netwerk. Alle resultaten uit de verschillende hoofdstukken samenvattend kan worden geconcludeerd dat alle resultaten eerder op een chemische dan op een fysische binding van de coupling agent aan het rubber molecule wijzen, waarbij een chemische brug tussen het polaire silica en het apolaire rubber wordt gevormd.

Dankwoord

Het is gelukt! U bent bijna aan het einde gekomen van dit proefschrift en ook ik ben aan het einde van mijn loopbaan als AIO beland. Van nature krijgt de mens op zo'n moment de drang om de achterliggende periode te overdenken. Maar wees gerust, ik zal u daar niet mee lastig vallen. Er is slechts één zaak die ik wil aanroeren, ik zou namelijk graag op deze plaats een aantal mensen willen bedanken die hebben bijgedragen aan de totstandkoming van dit proefschrift.

- Professor Noordermeer wil ik graag bedanken voor de kans die hij mij gegeven heeft om binnen zijn groep als AIO onderzoek te verrichten en voor de vele uren correctiewerk om alles goed op papier te krijgen. Ik heb er veel van geleerd.
- In het eerste jaar was Leen van der Does mijn dagelijkse begeleider. Leen, vooral wat presenteren betreft heb ik veel van jou geleerd. Vaak was jou beroemde (of beruchte?) "waarom" voldoende om in te zien waar het verhaal niet duidelijk was.
- De STW-begeleidingscommissie wil ik graag bedanken voor de prettige sfeer van de halfjaarlijkse bijeenkomsten. The following persons I would like to thank for their valuable discussions during these meetings; N. Gevers, A. Guillet, A. de Hoog, A. Labruyère, S. de Meij, K. Menting, T. Mergenhagen, J. Mol and J. Vancso.
- Zonder de hulp van Andries waren er heel wat minder resultaten geweest. In het begin hebben we heel wat uurtjes samen staan synthetiseren. Vooral toen ik in Utrecht en later bij DSM aan het werk was, kwam het mengwerk vooral op jou rekening en misschien was dat maar beter ook. Jouw mengcurves waren een stuk nauwkeuriger dan de mijne. Dries, bedankt voor al het werk dat je hebt verzet en de vele ideeën die je hebt ingebracht.
- Iets meer dan drie jaar heb ik mijn kantoor gedeeld met Louis, die ook nog eens in hetzelfde project zat. Heel wat uurtjes hebben we zitten discussiëren. Als ik het even niet meer zag zitten, wist je me altijd weer te motiveren. Ik denk met plezier terug aan de congressen in Lyon en Helsinki, die we samen hebben bezocht. Hoewel het culturele Sint-Petersburg mij niet echt aansprak heb jij me gelukkig weten te overtuigen toch mee te gaan. Ik had het niet graag willen missen. Louis, bedankt voor alles.
- De mensen van het van 't Hoff laboratorium in Utrecht wil ik bedanken voor hun hulp en gastvrijheid bij het maken van de silica-bolletjes. Judith, de "aardappelbollen" waren voor mij goed genoeg. Dank je wel voor je hulp bij het maken ervan en voor het plaatsnemen in de promotiecommissie.
- Gedurende ruim een maand heb ik bij DSM gebruik mogen maken van de vaste stof NMR onder begeleiding van Victor Litvinov. Victor, thank you for your help and patience in explaining the relaxation-principle again and again. For me it was a valuable experience.
- Voor problemen met mijn computer of wanneer één van de programma's weer eens niet deed wat ik wilde, kon ik altijd bij Geert terecht. Geert, bedankt voor je hulp, vooral de optie "format c:" zal ik onthouden.

- Jan wist altijd raad met praktische problemen op het lab. Als een reactie niet liep of een destillatie wilde niet “op-gang” komen, dan wist Jan wel raad. Bedankt.
- Met de komst van “the Indian-gang” werd de band in de groep misschien juist wel sterker. Thanks to my Indian-colleagues (Kinsuk, Pratip and Subhas) I have been in the most touristic places of the Netherlands. I’ll remember our trips to for example “de Deltawerken”, “de Keukenhof”, and the “Floriade”. Sorry, I should not have bought something at a “Pakistan-shop”, but I did not know.
- De secretaresses, Gerda, Karin en Geneviève, bedankt voor jullie hulp. Voor het afhandelen van alle “papierwerk” wil ik Gerda bedanken. Gerda en Karin ik denk met plezier terug aan de gezellige uurtjes “hupsen” op vrijdag. Karin, ik vond het geweldig dat je zomaar met mij meeging, zonder dat je wist wat je te wachten stond. Ik had het zelf, denk ik, niet gedaan. Jouw schaatsclinic met Falco Zandstra zal ik nooit vergeten.
- John en Zlata, bedankt voor het bestellen van de chemicaliën, kantoorartikelen en al die andere dingen die jullie hebben gedaan.
- De mensen bij Vredestein, met name Rob van Agen en Luc ter Bogt voor de metingen die door en bij jullie gedaan werden, het aanleveren van de grondstoffen en de waardevolle discussies over het project.
- De ongeveer twee-wekelijkse CT-vakgroepvolleybalcompetitie met Debby, Jeroen, Joost, Josien, MOR, Peter, Priscilla, Raymond, en Ype was een welkome onderbreking van de werkzaamheden op het lab of achter de PC.
- Montse, Richard, Vipin en Wilma en alle PBM-, STEP- en MTP-vakgroepgenoten die niet met name genoemd zijn, bedankt voor de prettige werksfeer in het lab en de gezellige vakgroepactiviteiten.
- Wim, zonder jou stimulans had ik nooit HLO gedaan, om over promoveren maar te zwijgen. Bedankt voor je vertrouwen en steun.
- Alle Harambeeërs die er in de afgelopen jaren voor gezorgd hebben dat ik elke week minstens enkele uren ontspanning kende, bedankt!
- Mijn vriendinnen Annemieke (en Jarno), Heidi (en Jan), Jolanda, Petra (en Bastiaan) en Tamara, bedankt voor de gezellige weekenden! Langzamerhand moeten we echt andere afspraken gaan maken, als we elkaar mog met enige regelmaat willen zien.
- Mijn paranimfen Marga en Fenghua. Marga dank je wel dat je me ondanks alles nooit hebt laten vallen. Fenghua, thank you for your friendship. I’ll never forget our first meeting in your appartment, sitting together on a “poef”. Sorry for the “wadlopen”, I did not know our guide would lead us through such deep waters.
- Iedereen die ik vergeten ben.
- Mijn ouders en verdere familie voor de steun die ik in al die jaren heb gekregen. Pap, ik mag oe geane ’n betje ploag’n, mear ik bedoele ’t allemoal wâ goôd.

Annemieke

Levensloop

Annemieke ten Brinke werd geboren op 6 september 1974 te Rijssen. Na het behalen van haar MAVO diploma in 1990 aan de Chr. Mavo te Rijssen, begon zij in september van dat jaar aan de Middelbare Laboratorium Opleiding te Hengelo. Gedurende deze studie heeft zij twee stage-opdrachten uitgevoerd, respectievelijk bij AKZO Coatings te Wapenveld en aan de Universiteit Twente te Enschede. Na het behalen van haar MLO-diploma met als differentiatie polymeerchemie in juli 1994 besloot zij haar studie te vervolgen aan de Hogere Laboratorium Opleiding te Utrecht. Voor afstudeeropdracht in de polymeerchemie ging zij weer naar Twente om binnen de groep van Dr. R. Gaymans onder de supervisie van Dr. Meike Niesten gesegmenteerde copolymeren op basis van uniforme aramide segmenten en poly(tetramethyleen-oxide) te onderzoeken. Nadat ze in februari 1998 haar HLO-diploma behaalde begon zij in mei van dat jaar aan een promotieonderzoek binnen de rubber technologie groep van Prof. J.W.M. Noordermeer. Het resultaat van dit onderzoek staat beschreven in het voor u liggende proefschrift.